SUPERINTENDENCIA DE INDUSTRIA Y COMERCIO
DIRECCIÓN DE NUEVAS CREACIONES

2020
Bogotá, D.C.,

Abogado
JUAN PABLO CADENA SARMIENTO

ASUNTO

Radicación	08 046 084
Trámite	011
Evento	378
Actuación	519
Oficio	
Folios	**39**

213029

Patente de Invención	☑		Patente de Modelo de Utilidad
Vía Nacional			
Via PCT (Fase Nacional)	☑	Capitulo I	☑ Capitulo II
No. Solicitud Internacional	PCT/US2006/043516		
Fecha de Presentación Internacional	08/Noviembre/2006		

Como resultado del examen de fondo realizado, con fundamento en el Artículo 45 de la Decisión 486 de la Comisión de la Comunidad Andina, se comunica:

1. **Documentos estudiados**

Descripción:	Folios 98 a 214	07/Mayo/2008
	Folios 231 a 295	07/Mayo/2008
	Folios 460 a 489	31/Enero/2011
Reivindicaciones:	Folios 215 a 218	07/Mayo/2008

	Folios 254 a 457	31/Enero/2011
Dibujos:	Folios 219 a 230	07/Mayo/2008
Oposiciones:	Folios 413 a 450	Lafrancol 06/Abril/2010
Respuesta del solicitante:	Folios 452 a 457	31/Enero/2011
Prioridad:	US 60 734 798	08/Noviembre/2005
	US 60 820 561	27/Julio/2006

2. Análisis de la prioridad

Se acepta la reivindicación de prioridad porque esta solicitud fue presentada dentro del plazo establecido (Art. 9 D 486) y su contenido técnico corresponde con el de la prioridad reivindicada.

3. Objeto de la invención

Título de la solicitud: "Antagonistas de Neuropilina".

El problema planteado en esta solicitud consiste en la necesidad de suministrar anticuerpos alternativos del tipo Anti- Neuropilina-1 (Anti-NRP-1).

Para resolver este problema técnico la solicitud en estudio proporciona anticuerpos anti-NRP1 novedosos capaces de modular por lo menos una actividad biológica mediada por neuropilina.

El objeto de la presente Solicitud se relaciona con la Clasificación Internacional de Patentes (CIP): C07K16/00, C07K 16/28

4. No es una invención (Art 15 D 486 literales (a) – (f))

El objeto de las reivindicaciones 23-24 no se considera una invención, de acuerdo con el Art citado. El método de las reivindicaciones 23-24 para producir un anticuerpo anti-NRP-1OX40L de expresión y recuperación de un anticuerpo se considera un proceso esencialmente biológico.

5. De la Solicitud de Patente

Reivindicaciones (Art 30 D 486, Art 22 PCT)

El capítulo reivindicatorio presentado carece de claridad y concisión por cuánto:

1) Las reivindicaciones independientes que se refieren a un anticuerpo deben caracterizarlo a partir de su estructura completa, mencionando las secuencias que lo conforman en la **cadena ligera y cadena pesada**, o las secuencias variables de las cadenas ligera y pesada o las secuencias de los 6 CDR´s que conforman **ambas cadenas**. La referencia a estructuras parciales del anticuerpo (por ejemplo solamente sus CDRs de cadena ligera o solamente las de cadena pesada) no son válidas puesto que no es una estructura activa, probada ni definida (reivindicaciones 1-4, 7-10);

2) Las reivindicaciones 19 y dependientes se refieren a polinucleótidos de determinada secuencia. Sin embargo, dado que el problema que resuelve la solicitud es proveer anticuerpos que se unen a NRP1 los polinucleótidos no hacen parte de la invención.

3) El vector reclamado en la reivindicación 20 y 21 carece de sustento en la descripción;

4) La línea celular mencionada en la reivindicación 22 debe ser caracterizada a partir de sus propias características, incluido el número del depósito del hibridoma al que se refiere, y estar plenamente sustentada en la descripción;

5) El método mencionado en la reivindicación 23-24 debe estar caracterizado por las etapas que lo conforman y estar plenamente sustentado en la descripción;

6) La composición farmacéutica y el kit mencionados en las reivindicaciones 25 y 26 deben caracterizarse a partir de los elementos y proporciones de los mismos que la componen, de acuerdo con la información sustentada en la descripción;
7) No se entiende a que se hace referencia con "artículo de fabricación" que comprende el anticuerpo anti-NRP1, se sugiere eliminar dicha reivindicación.

De esta manera, el capítulo reivindicatorio presentado no cumple con los requisitos establecidos en el art. 30 de la Decisión 486.

6. Unidad de invención (Art 25 D 486)

La solicitud no cumple con el requisito de unidad de invención porque se refiere a 2 grupos inventivos, definidos por las siguientes características esenciales:

1° Un anticuerpo Anti-Neuropilina-1 (Anti-NRP1) capaz de inhibir la intección de NRP-1 con semaforina (Reivindicaciones 1-6, 13-18). Un polinucleótido que codifica el anticuerpo Anti-NRP1, un vector que comprende dicho polinucleotido, una célula huésped que comprende dicho vector (Reivindicaciones 19-22). Una composición farmacéutica, un kit y un artículo de fabricación que comprende dicho anticuerpo (Reivindicaciones 25-27).

2° Un anticuerpo Anti-Neuropilina-1 (Anti-NRP1) capaz de inhibir la intección de NRP-1 con semaforina (Reivindicaciones 7-12, 13-18). Un polinucleótido que codifica el anticuerpo Anti-NRP1, un vector que comprende dicho polinucleotido, una célula huésped que comprende dicho vector (Reivindicaciones 19-22). Una composición farmacéutica, un kit y un artículo de fabricación que comprende dicho anticuerpo (Reivindicaciones 25-27).

El único concepto inventivo que comparten los anteriores grupos es proporcionar un anticuerpo Anti-Neuropilina-1 (Anti-NRP1). Sin embargo, este tipo de anticuerpos ya eran conocidos en el estado de la técnica mediante los documentos D1-D4, los cuales divulgan: un anticuerpo dirigido a NRP1 que inhibe por lo menos una actividad biológica mediada por neuropilina (D1, Discusión, pág. 481), un anticuerpo anti-NRP1 que inhibe la interacción de neuropilina 1 con semaforina (D2, pág. 40, primera columna, último párrafo), un anticuerpo anti-NRP1 que inhibe la interacción de neuropilina 1 con semaforina (D3, pág. 83, Abstract), un anticuerpo monoclonal que inhibe la interacción de neuropilina 1 con VEGF (D4, pág. 2341, Abstract).

El análisis anterior permite determinar que dicho único concepto no es nuevo ni inventivo y esto sumado a que no existen características técnicas adicionales entre los grupos permite concluir que no hay unidad de invención entre ellos.

Se sugiere presentar las solicitudes divisionales que considere necesarias, según los grupos mencionados o los considerados por el solicitante, ó limitar la solicitud inicial a una sola invención, eliminando de ella las otras invenciones.

El presente examen se llevará a cabo sobre el primer grupo inventivo.

7. Análisis de las Oposiciones

Argumentaciones de Lafrancol

Afirma el oponente que esta solicitud pretende obtener patente para composiciones y combinaciones farmacéuticas donde se involucran moléculas que se encuentran plenamente identificadas y que obstentan beneficios patentarios, moléculas como Vatalanib (WO9835958, US6258812), Sunitinib (WO0160814, US6573293), Imatinib (EP564409, US5521184), Lapatinib (WO9935146, US6727256). Además afirma que la presente solicitud pretende solicitar una patente de invención para métodos de tratamiento los cuales no se consideran invenciones. Por lo anterior, el oponente afirma que la presente solicitud no cumple con los requisitos esenciales para acceder al derecho patentario por cuanto no se encuentran presentes la novedad y el nivel inventivo.

Respuestas del Solicitante

En respuesta a los comentarios del señor opositor el solicitante presenta un nuevo capítulo reivindicatorio compuesto por 29 reivindicaciones y resalta que se han eliminado las reivindicaciones alusivas a usos. Además menciona que en la evidencia presentada por el señor opositor no hay documentos que divulguen anticuerpos NRP1 que inhiban la unión de NRP1 con semaforina sin bloquear la unión de NRP1 con VEGF ni anticuerpos que inhiban la unión de NRP1 con VEGF sin bloquear la unión de NRP1 con semaforina y que por consiguiente las reivindicaciones presentadas son nuevas e inventivas.

Respuesta del Examinador Técnico

Las nuevas reivindicaciones presentadas (Reivindicaciones 1-29) superan las objeciones resaltadas por el oponente ya que se eliminan las reivindicaciones correspondientes a método de tratamiento, así como las correspondientes a los usos

del anticuerpo y adicionalmente se eliminan las correspondientes a combinaciones del anticuerpo con agentes adicionales. En cuanto a los documentos presentados en la oposición, estos no desvirtúan la novedad o el nivel inventivo del objeto de esta solicitud, ya que el objeto de esos documentos de patente es la protección de la molécula solamente (Vatalanib, Sunitinib, Imatinib, Lapatinib), sin hacer referencia al anticuerpo objeto de la solicitud en estudio, por lo cual no se considerarán dentro del examen de patentabilidad.

8. Determinación del Estado de la Técnica

El estado de la técnica se determinó con base en la fecha de presentación de la solicitud de prioridad: noviembre 08 de 2005, y se encontraron los siguientes documentos que anticipan el objeto de esta solicitud:

Ítem	Documento	Título	Fecha de Publicación*
D1	Nature Immunology, vol. 3, n° 5, mayo 2002, págs. 477-482.	A neuronal receptor, neuropilin 1, is essential for the initiation of the primary immune response.	Mayo/2002
D2	Molecular and celular neuroscience, vol. 18, n°1, Julio 2001, págs. 26-43.	Age-dependent effects of secreted semaphorins 3ª, 3F. y 3E on developing hippocampal axons: In vitro effects and phenotype of semaphorin 3ª (-/-) mice.	Julio/2001
D3	Neoplasia, vol 5, n°1, enero 2003, págs. 83-92.	Semaphorin SEM3F and VEGF have opposing effects on cell attachment and spreading.	Enero/2003
D4	Cáncer, vol. 101, n°10, noviembre 2004, págs. 2341-2350.	Pancreatic carcinoma cells express neuropilins and vascular endotelial growth factor, but not vascular endotelial growth factor receptors.	Noviembre/2004
D5	Developmental cell, vol. 5, n°1, julio 2003, págs.45-57.	Neuropilin-1 conveys semaphoring and VEGF signaling during neural and cardiovascular development.	Julio/2003

D1
Divulga (Discusión, pág. 481) un anticuerpo dirigido a NRP1 que inhibe por lo menos una actividad

biológica mediada por neuropilina.

D2
Divulga (Pág. 40, primera columna, último párrafo) un anticuerpo anti-NRP1 que inhibe la interacción de neuropilina 1 con semaforina.

D3
Divulga (Pág. 83, Abstract) un anticuerpo anti-NRP1 que inhibe la interacción de neuropilina 1 con semaforina.

D4
Divulga (Pág. 2341, Abstract) un anticuerpo monoclonal que inhibe la interacción de neuropilina 1 con VEGF.

D5
Divulga (Pág. 45, Abstract) que NRP1 se enlaza a semaforina mediante el dominio a1a2 sin afectar el enlace a VEGF.

9. **Examen de Patentabilidad (Art 14 D486)**

Nivel Inventivo (Art18 D486)

La reivindicación 5 consiste en un anticuerpo anti-NRP1 el cual comprende las siguientes características técnicas:

Comparación de las características técnicas **esenciales**, con las del Estado de la Técnica:

Características **esenciales**	D1	D5
Anticuerpo anti-NRP1 que comprende las siguientes CDRs:	Divulga un anticuerpo anti-NRP1.	–
a) CDR-L1 que comprende la secuencia: SEC ID N° 123.		
b) CDR-L2 que comprende la secuencia: SEC ID N° 124.		
c) CDR-L3 que comprende la secuencia: SEC ID N° 125.		
d) CDR-H1 que comprende la secuencia: SEC ID N° 126.		
e) CDR-H2 que comprende la secuencia: SEC ID N° 127.		
f) CDR-H3 que comprende la secuencia: SEC ID N° 128.		

Que se une a NRP1 en el dominio a1a2 y bloquea la unión de NRP1 a semaforina sin bloquear la unión de NRP1 a VEGF.	–	Divulga que el enlace de NRP1 a semaforina se da mediante el dominio a1a2 sin afectar el enlace a VEGF (D5, Pág. 45, Abstract).

Los documentos D1 y D5 se consideran el estado de la técnica cercano a la invención definida en la reivindicación 5 porque divulgan un anticuerpo anti-NRP1 (D1, Discusión, pág. 481) y además que el enlace de NRP1 a semaforina se da mediante el dominio a1a2 sin afectar el enlace a VEGF (D5, Pág. 45, Abstract).

La diferencia entre el anticuerpo definido en la reivindicación 5 y el anticuerpo de D1 consiste en las secuencias de los CDRs para el anticuerpo de la invención.

El efecto técnico que se logra con dicho anticuerpo es bloquear la unión de NRP1 a semaforina sin bloquear la unión de NRP1 a VEGF. La información contenida en el capítulo descriptivo no permite evidenciar que el efecto técnico es sorprendente y no hay ninguna diferencia considerable en cuanto a especificidad de unión o actividad, o alguna ventaja técnica para el anticuerpo de la invención.

Por lo tanto, el problema técnico objetivo que pretende resolver esta invención se puede formular así: "cómo modificar el anticuerpo anti-NRP1 conocido en D1 para conseguir anticuerpos alternativos a los ya conocidos.

Sin embargo, el hecho de que el enlace de NRP1 a semaforina se da mediante el dominio a1a2 sin afectar el enlace a VEGF (D5, Pág. 45, Abstract) ya está divulgado en el documento D5.

En consecuencia, conociendo que el sitio de unión del anticuerpo es el domino a1a2 de NRP1 y que esto bloquea la unión a semaforina es obvio esperar que el anticuerpo de la invención tenga el mismo comportamiento y que se una al mismo sitio de unión produciendo los mismo efectos como el hecho de no interferir con el enlace a VEGF, por lo cual la invención se considera obvia.

La reivindicaciones 1-4, 6 y 13-18 no contiene características técnicas adicionales por lo tanto se considera que tampoco son inventivas.

Conclusión:
Las reivindicaciones 1-6 y 13-18 cumplen el requisito de novedad (Art. 16), pero no cumple con el requisito de nivel inventivo (Art. 18).

10. Conclusión

Los requisitos de patentabilidad de la presente solicitud están afectados así:

Ítem	Documento	Reivindicaciones afectadas	Requisito que afecta
D1	A neuronal receptor, neuropilin 1, is essential for the initiation of the primary immune response.	1-6 y 13-18	Nivel Inventivo
D5	Neuropilin-1 conveys semaphoring and VEGF signaling during neural and cardiovascular development.	1-6 y 13-18	Nivel Inventivo

En cumplimiento del artículo 45 de la Decisión 486 de la Comisión de la Comunidad Andina, se le indica que debe dar respuesta dentro del término de sesenta (60) días contados a partir de la fecha de notificación de la presente comunicación. En caso de no dar respuesta al presente requerimiento, o si a pesar de la respuesta subsistieran los impedimentos para la concesión, se denegará la patente.

Se invita al solicitante se sirva indicar, si así lo considera, su renuncia al término faltante de sesenta (60) días para dar respuesta a este requerimiento y presentarla por escrito.

Notifíquese el presente oficio conforme a lo dispuesto en el numeral 5.2, literal e), del capítulo quinto del título primero de la Circular Única No. 10 de 2001.

JESÚS FERNEL GARCÍA GARCÍA
Director de Nuevas Creaciones (E)

El anterior requerimiento fue notificado por fijación en lista, de fecha 27 JUL. 2012
Realizado por: Ximena Andrade.
Revisado por: Consuelo Leguizamón.
Aprobado por: Jesús Fernel García García.

Expediente 08 046 084 1er Art 45

A neuronal receptor, neuropilin-1, is essential for the initiation of the primary immune response

Rafaèle Tordjman[1], Yves Lepelletier[2], Valérie Lemarchandel[1], Marie Cambot[1], Philippe Gaulard[3], Olivier Hermine[2] and Paul-Henri Roméo[1]

Published online: 15 April 2002, DOI: 10.1038/ni789

The initiation of a primary immune response requires contact between dendritic cells (DCs) and resting T cells. However, little is known about the proteins that mediate this initial contact. We show here that neuropilin-1, a receptor involved in axon guidance, was expressed by human DCs and resting T cells both *in vitro* and *in vivo*. The initial contact between DCs and resting T cells led to neuropilin-1 polarization on T cells. DCs and resting T cells specifically bound soluble neuropilin-1, and resting T cells formed clusters with neuropilin-1–transfected COS-7 cells in a neuropilin-1–dependent manner. Functionally, preincubation of DCs or resting T cells with blocking neuropilin-1 antibodies inhibited DC-induced proliferation of resting T cells. These data suggest that neuropilin-1 mediates interactions between DCs and T cells that are essential for initiation of the primary immune response and show parallels between the nervous and immune systems.

Primary immune responses are initiated in the T cell areas of secondary lymphoid organs, where naive T lymphocytes encounter dendritic cells (DCs) that present antigens taken up in peripheral tissues or locally. Antigen-specific T lymphocyte activation requires the interaction of T cell receptors (TCRs) with specific major histocompatibility complex–peptide (pMHC) complexes, which are expressed on antigen-presenting cells (APCs)[1]. DCs, the major APCs, have the unique ability to present antigen to naive T cells and thus initiate the primary immune response. During this antigen recognition, a specific large-scale molecular complex is built at the DC–T cell interface that establishes a specialized junction called the immunological synapse; here, TCRs and costimulatory molecules are congregated in a central area surrounded by a ring of adhesion molecules. An initial contact between DCs and resting T cells—which is mediated by proteins such as DC-specific intercellular adhesion molecule 3 (ICAM-3)–grabbing nonintegrin (DC-SIGN) and ICAM-3, CD58 (also known as LFA-3) and CD2 or LFA-1 and ICAM-1 or ICAM-2—is required for the formation of the immunological synapse. This formation is also dependent on cytoskeletal rearrangement of DCs and T cells, which is associated with T cell activation[1].

The analogy between DCs and neurons, which was originally described in 1868 by Paul Langherans[4], together with the role of a neuronal receptor, neuropilin-1, in the regulation of the neurons cytoskeletal rearrangement prompted us to study neuropilin-1 expression by DCs. Neuropilin-1 is a transmembrane protein that was initially isolated from the optic tectum of *Xenopus laevis*. Neuropilin-1 is actually a receptor for a family of chemotropic cues that mediate axon guidance, the secreted semaphorins of subclass 3[5], in particular semaphorin 3A. An ordered series of axon guidance decisions during neurodevelopment ultimately leads to the establishment of precise connections between neurons and their appropriate targets. The leading edge of the axon, the growth cone, can drive the axon to its target in part through interactions with semaphorins[6]. The cytoplasmic domain of neuropilin-1 is not required for semaphorin signaling but members of the plexin family appear to act as the downstream signaling subunits of the semaphorin-neuropilin-1 receptor complex[11]. After the semaphorin-neuropilin interaction, plexins are able to modulate the activity of small GTPases and induce structural changes to the cytoskeleton such as axonal cytoskeleton retraction and growth cone collapse[11].

We show here that neuropilin-1 was expressed by DCs and resting T cells. In addition, we observed a neuropilin-1 polarization on T cells after contact between DCs and resting T cells. We therefore analyzed the role played by neuropilin-1 in adhesion and clustering between DCs and T cells. Soluble neuropilin-1 bound DCs and resting T cells. Resting T cells formed clusters with COS-7 that expressed neuropilin-1 in a neuropilin-1–dependent manner. Finally, DC-induced proliferation of resting T cells was inhibited by DCs or T cells that had been preincubated with blocking neuropilin-1 antibodies. Together, these data suggest a role for neuropilin-1 in initiation of the primary immune response.

Results

Neuropilin-1 is expressed by human DCs

Neuropilin-1 expression has predominantly been studied in the developing embryonic nervous system, but some adult tissues have also been assessed[11]. Because neurological and immunological synapses show similarities, we analyzed whether DCs expressed neuropilin-1, by reverse-transcribed polymerase chain reaction (RT-PCR) analysis. We found neuropilin-1 transcripts in human DCs derived from monocytes *in vitro*, but not in monocytes themselves (data not shown). Using immunofluorescence analysis, we showed that the neuropilin-1 protein was indeed expressed by human DCs (Fig. 1a) and not by monocytes (data not shown). The specificity of the neuropilin antibodies used for these experiments was confirmed by immunoblot analysis. The antibody to rat neuropilin-1 recognized one protein product that migrated on SDS–polyacrylamide gel electrophoresis (SDS-PAGE) as a 130-kD polypeptide—the expected size of human neuropilin-1—in human neuropilin-1–transfected COS-7 cells, but not in nontransfected COS-7 cells (Fig. 1b, lanes 1 and 2). Using this antibody, we detected a 130-kD doublet that corresponds to neuropilin-1 in human DCs but not in monocytes (Fig. 1b, lanes 3 and 4). A similar doublet was found in neuropilin-1–expressing human PC3 prostate carcinoma cells[11].

During *in vitro* DC differentiation induced by granulocyte macrophage colony-stimulating factor (GM-CSF) and interleukin 4 (IL-4), CD14 expression is down-regulated, whereas CD1a and DC-SIGN expression is up-regulated[11]. We studied neuropilin-1 protein expression during DC differentiation using flow cytometry. Purified monocytes lacked neuropilin-1 expression but expressed a high amount of CD14 (Fig. 1c, d0). However, neuropilin-1 expression increased during DC differentiation *in vitro* and its appearance followed a time-course similar to that of DC-SIGN or CD1a (Fig. 1c). Further DC maturation induced by cytokines (tumor necrosis factor-α and IL-1) did not greatly modify the expression of neuropilin-1 (data not shown).

[1]Institut Cochin, Departement d'Hematologie, INSERM U567, CNRS UMR 8104, Paris, France. [2]CNRS UMR 8603 and Service d'Hematologie, Hopital Necker, Paris, France. [3]Departement de Pathologie EA 2348, Hôpital Henri Mondor, Creteil, France. Correspondence should be addressed to R.T. (tordjman@cochin.inserm.fr) or O.H. (hermine@necker.fr).

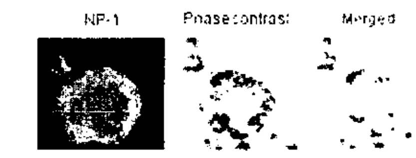

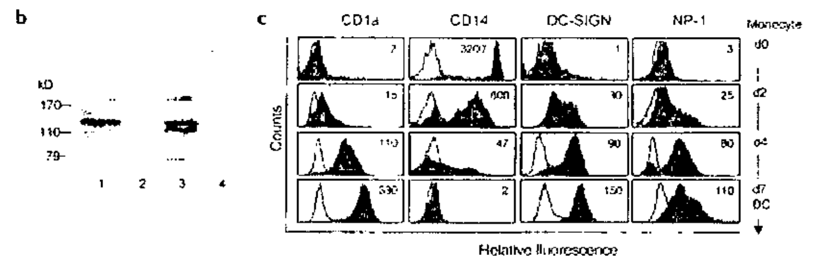

Figure 1. Neuropilin-1 is expressed by *in vitro* human monocyte-derived DCs. (a) Immature DCs were plated on poly-L-lysine–coated slides and expression of neuropilin-1 was assessed by immunocytofluorescence (red) (see Methods). Controls included rabbit-purified IgG as a primary antibody and the absence of neuropilin-1 expression by monocytes. (b) Protein extracts from COS-7 cells (lane 2), COS-7 cells that expressed human neuropilin-1 (lane 1), human immature DCs (lane 3) and human monocytes (lane 4) were resolved by SDS-PAGE. Immunoanalysis was done with the neuropilin-1 antibody that was used for immunocytofluorescence. (c) Increase of neuropilin-1 expression during DC differentiation *in vitro*. Immature DCs were obtained after culture of purified monocytes in the presence of GM-CSF and IL-4. At the indicated time-points the cells were analyzed by flow cytometry for expression of the monocyte marker CD14, the DC markers CD1a and DC-SIGN and neuropilin-1 (28.4). Cells were gated on forward side scatter; the numbers denote mean fluorescence. One representative of four experiments is shown.

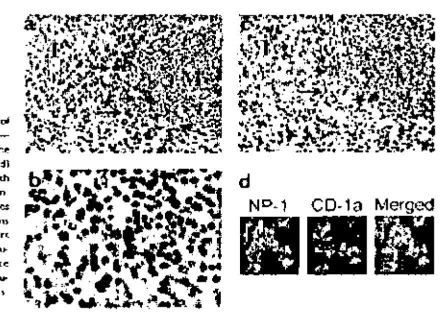

Figure 2. Expression of neuropilin-1 in human lymphoid tissues. Analysis of neuropilin-1 expression in reactive dermatopathic lymphadenopathy samples—which contain a high number of DCs in the interfollicular areas—was done with the use of (a–c) immunohistochemistry (the APAAP technique with Naphthol fast red) and (d) immunofluorescence. (a,b) Cytoplasmic neuropilin-1 staining of cells with DC morphology (short arrows) was observed in interfollicular areas (I) but the mantle cells in follicles (M) were not stained. In addition, the surrounding lymphocytes (long arrows) in the interfollicular areas also stained positively. (c) The serial sections used in a were stained with anti-CD1a. Strong staining of DCs was observed (short arrows), but lymphoid cells were not stained (long arrow). (d) Expression of neuropilin-1 (green) and CD1a (red) was detected with the use of immunofluorescence in human reactive dermatopathic lymphadenopathy samples. Coexpression of neuropilin-1 and CD1a in DCs was detected with the use of double immunofluorescence (yellow).

499

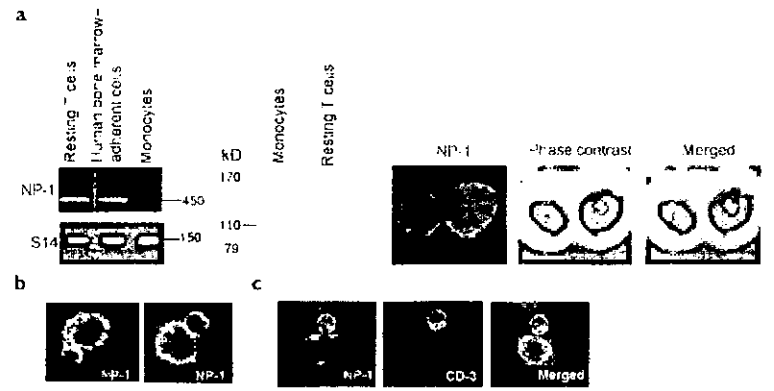

Figure 3. Neuropilin-1 is expressed by resting T cells and T cell–DC interaction induces neuropilin-1 polarization. (a) Expression of neuropilin-1 mRNA and protein by resting T cells. (Left panel) RT-PCR was done with total RNA isolated from resting T cells, human bone marrow–adherent cells were used as a positive control and human monocytes were used as a negative control. The expected neuropilin-1 PCR product was 450 bp. As a control, we used an amplification of the same reverse-transcribed products with S14 primers (150 bp). (Middle panel) Protein extracts from human monocytes and resting T cells were resolved by SDS-PAGE and immunoanalysis was done as in Fig. 1b. (Right panel) Neuropilin-1 protein (blue) was detected in resting T cells with the use of immunocytochemistry. (b) Polarization of neuropilin-1 in T cells that contact DCs. Localization of neuropilin-1 (red) on fixed allogeneic DC–T cell conjugates. (Left panel) Polarization of neuropilin-1 was found in T cells but not in DCs contact zone. (Right panel) The bipolar polarization of neuropilin-1 was detected in a few DC–T cell conjugates. (c) Colocalization of neuropilin-1 with CD3 at the DC–T cell contact site. Neuropilin-1 (red) and CD3 (green) were detected in allogeneic DC–T cell conjugates. Polarization and colocalization of neuropilin-1 and CD3 were also detected (yellow).

To determine whether neuropilin-1 expression *in vitro* reflected its expression *in vivo*, sections of human lymph nodes were stained with neuropilin-1 antibodies. We selected samples from patients with reactive dermatopathic lymphadenopathy, because such samples contain high numbers of DCs in the interfollicular areas[26]. Neuropilin-1–expressing cells were found in lymph node T cell areas (Fig. 2a,b, short arrows). These stained cells were large with irregular nuclei and abundant cytoplasm, which was consistent with the distribution and morphology of DCs. Analysis of serial sections of the same biopsy samples, stained for CD1a, indicated that these large cells were indeed DCs (Fig. 2c). Finally, using double immunofluorescence with antibodies to neuropilin-1 and CD1a, we showed that the CD1a$^+$ cells also expressed neuropilin-1 (Fig. 2d).

Neuropilin-1 expression by T cells

Careful analysis of the staining of lymph nodes with neuropilin-1 antibodies indicated that, in addition to DCs, T lymphocytes might also express neuropilin-1 (Fig. 2a,b, long arrows). We therefore analyzed whether resting T cells purified from adult peripheral blood expressed neuropilin-1. Neuropilin-1 mRNA (Fig. 3a, left panel) was detected in resting T lymphocytes, and immunoblot analyses and immunofluorescence revealed the presence of neuropilin-1 protein in these cells (Fig. 3a, middle and right panels).

The initial interaction between T lymphocytes and DCs results in formation of the immunological synapse. The formation of this structure leads to polarization of molecules such as CD3, CD4 or CD8$^+$ on the effector T lymphocyte. Using immunofluorescence,

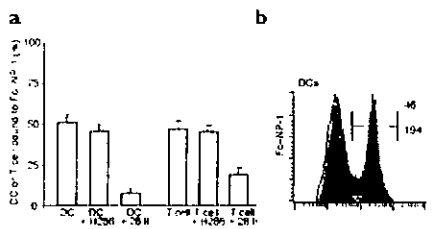

Figure 4. Adhesion of soluble neuropilin-1 to DCs and T cells. (a) We assessed the binding of soluble neuropilin-1 to DCs or resting T cells by measuring the percentage of DCs or T cells bound to Fc–neuropilin-1 by flow cytometry using an FITC-conjugated human Fc antibody. Binding of Fc neuropilin-1 to DCs was inhibited when DCs or resting T cells were preincubated with blocking neuropilin-1 antibodies (DC + 2B11 and T cells + 2B11), it was not inhibited when a nonblocking neuropilin-1 antibodies (DC + H286 and T cells + H286) were used. In each assay, DCs and T cells were first preincubated with human IgG to block the Fc receptors on DCs. Data are means ± s.e.m. of three independent experiments. (b) FACS analysis showing the binding of Fc neuropilin-1 to DCs (46 is the percentage of DCs bound to Fc–neuropilin-1, 194 is mean fluorescence).

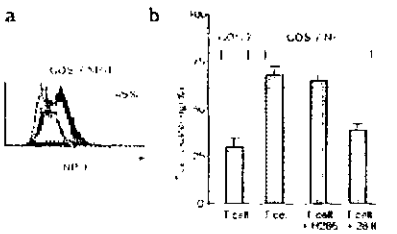

Figure 5. Heterotypic T cell clustering with neuropilin-1–expressing COS-7 cells. (a) COS-7 cells were transfected with a vector that allowed a high amount of neuropilin-1 expression (>95%) as shown by flow cytometry. (b) COS-7 cells and neuropilin-1–expressing COS-7 cells (COS-7 / NP-1) were incubated with T cells that had been labeled with the fluorescent dye hydroethidine at 37 °C; heterotypic cell clustering was measured by flow cytometry. The specificity of binding was tested by preincubating T cells with blocking neuropilin-1 antibodies (T cells + 2B11) or with neuropilin-1 antibodies that did not block function (T cells + H286). Data are means ± s.e.m. of three independent experiments.

we studied neuropilin-1 distribution on DC allogeneic T cell conjugates. Only T cells that showed an obvious contact with DCs were analyzed. We found the polarization of neuropilin-1 towards the contact zone (Fig. 3b, right panel) in 78.5 % (*n* 521) of the T lymphocytes present in these conjugates. To study the colocalization of neuropilin-1 with proteins known to be present at the DC–T cell contact site, double immunofluorescence with anti-CD3 was done, which showed that neuropilin-1 and CD3 do colocalize (Fig. 3c). This pattern of polarization indicated that neuropilin-1 is positioned at the T lymphocyte pole of the immunological synapse. In a few DC–T cell conjugates (11.5 %, *n* 52), we did see a bipolar distribution of neuropilin-1, with neuropilin-1 concentrated at the contact zone and at the opposite pole of the T lymphocyte (Fig. 3b, left panel). A similar bipolar distribution of CD3, also observed in the DC allogeneic T cells conjugates, has been described during antigen-specific T cell–B lymphoma cells interactions[27] and during antigen-independent DC–T cell interactions[28]. Taken together, these data show that neuropilin-1 is expressed by DCs and resting T cells both *in vitro* and *in vivo* and suggest a potential function for this receptor in DC–T cell interactions during the initiation of the immune response.

Neuropilin-1 promoted cell-cell interactions

Neuropilin-1 was initially described as a receptor for semaphorin 3A, but it is able to bind other secreted semaphorins, such as semaphorin 3B, semaphorin 3C[29] and vascular endothelial growth factor (VEGF)[30]. In addition, neuropilin-1 can also act through homophilic interactions in the absence of its major ligand, semaphorin 3A[31]. Because mRNA expression by neuropilin-1 ligand was low in DCs and resting T cells (data not shown), we analyzed whether neuropilin-1 promoted DC–T cell interactions via homophilic binding of neuropilin-1. Using a Fc–neuropilin-1 adhesion assay[26], we tested whether DCs could bind soluble Fc–neuropilin-1 (Fig. 4). We found that Fc–neuropilin-1 could bind DCs (Fig. 4b) and that binding was inhibited in the presence of blocking neuropilin-1 antibodies, whereas neuropilin-1 antibodies without blocking activity had no effect. We obtained a similar result with Fc–neuropilin-1 and resting T cells (Fig. 4a). These results showed that the adhesion of DCs or T cells to Fc–neuropilin-1 is mediated by neuropilin-1 and suggested that the interaction between DCs and resting T cells might involve homophilic neuropilin-1–neuropilin-1 interactions.

We then studied whether neuropilin-1 can mediate binding in *trans* when neuropilins are embedded in the plasma membranes of different cells. For this purpose, we analyzed whether neuropilin-1 can generate clusters of resting T cells when expressed in heterologous cells. We transfected COS-7 cells with a neuropilin-1 expression vector to generate neuropilin-1–expressing COS-7 cells (Fig. 5a). Resting T cells were able to form clusters around the neuropilin-1–expressing COS-7 cells in a neuropilin-1 dependent manner, as shown with blocking neuropilin-1 antibodies, which inhibited the interaction (Fig. 5b). Neuropilin-1 antibodies without blocking function had no

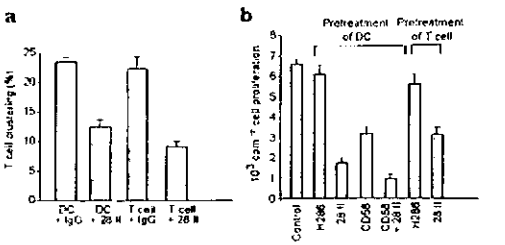

Figure 6. Neuropilin-1 mediates DC–T cell clustering and DC-induced proliferation of resting T cells. (a) Neuropilin-1 is required for clustering of DCs with resting T cells. DCs and T cells were first preincubated with human IgG to block the Fc receptors on DCs. DCs were then preincubated with blocking neuropilin-1 antibody (DC + 2B11) or rabbit-purified polyclonal IgG (DC + IgG) and mixed with labeled allogeneic resting T cells. In separate experiments, labeled allogeneic resting T cells were preincubated with blocking neuropilin-1 antibody (T cells + 2B11) or rabbit-purified polyclonal IgG (T cells + IgG) and then mixed with DCs. The clustering was determined by measuring the percentage of DCs that had bound fluorescent T cells by flow cytometry. Data are mean ± s.e.m. from three independent experiments. (b) Neuropilin-1 is required for DC-induced allogeneic T cell proliferation. DCs and resting T cells were first preincubated with human IgG to block the Fc receptors on DCs. DCs were then preincubated with a nonblocking neuropilin-1 antibody (H286), blocking neuropilin-1 antibody (2B11), blocking CD58 antibody (CD58) or a combination of blocking CD58 and neuropilin-1 antibodies (CD58 + 2B11). The allogeneic resting T cells were then added to these pretreated DCs. In separate experiments, the allogeneic resting T cells were preincubated with nonblocking neuropilin-1 antibody (H286) or blocking neuropilin-1 antibody (2B11), then were cocultured with DCs. The 'control' represents DCs and T cells that were not preincubated with antibodies. DCs and allogeneic resting T lymphocytes were cocultured for 4 days. T cells were then pulsed for 16 h with [^{3}H]-thymidine and T cell proliferation was measured by thymidine incorporation. Data are the means ± s.e.m. from triplicate wells.

effect on cluster formation (Fig. 5b). The neuropilin-1-independent clustering of T cells to untransfected COS-7 cells might be explained by the expression of adhesion molecules such as CD58 by COS-7 cells (data not shown), which can interact with CD2 on T cells, or by the low amount of neuropilin-1 expression (< 10%) in untransfected COS-7 cells (data not shown). However, as the blocking neuropilin-1 antibody had no effect on the neuropilin-1-independent clustering of T cells on COS-7 cells, we favored the former hypothesis.

Neuropilin-1 effects on T cell proliferation

Characterization of molecules that participate in DC–T cell interactions is hampered by the numerous interactions that simultaneously contribute to the establishment and function of the immunological synapse. To demonstrate that neuropilin-1 is required on both DCs and T cells for DC–T cell binding and T cell activation, we studied the involvement of this receptor in DC–T cell clustering and in DC-induced T cell proliferation. DC clustering with allogenic resting T cells was partially inhibited when DCs or T cells were preincubated with blocking neuropilin-1 antibodies (Fig. 6a). The relative inhibition of preincubated DCs and T cells (50% and 40%, respectively) indicated that the DC–T cell clustering was not totally dependent on neuropilin-1 activity and might reflect the numerous adhesion molecules involved in the stabilization of the DC–T cell contact. Finally, to determine whether neuropilin-1-mediated interactions are required for initiation of the primary immune response, we studied the effect of the neuropilin-1 antibodies on the DC-induced proliferation of resting T cells. DC-induced proliferation of resting T cells was inhibited by 60% when DCs were preincubated with the blocking neuropilin-1 antibodies and inhibited by 50% when T cells were preincubated with the same antibodies. The amount of inhibition in these experiments was equivalent to that obtained when antibodies to CD58 were used in the same assay (Fig. 6b). The involvement of neuropilin-1 in the initial DC–T cell contact was further supported when we found that blocking neuropilin-1 antibodies had no effect on the proliferation of activated T cells (data not shown). Together, these data argue that neuropilin-1–mediated interactions are necessary to initiate the primary immune response.

Discussion

DCs have the unique capacity to stimulate naïve T cells and initiate primary immune responses. T cell recognition of antigen presented by DCs requires the formation of a specialized junction between these cells called the immunological synapse. The formation of this highly specialized tight interaction is a multistep process that begins with adhesion of the T cell and the DC. Among the proteins involved in the initial contact between DCs and T cells, integrins such as LFA-1 and ICAM-1 and nonintegrins such as DC-SIGN and ICAM-3[21] play key roles. The importance of DC-SIGN–ICAM-3 in the primary immune response was first shown with ICAM-3 transfectants that induced DC clustering and by the inhibition of DC-induced proliferation of resting T cells, but not of activated T cells, with antibodies to DC-SIGN[21]. We have identified here a neuronal receptor, neuropilin-1, as another essential element of the primary immune response. We showed that preincubation of DCs or T cells with blocking neuropilin-1 antibodies inhibited DC clustering with allogenic resting T cells and DC-induced proliferation of resting T cell but not of activated T cells. Because T cell proliferation was blocked if either DCs or T cells were preincubated with blocking neuropilin-1 antibodies before DC–T cells were mixed, this supported a role played by neuropilin-1 in both DCs and T cells.

Formation of the synapse between DCs and allogenic resting T cells was associated with a neuropilin-1 polarization in T cells, but not in DCs, and neuropilin-1 was positioned at either pole of the T cell. CD3 and TCR[1] also show bipolar polarization, which is probably caused by myosin I activation and actin filament contraction at the original trailing edge[1]. Indeed, the bipolar distribution of neuropilin-1 could be explained if neuropilin-1 is also involved in the formation and function of the immunological synapse by promoting subsequent low-avidity interactions of adhesion molecules that can, thus, enable productive TCR engagement followed by adhesion strengthening.

In the nervous system, neuropilin-1 interacts with semaphorins[6,7], but neuropilin-1 also forms homo-oligomers, which suggests that neuropilin-1–neuropilin-1 interactions could also occur in *trans*. However, no function has been reported for this interaction. We showed here that neuropilin-1 is expressed on both DCs and resting T cells and is likely to mediate contacts between these two cells *via* homophilic interaction. We do not exclude the possibility that this DC–T cell interaction might also be mediated by neuropilin-1–interacting protein expressed by DCs and/or T cells. In addition, this neuropilin-1–mediated interaction might also be involved in the formation of homotypic clusters, which has been described for activated T cells and DCs[22].

Previously, neuropilin-1 was known as a receptor that mediates chemorepulsion associated with induction of growth cone collapse and axonal cytoskeleton retraction induced by semaphorins. The data we present here suggest that neuropilin-1–mediated interactions between DCs and T cells might induce similar cytoskeletal rearrangements in T cells and DCs. These cytoskeletal rearrangements are critical for both the clustering and the activation of resting T cells[1]. In addition, in axon guidance, neuropilin-1 function is required for both repulsion and attraction of neuronal connections[23]; this dual role played by neuropilin-1 is mediated by multiprotein complexes that include molecules such as semaphorins, plexin and L1 CAM (L1 cell adhesion molecule)[24]. We hypothesize that these attractive or repulsive neuron guidance cues may also regulate the immune response by triggering or extinguishing the contact between T lymphocytes and DCs during initiation of the immune response. This type of regulation could eventually give rise to distinct functional outputs such as effector and memory T cell generation or T cell tolerance.

Two reports have hinted at commonalities between the nervous and immune system. Immunological and neurological synapses use a common molecule, agrin[25], and the neuronal repellent Slit regulates leukocyte migration[26]. The data we present here demonstrate another parallel between the nervous and immune systems in the capacity of the neuronal guidance cue to play a role in initiation of the primary immune response.

Methods

Isolation and culture of monocytes, DCs and T cells. Human monocytes and resting T cells were isolated from the peripheral blood mononuclear cells of healthy volunteers, after their informed consent, with the use of monocyte and pan T cell isolation kits (Miltenyi Biotec, Bergisch Gladbach, Germany) as described[1]. The purity of monocytes, evaluated by CD14 staining, and of resting T cells, evaluated by CD4 and CD8 staining, was always higher than 95%. Immature DCs were obtained from monocytes as described[1]. Culture of human bone marrow adherent cells was done as described[12].

Fluorescence microscopy. Cells were fixed in 3% paraformaldehyde, quenched with 0.1 M glycine, plated on slides coated with poly-L-lysine (Sigma, St. Louis, MO) and permeabilized with 0.01% saponin. Slides were examined with a confocal laser microscope system (LSM 510; Carl Zeiss, Oberkochen, Germany) for neuropilin-1. The primary antibody raised were rabbit anti-extracytoplasmic neuropilin-1; the secondary antibodies used were cyanine 3–conjugated goat anti-rabbit whole IgG (Jackson ImmunoResearch, West Grove, PA). Controls included rabbit purified IgG as a primary antibody and the negative immunostaining of monocytes. Clustering between DCs and allogenic resting T cells (1:3) was assayed as described[1] and DC–T cell conjugates were fixed in 3% paraformaldehyde after 20 min of contact. We also used fluorescein isothiocyanate (FITC)-conjugated mouse anti-human CD11 (Jackson ImmunoResearch).

Immunoanalysis. Total protein extracts from COS-7 cells, human DCs, human resting T cells and monocytes were obtained with a lysis buffer (50 mM Tris HCl, pH 7.4, 150 mM NaCl, 1% NP-40, [illegible]). The lysates were collected and washed [illegible] then resuspended in [illegible] buffer for [illegible]. The solution was then incubated [illegible] and centrifuged at [illegible] × *g*. Supernatants were used for immunoblotting. Protein concentration was measured with a commercial kit (BioRad, Richmond, CA). Total protein extracts were separated by electrophoresis in 7.5% SDS-PAGE and transferred to Hybond-P PVDF membranes (Amersham Pharmacia). An immunoblot analysis was done with the neuropilin-1 antibody anti-extracytoplasmic neuropilin-1 used at [illegible] dilution, which was used at a [illegible] dilution and was revealed by the enhanced chemiluminescence detection system (Amersham).

Immunohistochemistry. DCs and T cells from two dermatopathic lymphadenopathy biopsy samples were obtained. Biopsy specimens were fixed in formol, routinely embedded in paraffin. Paraffin-embedded sections were stained for neuropilin-1 and CD1a antigens with the use of the alkaline phosphatase anti-alkaline phosphatase (APAAP) method[27] as described[1]. The neuropilin-1 antibody was the same one that was used in fluorescence microscopy; the anti-CD1a was from Immunotech. Controls included omission of the primary antibody and use of an irrelevant polyclonal antibody (Dako, Carpinteria, CA). To evaluate the coexpression of neuropilin-1 and CD1a in DCs, a double immunofluorescence method, as described[1], was used on paraffin-embedded dermatopathic lymphadenopathy sections. The surgical specimens were obtained and processed for routine diagnostic purpose (routinely fixed paraffin-embedded tissue for histology and immunophenotype). The experiments on human samples were approved by the French Health Department and the Necker Hospital Ethical Committee (agreement 30F-65).

RT-PCR analysis. RT-PCR analysis was done as described[1]. Primer sequences for human neuropilin-1 and human S14 were as follows: neuropilin-1 forward, 5′-ACGAATGAAC-GTGGGCGAGAC-3′ and reverse, 5′-AGGCCATTCAAGGCTGTTGG-3′ (35 cycles; annealing at 60 °C); S14 forward 5′-GGCAGACCGAGATGAATCCTCA-3′ and reverse, 5′-CAGGTCCAGGGGTCTTGGTCC-3′ (28 cycles, annealing at 64 °C).

Antibodies. The following antibodies were used in flow cytometry: 3F2 (anti–DC-SIGN), 28H (anti–neuropilin-1 to neuropilin-1 extracellular domain)[4], phycoerythrin (PE)-anti-CD11 (Becton Dickinson, Pont de Claix, France), anti-CD1a (Chemicon, Montrouge, France). For the neuropilin-1 functional blocking test, the blocking neuropilin-1 antibody 28H (to amino acids 265–557) was used, as described[4], at 10 µg/ml; the control used was a nonblocking neuropilin-1 antibody, H286 (to amino acids 570–835; Santa Cruz Biotechnology, Santa Cruz, CA). These two antibodies recognized extracellular epitopes.

Neuropilin-1 ectodomain Fc-binding assay. DCs were first preincubated with human IgG (10 mg/ml) to block the Fc receptor sites for antibodies. The rat neuropilin-1 extracellular domain fused to human IgG1 Fc (Fc-neuropilin-1; 50 µg/ml; R&D Systems, Abingdon, UK) was preincubated with FITC-conjugated goat anti–human IgG F(ab′)[2] Fc(γ) fragment specific (FITC-anti–human Fc, Jackson ImmunoResearch) for 1 h at 37 °C. DCs that were preincubated with or without the anti–neuropilin-1 blocking rabbit IgG (25 µg/ml) or the anti–neuropilin-1 without blocking function (H286) were then incubated with the immune complexes FITC–anti-human Fc and FITC–anti-human Fc–neuropilin-1 for 30 min at room temperature. The binding assay was evaluated by flow cytometric analysis. Controls included the binding of FITC-anti–human Fc without Fc–neuropilin-1 to DCs that had been preincubated with or without neuropilin-1 antibody.

Heterotypic cell clustering and DC-induced T cell proliferation. Clustering of resting T cells was analyzed with the use of wild-type COS-7 cells or with COS-7 cells that had been transfected with neuropilin-1. Neuropilin-1 cDNA was cloned into the expression vector pXM121 and transiently transfected into COS-7 cells with Lipofectamine (Gibco-BRL, Gaithersburg, MD).

Clustering with allogenic resting T cells was analyzed as described[1] with the use of one color to stain T cells that were in clusters with either COS-7 cells or DCs. T cells were labeled with hydroethidine (40 µg/ml; Molecular Probes, Eugene, OR) for 1 h at 37 °C before mixing with DCs or COS-7 cells (at a ratio of 1:10[?]). The clustering was determined by measuring percentage of fluorescent T cells that had bound COS-7 cells or DCs by flow cytometry.

DC-induced resting allogenic T lymphocyte proliferation was evaluated as described[1]. Briefly, immature DCs (1×10[4]) and allogenic resting responder T lymphocytes (100×10[3]) were mixed, cultured for 5 days and pulsed for 16 h with [3H]thymidine; thymidine incorporation was then quantified.

In the [illegible] assays, DCs or T cells were [illegible] blocked with human IgG [illegible] and preincubated with or without the [illegible] antibodies [illegible] for 30 min at [illegible].

Acknowledgments

We thank H. Fesser-Langre and Z. He for the gift of the NP-1 construct and of [illegible] neuropilin-1 (extracytoplasmic) and blocking anti-neuropilin-1); A. Amara for the gift of anti–DC-SIGN; A. Trautmann, G. Bismuth and A. Chaoul for their advice; and [illegible] Saraceni for his advice and encouragement. Supported by the INSERM, the CNRS and the Association pour la Recherche sur le Cancer (grant number 57-51). M.C. was supported by the Fondation pour la Recherche Médicale.

Competing interests statement

The authors declare that they have no competing financial interests.

Received 8 January 2002; accepted 28 March 2002

1. Banchereau, J. & Steinman, R. M. Dendritic cells and the control of immunity. *Nature* 392, 245–252 (1998).
2. Dustin, M. L. & Cooper, J. A. The immunological synapse and the actin cytoskeleton: molecular hardware for T cell signaling. *Nature Immunol.* 1, 23–29 (2000).
3. Al-Alwan, M. M., Rowden, G., Lee, T. D. & West, K. A. The dendritic cell cytoskeleton is critical for the formation of the immunological synapse. *J. Immunol.* 166, 1452–1456 (2001).
4. Langerhans, P. Über die Nerven der menschlichen Haut. *Virchows Arch. path. Anat.* 44, 325–337 (1868).
5. Semaphorin Nomenclature Committee. Unified nomenclature for the semaphorins/collapsins. *Cell* 97, 551–552 (1999).
6. Kolodkin, A. L. et al. Neuropilin is a semaphorin III receptor. *Cell* 90, 753–762 (1997).
7. He, Z. & Tessier-Lavigne, M. Neuropilin is a receptor for the axonal chemorepellent semaphorin III. *Cell* 90, 739–751 (1997).
8. Kolodkin, A. L., Matthes, D. J. & Goodman, C. S. The semaphorin genes encode a family of transmembrane and secreted growth cone guidance molecules. *Cell* 75, 1389–1399 (1993).
9. Kolodkin, A. L. Semaphorin-mediated neuronal growth cone guidance. *Prog. Brain Res.* 117, 115–132 (1998).
10. Yu, H. H. & Kolodkin, A. L. Semaphorin signaling: a little less per-plexin. *Neuron* 22, 11–14 (1999).
11. Takahashi, T. & Strittmatter, S. M. Plexina1 autoinhibition by the plexin sema domain. *Neuron* 29, 429–439 (2001).
12. Tordjman, R. et al. Neuropilin-1 is expressed on bone marrow stromal cells: a novel interaction with hematopoietic cells? *Blood* 94, 2301–2309 (1999).
13. Soker, S., Takashima, S., Miao, H. Q., Neufeld, G. & Klagsbrun, M. Neuropilin-1 is expressed by endothelial and tumor cells as an isoform-specific receptor for vascular endothelial growth factor. *Cell* 92, 735–745 (1998).
14. Gagnon, M. L. et al. Identification of a natural soluble neuropilin-1 that binds vascular endothelial growth factor: in vivo expression and antitumor activity. *Proc. Natl Acad. Sci. USA* 97, 2573–2578 (2000).
15. Geissmann, F. et al. Transforming growth factor β1, in the presence of granulocyte/macrophage colony-stimulating factor and interleukin 4, induces differentiation of human peripheral blood monocytes into dendritic Langerhans cells. *J. Exp. Med.* 187, 961–966 (1998).
16. Krenacs, L., Tiszalvicz, L., Krenacs, T. & Boumsell, L. Immunohistochemical detection of CD1A antigen in formalin-fixed and paraffin-embedded tissue sections with monoclonal antibody O10. *J. Pathol.* 171, 99–104 (1993).
17. Leupin, O., Zaru, R., Laroche, T., Müller, S. & Valitutti, S. Exclusion of CD45 from the T-cell receptor signaling area in antigen-stimulated T lymphocytes. *Curr. Biol.* 10, 277–280 (2000).
18. Revy, P., Sospedra, M., Barbour, B. & Trautmann, A. Functional antigen-independent synapses formed between T cells and dendritic cells. *Nature Immunol.* 2, 925–931 (2001).
19. Chen, H., Chédotal, A., He, Z., Goodman, C. S. & Tessier-Lavigne, M. Neuropilin-2, a novel member of the neuropilin family, is a high affinity receptor for the semaphorins Sema E and Sema IV but not Sema III. *Neuron* 19, 547–559 (1997).
20. Chen, H., He, Z., Bagri, A. & Tessier-Lavigne, M. Semaphorin-neuropilin interactions underlying sympathetic axon responses to class III semaphorins. *Neuron* 21, 1283–1290 (1998).
21. Geijtenbeek, T. B. et al. Identification of DC-SIGN, a novel dendritic cell-specific ICAM-3 receptor that supports primary immune responses. *Cell* 100, 575–585 (2000).
22. Delemarre, F. G., Hoogeveen, P. G., De Haan-Meulman, M., Simons, P. J. & Drexhage, H. A. Homotypic cluster formation of dendritic cells, a close correlate of their state of maturation. Defects in the biobreeding diabetes-prone rat. *J. Leukoc. Biol.* 69, 373–380 (2001).
23. Song, H. et al. Conversion of neuronal growth cone responses from repulsion to attraction by cyclic nucleotides. *Science* 281, 1515–1518 (1998).
24. Castellani, V., Chédotal, A., Schachner, M., Faivre-Sarrailh, C. & Rougon, G. Analysis of the L1-deficient mouse phenotype reveals cross-talk between Sema3A and L1 signaling pathways in axonal guidance. *Neuron* 27, 237–249 (2000).
25. Khan, A. A., Bose, C., Yam, L. S., Soloski, M. J. & Rupp, F. Physiological regulation of the immunological synapse by agrin. *Science* 292, 1681–1686 (2001).
26. Wu, J. Y. et al. The neuronal repellent Slit inhibits leukocyte chemotaxis induced by chemotactic factors. *Nature* 410, 948–952 (2001).
27. Cordell, J. L. et al. Immunoenzymatic labeling of monoclonal antibodies using immune complexes of alkaline phosphatase and monoclonal anti-alkaline phosphatase (APAAP complexes). *J. Histochem. Cytochem.* 32, 219–229 (1984).
28. Tordjman, R. et al. Erythroblasts are a source of angiogenic factors. *Blood* 97, 1968–1974 (2001).

501

Corrigenda

A neuronal receptor, neuropilin-1, is essential for the initiation of the primary immune response

[illegible] Yves Lepelletier, Valérie Lemarchandel, Marc [illegible], Philippe [illegible], Olivier Hermine and Paul-Henri Roméo

Nature Immunology 3, 477–482

In the May 2002 issue of *Nature Immunology*, an [illegible] The correct version is shown below. This mistake does not affect the main message of the paper.

c

Angiogenin: an antimicrobial ribonuclease

Tomas Ganz

Nature Immunology 4, 213–214

In the March 2003 issue of *Nature Immunology*, page 213, second column, the last sentence should have read: "In this issue of *Nature Immunology*, Hooper *et al.*[1] describe angiogenin 4 (Ang4) as a previously unrecognized and abundant antimicrobial constituent of mouse Paneth cell granules."

502

MCN

Molecular and Cellular Neuroscience 18, 26–[illegible] (2001)
doi:10.1006/mcne.2001.0999, available online at http://www.idealibrary.com on IDEAL

Age-Dependent Effects of Secreted Semaphorins 3A, 3F, and 3E on Developing Hippocampal Axons: *In Vitro* Effects and Phenotype of *Semaphorin* 3A (−/−) Mice

Esther Pozas,[1] Marta Pascual,[1,2] Kim Tuyen Nguyen Ba-Charvet,[2] Patricia Guijarro,[1,2] Constantino Sotelo,[2] Alain Chédotal,[2] José A. Del Río,[1,2] and Eduardo Soriano[1,2]

[1]*Department of Cell Biology and Neuroscience Research Center (CERN), University of Barcelona, E-08028, Spain; and* [2]*INSERM U106, Bâtiment de Pédiatrie, Hôpital de la Salpêtrière, 47 Boulevard de l'Hôpital, 75013 Paris, France*

We studied the role of Semaphorins in the formation of hippocampal connections at embryonic and early postnatal stages. We show that the embryonic entorhinal cortex has a repulsive effect on embryonic hippocampal axons that disappears gradually at postnatal stages. Such chemorepulsion is blocked by Neuropilin-1 and -2 blocking antibodies. However, at perinatal stages, the inner layers of the entorhinal cortex attract CA1 axons. At these stages, Sema3A and Sema3F bind commissural and entorhinal axons. Sema3A and Sema3F repel hippocampal axons at E14-P2, but not at E13. A similar spatiotemporal pattern of chemorepulsion is observed for Sema3A on entorhinal axons, in contrast to Sema3F, which repels these axons only at postnatal ages. Sema3E also repels hippocampal axons but exclusively at E14. We show that Sema3A and Sema3F can induce the collapse of hippocampal growth cones and that membrane-bound Sema3A and Sema3F can guide hippocampal axons in the stripe assay. In *sema3A* (−/−) mice, the entorhinohippocampal projection is largely normal although single axons innervate aberrantly the stratum radiatum and the hilus. Thus, the chemorepulsion evoked by Sema3A, Sema3F, and Sema3F is dynamically regulated in the developing hippocampal formation.

INTRODUCTION

The major hippocampal afferents arise from the entorhinal cortex, the CA3/hilar region and the septum (Amaral and Witter, 1995). Developing studies have shown that these afferents invade their appropriate target regions and layers in a highly specific fashion before birth (Supèr and Soriano, 1994; Linke *et al.*, 1995; Supèr *et al.*, 1998), suggesting the existence of specific guidance mechanisms involving substrate-bound, short-range and long-range diffusible signals (Tessier-Lavigne and Goodman, 1996; Polleux *et al.*, 1998; Chédotal *et al.*, 1998; Forster *et al.*, 1998). Recent studies have shown that pioneer Cajal-Retzius cells provide signals necessary for the ingrowth of entorhinal axons in their termination zone, the stratum lacunosum moleculare, and that Reelin, an extracellular protein secreted by Cajal-Retzius cells, regulates the targeting and the elaboration of entorhinal fibers (Soriano *et al.*, 1994; Del Río *et al.*, 1997; Deller *et al.*, 1999; Borrell *et al.*, 1999a,b). In addition, different secreted Semaphorins have been shown to repel developing hippocampal axons *in vitro*, which suggests they have a function in the patterning of hippocampal connections (Chédotal *et al.*, 1998; Steup *et al.*, 1999; 2000).

Vertebrate Class 3 secreted Semaphorins (Sema3A-F) exert chemorepellent effects on developing axons in both the PNS and CNS, although some of them can also be chemoattractants (Kapfhammer and Raper, 1987a,b; Luo *et al.*, 1993; Kolodkin, 1996; Adams *et al.*, 1997; Mark *et al.*, 1997; Varela-Echevarría *et al.*, 1997; Bagnard *et al.*, 1998; Chédotal *et al.*, 1998; de Castro *et al.*, 1999; Raballo *et al.*, 1999; Semaphorin Nomenclature Committee, 1999; Steup *et al.*, 1999, 2000; Raper, 2000). It has also been suggested that class 3 Semaphorins may play a role in axon fasciculation and branching (Mark *et al.*, 1997). These effects are mediated by Neuropilin-1 and Neuropilin-2, which are high affinity receptors for class 3 Semaphorins (Chen *et al.*, 1997; Feiner *et al.*, 1997; He and Tessier-Lavigne, 1997; Kolodkin *et al.*, 1997). In addition, Plexins bind to Neuropilins and are functional co-receptors for Class 3 secreted Semaphorins (Takahashi *et al.*, 1999; Tamagnone *et al.*, 1999). Most studies on secreted Semaphorins focused on the specific developmental stages at which axons exit from the parent brain region, and indicated that these molecules play a role in the initial paths of developing axons. However, secreted Semaphorins are expressed through later developmental stages and in the adult, and they may be involved in processes such as layer-specific targeting, synaptogenesis or reactive synaptogenesis (Luo *et al.*, 1993; Giger *et al.*, 1996; 1998; Shepherd *et al.*, 1996; Pasterkamp *et al.*, 1998a,b). In fact, Sema3A has been shown to collapse adult nociceptive sensory afferents (Tanelian *et al.*, 1997; Reza *et al.*, 1999).

To understand the role of Semaphorins throughout development, we analyzed the effects of secreted Semaphorins on the hippocampal system at different stages, from the onset of axon outgrowth to the stages when the layer-specific connections were formed. In addition, we cocultured different regions of the hippocampal system in order to investigate the age-dependent action of endogenous chemorepellent signals and analyzed the implication of Neuropilin receptors. Finally, phenotypic analyses of *sema3A*-deficient mice were carried out.

To whom correspondence and reprint requests should be addressed. [illegible]

[illegible] Copyright © 2001 by Academic Press. All rights of reproduction in any form reserved. [illegible]

RESULTS

Sema3A and Sema3F Induce Growth Cone Collapse and Orient Hippocampal Axons

Previous studies have shown that Sema3A and Sema3F repel hippocampal (H) and entorhinal cortex (EC) axons in three-dimensional collagen gels at embryonic days E15–E17 (Chédotal *et al.*, 1998). To determine whether Semaphorin-induced chemorepulsion of hippocampal axons was mediated by growth cone collapse and/or reorientation of axons, we performed collapse and stripe assays. For the collapse assay, embryonic (E16) explants from the hippocampus (CA1 region) and the EC were cultured on coverslips, and then exposed to recombinant secreted Semaphorins for 30–45 min. In hippocampal and EC axons treated with control medium (from mock-transfected COS cells), growth cones exhibited large sizes and characteristic triangular shapes with lamellipodia and filopodia (Figs. 1A, 1C, 1E, and 1F). After 30–45 min of incubation with

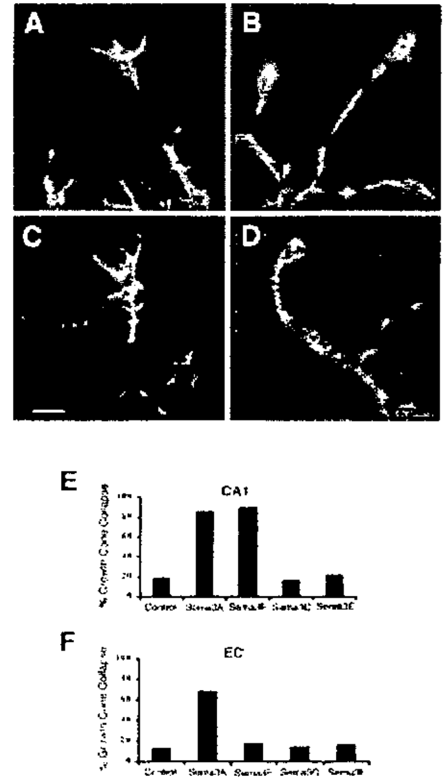

FIG. 1. Representative phalloidin rhodamine-stained neuronal processes of cultured hippocampal and entorhinal explants from E16 embryos [illegible] Semaphorin-induced growth cone collapse. Explants from the CA1 region (A, B) and from the EC are shown (C, D). Normal growth cones with lamellipodia and filopodia in hippocampal (A) and entorhinal explants (C) cultured with control medium. After incubation with Semaphorin 3F (B) and 3A (D)-containing medium, the majority of growth cones show collapsed morphologies. [illegible] percentages of collapsed growth cones after [illegible] CA1 (E) and EC (F) explants with secreted Semaphorins. Results represent the mean values of three separate experiments. Scale bar: [illegible]

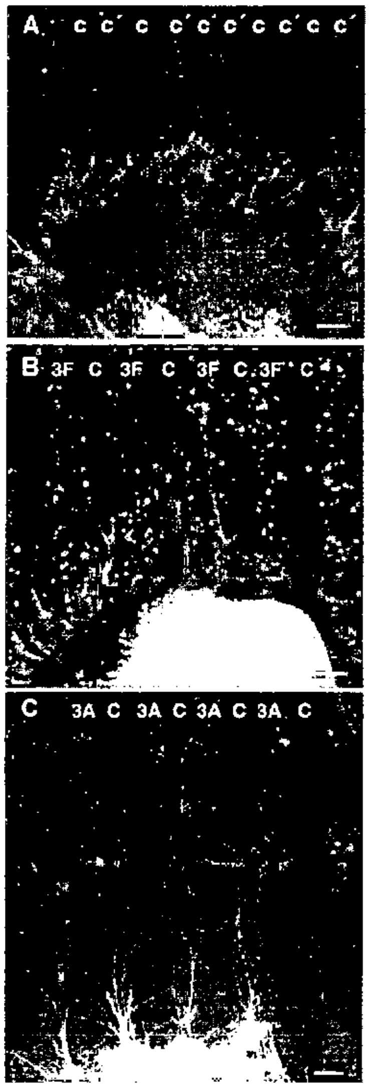

Sema3A, the majority of hippocampal and entorhinal growth cones (86 and 69%, respectively) had round-tipped or "pencil-like" shapes and lacked filopodia and lamellipodia (Figs. 1D-1I), which is characteristic of collapsed growth cones (Luo *et al.*, 1993; Goshima *et al.*, 1995; Fe and Tessier-Lavigne, 1997; Jin and Strittmatter, 1997). In contrast, Sema3F induced a selective increase in the number of collapsed growth cones in hippocampal axons (90%) but not in EC axons (Figs. 1B, 1E, and 1H), consistent with studies showing that Sema3F does not repel entorhinal fibers at E15-E17 (Chedotal *et al.*, 1998). Incubation with Sema3C and Sema3E had no effects on growth cone morphology (Figs. 1F and 1I). We conclude that secreted Sema3A and Sema3F differentially induce the collapse of hippocampal and EC growth cones.

In mammals, secreted Semaphorins have a short stretch of basic amino acids at their carboxy terminus, which is likely to limit the diffusion of Semaphorins (Cutoff and Kolodkin, 1996; Bagnard *et al.*, 1998). To further explore the hypothesis that developing hippocampal axons could be spatially reoriented by restricted presentations of membrane-bound secreted Semaphorins, we used the stripe assay. Hippocampal axons grew uniformly irrespective of the stripes when confronted with alternating lanes of membranes from mock-transfected and untransfected COS cells (Fig. 2A). In contrast, and as expected from the chemorepulsive and collapsing activities of Sema3F and Sema3A, hippocampal axons confronted with alternating lanes of membranes from COS cells expressing Sema3F or Sema3A and those from control COS cells, invariably avoided Semaphorin membranes (Figs. 2B and 2C). We conclude that membrane-bound Sema3F and Sema3A can act as a short-range cue for hippocampal axons, inhibiting their growth and reorienting it toward the Semaphorin-free stripes.

FIG. 2. Membrane stripe assay on hippocampal explants. Hippocampal axons [illegible] (B) and Sema3A (C). When confronted [illegible] control membranes [illegible] and mock-transfected membranes [illegible] grow out randomly (A). When confronted to alternating stripes of Sema3F or Sema3A expressing membranes and control membranes (B, C), they constantly avoid the Sema3F [illegible]. Cell body and axonal processes were stained with the vital dye [illegible] and [illegible]. Scale bar [illegible].

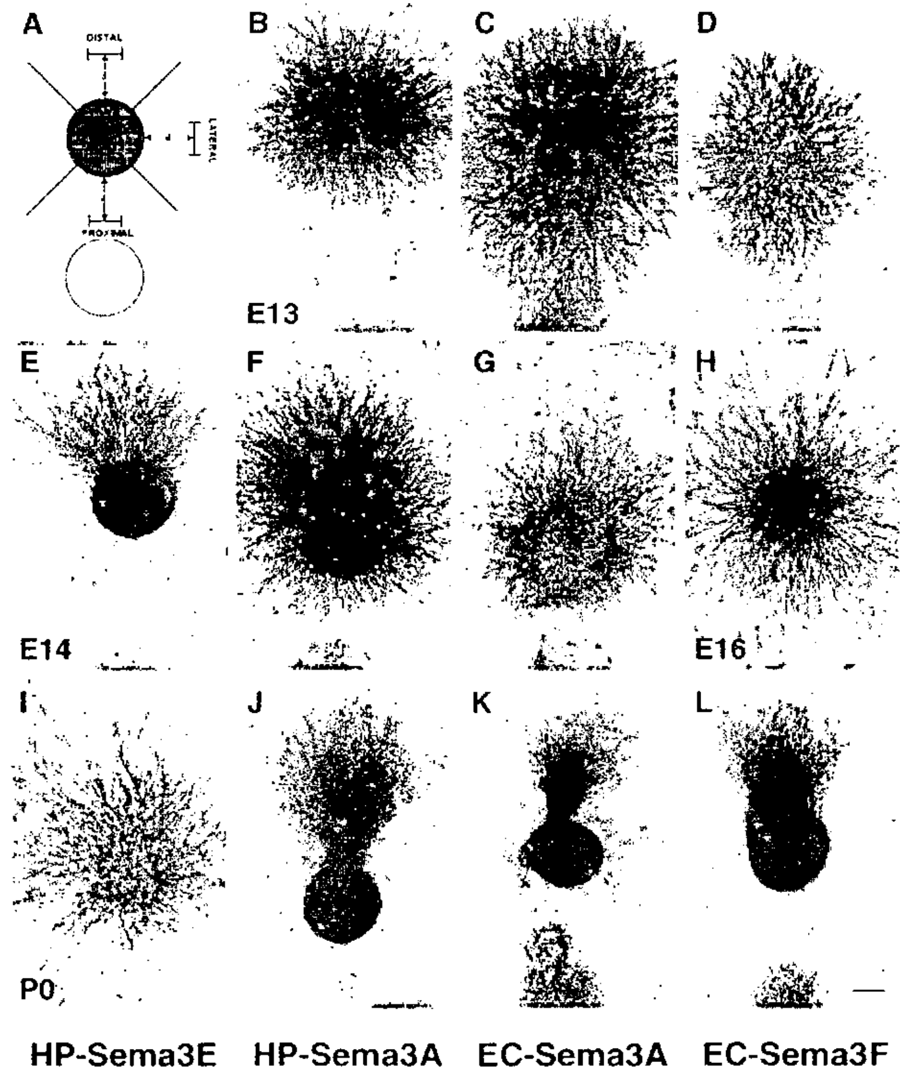

904

Age-Dependent Effects of Secreted Semaphorins in the Hippocampal Formation

In a previous study we showed that Sema3A and Sema3F repel hippocampal axons at E15–E17 (Chedotal *et al.* 1998). However, both Semaphorins and their receptors are expressed in the hippocampal area at earlier and later developmental stages, which suggests additional functions (Giger *et al.*, 1996, 1998; Chedotal *et al.*, 1998). To determine the onset of Semaphorin actions and additional functions of secreted Semaphorins, we performed a time course analysis of Semaphorin effects on explants from E13 to postnatal day 2 (P2). Explants were cocultured at a distance with aggregates of transfected COS cells in collagen gels. Axonal growth was monitored by immunostaining against the neuronal specific β-III tubulin, and the number of fibers was counted in the distal and proximal quadrants (Fig. 3A). Hippocampal and entorhinal explants cocultured with control, mock-transfected cells, exhibited radial axonal growth at any age assayed (E13–P2) (Figs. 4A–4E). Similar results were obtained when E13 explants were confronted with Semaphorin-transfected COS cells (Figs. 3B, 3C, and 4A). However, a consistent chemorepulsion was observed when hippocampal and entorhinal explants were cultured with Sema3A at E14 (Figs. 3F, 3G, and 4B), and for hippocampal explants (but not for entorhinal explants) confronted with Sema3F secreting COS cells (Fig. 4B; see also Fig. 3H). A similar, but more dramatic, chemorepulsive effect was apparent at E16 in both hippocampal and EC explants (Fig. 4C), which confirm our previous observations at E15–E17 (Chedotal *et al.* 1998). These data indicate that the onset of Sema3A and Sema3F-mediated chemorepulsion begins at E14 in the hippocampal system.

Next, we wanted to determine whether these effects lasted at early postnatal stages (P0–P2), when hippocampal afferents had already reached their target regions and layers in the hippocampus (Super and Soriano, 1994; Supèr *et al.*, 1998). The strong chemorepulsive effect of Sema3A and Sema3F on hippocampal axons was maintained at P0–P2, with a robustness similar to that at E16 (Figs. 3J, 4D, and 4E). For the EC, we divided the cortical plate into an upper (EC-u) and inner (EC-i) half, because it is known that only the upper layers II–III project to the hippocampus (Amaral and Witter, 1995). Sema3A elicited a chemorepulsive effect on both the upper and inner EC, although, particularly at P2, the effect was less dramatic than at embryonic stages (Figs. 3K, 4D, and 4E). In addition, and contrary to previous stages, both the inner and lower entorhinal cortex were strongly repelled by Sema3F at P0 (Figs. 3L and 4D). At P2, however, such Sema3F-induced chemorepulsion was only maintained for the inner EC, but not for the upper EC (Fig. 4E). The present findings show clear age-dependent effects of Sema3A and Sema3F on hippocampal axons and a striking chemorepulsive effect of Sema3F on entorhinal axons only within a narrow developmental window.

We were unable to detect any effect of Sema3C on the growth of hippocampal and entorhinal axons at any tested age (E13–P2) (Figs. 4A–4E), consistent with our previous data at E15–E17. The same holds true for Sema3E at all the developmental stages tested except for E14 (Figs. 3E and 4B). Only at this stage did we find that hippocampal, but not entorhinal axons, were repelled in the presence of Sema3E secreting COS cells (Figs. 3F and 4B). Again, these observations support the notion that secreted Semaphorins act at very strict developmental stages.

Binding Sites for Sema3A and 3F Are Dynamically Regulated During Hippocampal Development

Previous studies have shown that both *neuropilin-1* and *neuropilin-2* transcripts are highly expressed in the hippocampal formation, including the EC, from E14 to postnatal stages (Kawakami *et al.*, 1996; Chédotal *et al.*, 1998). This contrasts, for instance, with the lack of effect of Sema3F on embryonic entorhinal axons. To clarify this discrepancy, and to better understand the dynamic effects of Sema3A and Sema3F on developing hippocampal axons, we mapped *in situ* the binding sites for recombinant Sema3A and Sema3F tagged with alkaline phosphatase (AP). Brain sections from E16–E18 embryos and P0–P5 postnatal mice were incubated with Semaphorin–AP fusion proteins and developed with an AP enzymatic reaction. At E16–E18 Sema3A–AP-binding sites were observed through the fimbria and alveus, the developing white matter (Fig. 5A). In addition, staining was also present in the plexiform layers, including the stratum lacunosum moleculare (slm) (the entorhinal termination zone), the stratum oriens (so), and stratum radiatum (sr) (the commissural/associational termination zones) (Fig. 5A). A similar pattern of Sema3A binding sites, although less intense, was found at P0–P5 (not shown). This pattern of binding is consistent with the chemorepulsion exerted by Sema3A on both hippocampal and entorhinal axons.

Sema3F–AP staining at E16–E18 was evident in the developing white matter and fimbria, and in the stratum oriens and radiatum, which are the layers of termination for the commissural/associational pathway (Fig. 5B). In contrast, AP staining was undetectable in the stratum lacunosum moleculare. This is consistent with the observation that Sema3F repels embryonic hippocampal axons, but not embryonic entorhinal fibers (Chédotal *et al.* 1998; present findings Fig. 1). However, sections from postnatal (P0–P5) brains showed a wide distribution of Sema3F–AP binding sites, with labeling in both fiber tracts and the different plexiform layers of the hippocampus, including the stratum lacunosum-moleculare (the entorhinal termination zone) (Fig. 5C). The data indicate that, at these stages, both commissural/associational and entorhinal axons display binding sites for Sema3F.

Hippocampal Axons Are Transiently Repelled by Diffusible Signals Released from the EC

Previous investigations have shown that the EC releases long range diffusible signals that repel E15–E17 hippocampal axons (Chedotal *et al.* 1998). These observations agree with the early patterning and trajectories of hippocampal afferents in which both CA1 and CA3 fibers grow through the fimbria towards the hippocampal midline, but do not invade the EC (Super *et al.*, 1994; Super and Soriano, 1998). To determine whether EC-derived chemorepulsive signals varies during development, we analyzed the effect of entorhinal explants on hippocampal axonal growth at distinct stages. Explants from the EC and hippocampus were cocultured in collagen gels and hippocampal axonal growth was monitored by injecting DiI (1,1'-dioctadecyl-3,3,3',3'-tetramethylindocarbocyanamine) crystals. As in our previous study (Chédotal *et al.* 1998), we found that EC explants consistently repelled the outgrowth of CA1 and CA3 axons at E16 (Figs. 6B and 7B). Such a marked chemorepulsive effect was already detected at E14 (Figs. 6A and 7A). However, EC-induced chemorepulsion was virtually absent at postnatal stages (P0–P2), when mild chemorepulsion was observed only at P0 when the CA3 region was confronted with the upper EC (Figs. 6C and 7C). In addition, we noted that the inner layers of the EC, but not the upper EC, exerted strong chemoattraction on CA1 hippocampal axons at P0–P2 (Figs. 6D, 7C, and 7D). CA1–CA3 cocultures exhibited neither chemorepulsive nor chemoattractive responses at any of the ages tested (Figs. 7B and 7D). We conclude that the EC exerts a chemorepulsive effect on developing hippocampal axons at embryonic stages, which disappears gradually at postnatal stages. Conversely, the inner layers of the entorhinal cortex attract at a distance CA1 axons only at perinatal stages, which is consistent with the fact that CA1, but not CA3 pyramidal neurons, send axon collaterals that innervate the inner layers of the EC (Amaral and Witter, 1995).

Neuropilin-1 and Neuropilin-2 Receptors Mediate EC-Induced Chemorepulsion

To test whether EC-induced chemorepulsion on hippocampal axons was mediated by Neuropilin receptors, we cocultured hippocampal and EC explants in the presence of anti-NP-1 or anti-NP-2 blocking antibodies (Chedotal *et al.* 1998; Giger *et al.*, 1998) and hippocampal axonal growth was monitored by injecting DiI. These experiments showed that at E14 and E16, EC-induced chemorepulsion of hippocampal axons was abolished in the presence of anti-NP-1, but not in the presence of anti-NP-2 or control IgGs (Figs. 8A–8C, 8E, and 8F). In contrast, at P0 both anti-NP-1 and NP-2 antibodies blocked chemorepulsion of hippocampal axons induced by the upper EC (Figs. 8D and 8G). These data support the participation of endogenous secreted Semaphorins and the specific activation of Neuropilin receptors in the EC-induced chemorepulsion of hippocampal axons.

Analysis of sema3A-Deficient Mice

Finally, we analyzed the impact of the lack of *sema3A* on the development of entorhinohippocampal connections *in vivo*. For this, DiI was injected in the EC of wild type and *sema3A* deficient mice at P0–P2. As in previous studies, entorhinohippocampal fibers were es-

FIG. 4. ... samples showing ... [illegible]

505

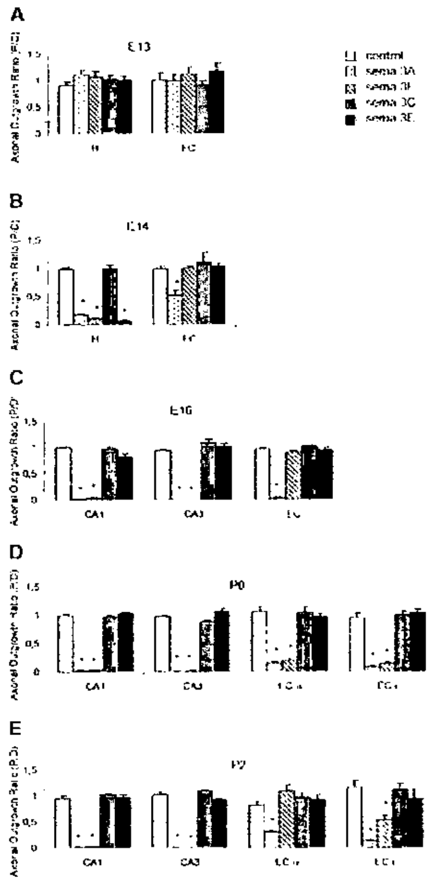

FIG. 4. Age-dependent effect of [illegible] hippocampal and entorhinal axons at E13 (A), E14 (B), E16 (C), P0 (D), and P2 (E). Histograms showing [illegible] of hippocampal and entorhinal explants [illegible] secreting different Semaphorins or with [illegible] mock-transfected cells. Ratios close to 1 represent [illegible] lower than 1 represent a chemorepulsive [illegible]. Data are means ± SEM [illegible] indicated by asterisks (P < 0.01 [illegible]).

stricted in wild-type mice to the ipsilateral stratum lacunosum-moleculare with no fibers present in the stratum radiatum and stratum oriens (Fig. 9A). At these stages, a few axons invaded the molecular layer of dentate gyrus as well. Entorhinal axons were also present in the fimbria and white matter (Fig. 9A).

In *sema3A*-deficient mice, an essentially similar pattern of termination was observed (Figs. 9B–9D). Thus, entorhinohippocampal axons terminated in the stratum lacunosum-moleculare of the ipsilateral hippocampus and fibers ran into the fimbria and the white matter. However, there were both single fibers and axonal fascicles that innervated ectopic layers, such as the stratum radiatum and the hilus (Figs. 9B–9D). Also, scattered neurons were retrogradely labeled in the hilus (Fig. 9D). We thus conclude that the lack of Sema3A does not alter essentially the basic pattern of termination of entorhinohippocampal axons *in vivo* at early postnatal stages, although it causes minor targeting errors.

DISCUSSION

A Combination of Endogenous Chemorepellent and Chemoattractive Factors Play a Role in the Development of Hippocampal Connections

During the early development of hippocampal connections, the CA1 and CA3 pyramidal neurons send axons toward the telencephalic midline (hippocampal commissure) through the fimbria. However, hippocampal axons do not invade the entorhinal area (Super and Soriano, 1994; Amaral and Witter, 1995; Super *et al.*, 1998; Borrell *et al.*, 1999a,b). In a previous study, we showed that the EC releases chemorepellent diffusible factors for the growth of hippocampal axons at E15–E17 and we proposed that such chemorepellent activity prevent hippocampal axons to invade the EC (Chedotal *et al.*, 1998). Here we show that EC-induced chemorepulsion of hippocampal axons is already present at E14, and that it disappears completely at early postnatal stages. Such an age-dependent pattern of EC-evoked chemorepulsion on hippocampal axons is consistent with the onset of developing hippocampofugal connections, which starts at E14 (Super and Soriano, 1994; Super *et al.*, 1998). Furthermore, the lack of endogenous chemorepulsive activity at early postnatal stages, when hippocampal axons have already reached their target areas, suggests that the role of long range chemorepellent factors secreted by EC may be related to the early guidance of hippocampal axon trajectories.

In addition to the repulsive action of molecules re-

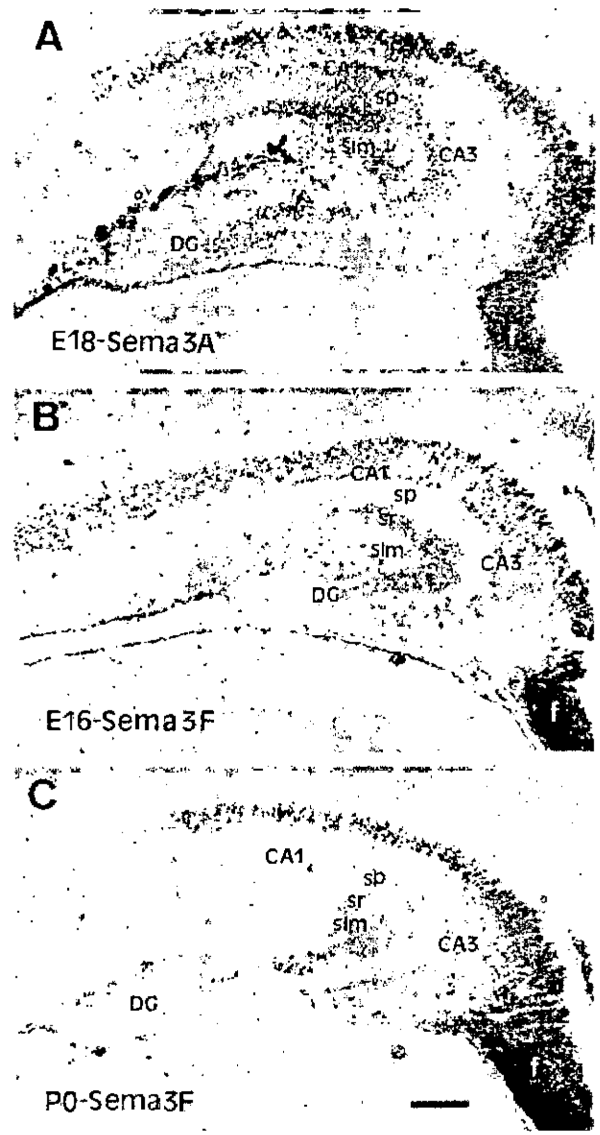

506

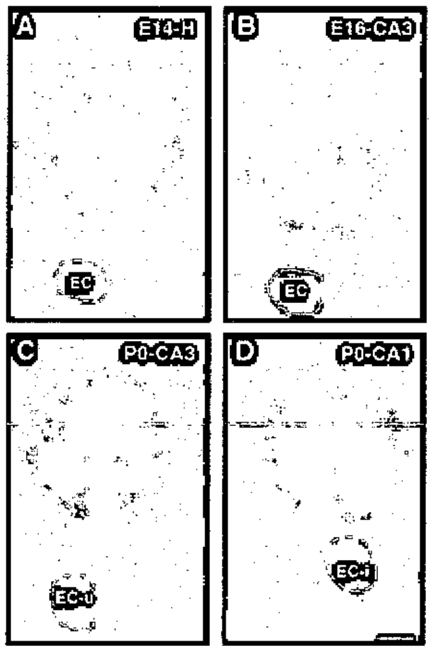

FIG. 6. Cocultures of the entorhinal cortex and the hippocampus illustrating long-range effects of the EC on developing hippocampal axons. In all panels the hippocampal explants were injected with DiI; dotted lines label the contour of EC explants. Fluorescence photomicrographs (A–D) of collagen gel cocultures are shown. A: E14, hippocampal axons were repelled by entorhinal explants. At E16, CA3 axons (B) were also repelled by EC explants. At P0 the upper layers of the EC (EC-u) weakly repelled CA3 axons (C), while the deep layers (EC-l) exerted chemoattraction on CA1 axons (D). Scale bar: 125 μm.

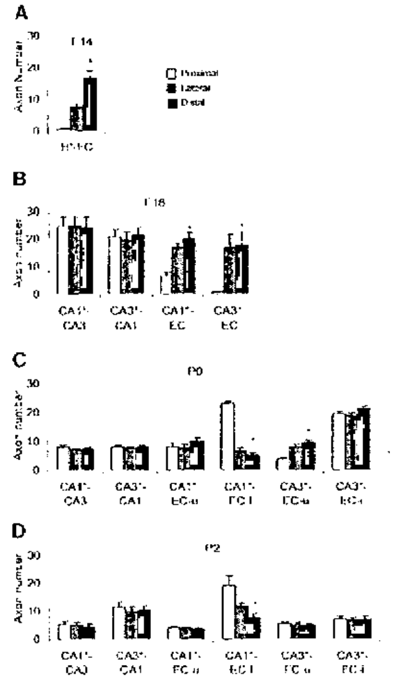

FIG. 7. Histograms showing axon numbers (per 100 μm) in the proximal (white bars), lateral (striped bars) and distal (filled bars) quadrants of hippocampal explants cocultured with the EC at different stages. Hippocampal axons (H, CA1, CA3) were strongly repelled by entorhinal explants at embryonic stages (A, B). At postnatal stages this repulsive effect decreases or disappears (CA1 and CA3 regions (C, D)). The CA1 region showed a chemoattractive effect towards the inner layers of the EC (EC-l) but not toward the upper layers of the EC (EC-u) (C, D). For statistical analysis axon numbers in the distal quadrants were compared to those in proximal quadrants. Data are means ± SEM. Significant differences are indicated by asterisks (P < 0.05; LSD test).

[illegible]ased from the EC, chemoattractive factors present in the fimbria, the septum or hippocampus itself could cooperate in directing hippocampal axons towards the

FIG. 5. Distribution of binding sites for AP-Sema3A (A) and AP-Sema3F (B, C) in [illegible] sections of the developing hippocampus at E16 (B), E18 (A) and P0 (C). At E18 AP-Sema3A binding sites were present in the developing white matter and fimbria and in the [illegible] layers of hippocampus (A). At E16 [illegible] binding sites for Sema3F labeled strongly the white matter, fimbria and stratum radiatum, but not the stratum lacunosum-moleculare (B). At P0 this pattern was maintained, but labeling was also observed in the stratum lacunosum-moleculare (C). CA1 and CA3, hippocampal regions; DG, dentate gyrus; Fimbria; [illegible] stratum lacunosum-moleculare; sp, stratum pyramidale; sr, stratum radiatum. Scale bar: 200 μm.

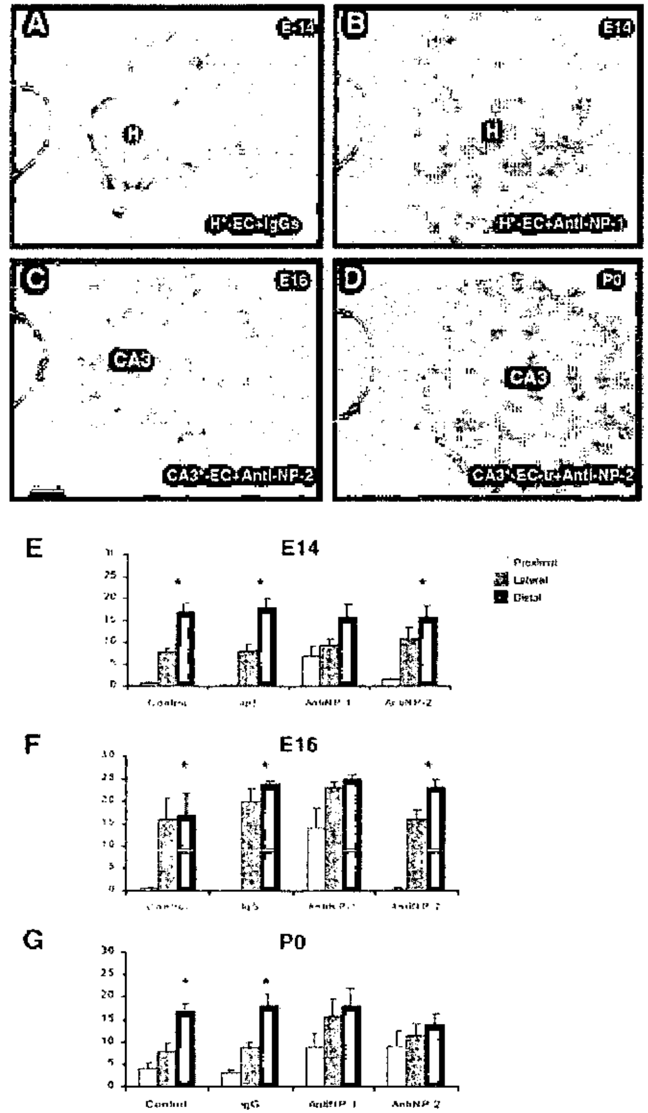

507

midline. In fact, in a recent study we showed that the fimbria exerts a chemoattractive influence on developing hippocampal axons, which is most likely mediated by Netrin-1 (Barallobre et al., 2000). We show also that only at postnatal stages did the inner EC (but not the upper EC) exerts a chemoattractive influence on CA1, but not on CA3 axons. This pattern of chemoattraction correlates with the fact that CA1, though not CA3, pyramidal neurons send axon collaterals that innervate the inner layers of the EC, but not the upper EC (Amaral and Witter, 1995; Super and Soriano, 1994). Thus, the inner EC shifts from a chemorepulsive to a chemoattractive activity on CA1 pyramidal cell axons just around birth, suggesting that this chemoattraction may be responsible for the directional growth of CA1 axon collaterals to the inner EC. Taken together, these data indicate that the activity of endogenous chemoattractive and chemorepulsive signals are dynamically regulated during hippocampal development, and that both factors combine in the early guidance of hippocampal connections.

Mechanism of Action of Sema3A and Sema3F-Induced Chemorepulsion

Consistent with studies in other brain regions (Luo et al., 1993; Goshima et al., 1995; Püschel et al., 1995; Bagnard et al., 1998), we found here that Sema3A and Sema3F induce the collapse of hippocampal growth cones at E16, and that Sema3A, but not Sema3F, induce the collapse of entorhinal axons at this age. Since such a collapsing activity correlates well with the pattern of chemorepulsion in collagen gel cocultures (see results), growth cone collapse may precede chemorepulsion and redirectioning of growing axons in vivo. In addition, the stripe assay shows that membrane bound Sema3A and Sema3F are able to guide and reorient hippocampal axons. This suggests that membrane bound secreted Semaphorins may convert a permissive substratum into a nonpermissive one, reorienting axonal trajectories, and/or inducing axonal fasciculation. Similar effects have been proposed previously for sensory and cortical axons (Messersmith et al., 1995; Püschel et al., 1995; Bagnard et al., 1998). Taken together, these results suggest that Semaphorin effects on developing hippocampal axons are caused by both long-range and local presentations, resulting in collapse and reorientation of growth cones.

Age-Dependent, Dynamic Effects of Sema3A and Sema3F on Developing Hippocampal Axons

We show that recombinant Sema3A and Sema3F, but not Sema3C, repel hippocampal axons at E14–E16. In addition, we show that Sema3A- and Sema3F-induced chemorepulsion does not occur at E13 and that it lasts for hippocampal axons at least until P2. A similar age-dependent pattern of chemorepulsion is observed with Sema3A for the EC, although in this cortical region the chemorepulsion is weaker at postnatal stages. Furthermore, the present study shows that while Sema3F does not repel embryonic EC axons, Sema3F exerts a strong chemorepulsion on entorhinal fibers at P0, which decreases markedly at P2. Finally, and unlike Steup et al. (2000), in rats, we were unable to observe Sema3C-induced chemorepulsion of hippocampal or entorhinal axons at any age tested. The reasons for this discrepancy may be related to the different species used or to a differential expression of plexins or other signaling molecules in rats and mice.

The mRNAs for class 3 secreted semaphorins, *neuropilin 1* and *neuropilin 2*, are highly expressed in the embryonic and early postnatal hippocampal region (Kawakami et al., 1996; Chédotal et al., 1998; Skaliora et al., 1998; Steup et al., 2000). In addition, NP-1 protein is present in developing entorhinohippocampal and commissural–associational axons (Kawakami et al., 1996; Steup et al., 2000). The onset of Sema3A and Sema3F chemorepulsion at E14 coincides with the emerging expression of Neuropilins (Kawakami et al., 1996; Chédotal et al., 1998; Skaliora et al., 1998; Steup et al., 2000). *Sema3F* and *sema3A* are strongly expressed in the EC and they are expressed at lower levels in the embryonic and postnatal hippocampus (Chédotal et al., 1998). This suggests that decreasing gradients of Semaphorin expression from the EC to the hippocampus may prevent hippocampal axons growing into the EC and guide hippocampofugal axons to the fimbria. Our binding analyses showing Sema3A and Sema3F binding sites in the commissural/associational projection layers (stratum oriens and stratum radiatum) agree with the Sema3A and Sema3F-induced chemorepulsion of hippocampal and entorhinal axons (Fig. 10). However, the present blocking experiments showing that EC-induced repulsion of hippocampal axons at embryonic stages (E14–E16) is only blocked by anti-NP-1, but not by anti-NP-2 antibodies, suggest that Sema3A is the endogenous factor mediating repulsion of CA3–CA1 axons at these ages. Thus, although recombinant Sema3F causes collapse and reorientation of embryonic hippocampal axons, and these axons display Sema3F binding sites, EC-derived Sema3F does not appear to contribute significantly to long-range chemorepulsion of hippocampal axons. In agreement with our stripe assay, restricted diffusion and local presentations of Sema3F may serve as a short-distance guidance cue for embryonic hippocampal axons. In line with this, the fact that Sema3F and Sema3A still chemorepel hippocampal axons at postnatal stages, long after these axons have reached their target layers, suggests the participation of these secreted Semaphorins in processes such as target layer and cell selection, and axonal branching and synaptogenesis. Since EC-induced chemorepulsion of hippocampal axons at postnatal stages is significantly reduced in the presence of NP-1 or NP-2 blocking antibodies, it is likely that both Sema3A and Sema3F contribute to this process.

For the entorhinohippocampal connection, we show that the embryonic EC is repelled only by Sema3A. In contrast, both Sema3A and Sema3F chemorepel postnatal EC axons. The spatiotemporal pattern of binding showing Sema3F binding sites in the entorhinal termination zone (the stratum lacunosum moleculare) only at postnatal ages, is consistent with the developmental pattern of Sema3F-induced chemorepulsion. Taken together with our previous study (Chédotal et al., 1998) the data indicates that Sema3A is responsible for the early guidance of entorhinohippocampal axons from the EC to the hippocampus. Since at postnatal stages EC axons have already reached the target hippocampus and termination layer (the stratum lacunosum moleculare; Super and Soriano, 1994), Sema3A- and Sema3F-induced chemorepulsion of postnatal entorhinal axons may play a role in late processes, such as target layer, cell selection, and synaptogenesis (Fig. 10).

The embryonic EC express high levels of *neuropilin-2* mRNA; whereas Sema3F does not repels nor causes growth cone collapse of embryonic entorhinal axons. Moreover, embryonic EC axons do not display Sema3F binding sites. These data suggest that *in vivo*, both the binding and the signaling of Sema3F may need additional factors or coreceptors, most likely plexins (Takahashi et al., 1999; Tamagnone et al., 1999; Rhom et al., 2000). Alternatively, posttranscriptional or posttranslational regulation of Neuropilin-2 may account for the lack of Sema3F binding and signaling in embryonic EC axons (Rossignol et al., 2000).

Sema3E Induces Chemorepulsion of Hippocampal Axons Selectively at E14

Although Sema3E is highly expressed in many CNS and PNS regions, including the forebrain, no biological effects of this Semaphorin have been described to our knowledge except on DRG axons. In DRG sensory neurons responding to NGF Sema3E induces collapse and chemorepulsion of growth cones, probably acting through NP-1 receptors (Miyazaki et al., 1999a,b). Here we consistently found that Sema3E exerts strong chemorepulsion of hippocampal axons at E14, but not at E13 nor at E16–P2. Sema3E expression in the hippocampal system, including the EC and hippocampus, starts at E14, with expression increasing with age to peak around P0 (Miyazaki et al., 1999a; E.P., unpublished observations). The function of such extremely short period of Sema3E-induced chemorepulsion is difficult to ascertain, although it is possible that it may be related to the early guidance of hippocampofugal axons. One possibility is that Sema3E produced by pyramidal neurons may act in an autocrine manner on pyramidal neurons themselves, helping their axons to exit the hippocampus. In addition, since Sema3E induces morphological differentiation of PC-12 cells apparently through receptors other than Neuropilins (Sakai et al., 1999), this Semaphorin may affect the differentiation of hippocampal cells.

The Development of Hippocampal Connections Is a Multifactorial Process Involving Different Guidance Cues

Consistent with previous studies (Catalano et al., 1998), we were unable to detect major alterations in the hippocampus of postnatal *sema3A*-deficient mice. These results, together with recent findings showing an ap-

FIG. 8. Neuropilin-1 and Neuropilin-2 receptors are involved in EC-induced chemorepulsion of hippocampal axons. Long-range effects of the EC [illegible] hippocampal [illegible] cultured at E14 (A, B), E16 (C) and P0 (D) in the presence of control IgGs (A), anti-NP-1 (B) or anti-NP-2 (C, D) antibodies. [illegible] were injected with DiI; dotted lines label the contour of EC explants. [illegible] chemorepulsion of hippocampal axons (A). In contrast, anti-NP-1 antibodies abolish repulsion of hippocampal axons at E14 (B). [illegible] block EC-induced chemorepulsion at E16 (C). NP-2 blocking antibodies abolish chemorepulsion at P0 (D). [illegible] 100 μm in the proximal and distal quadrants of hippocampal explants at [illegible] for statistical analysis [illegible] in the proximal and distal quadrants [illegible] indicated by asterisk (**P < 0.01, LSD test). Scale bar: 100 μm.

508

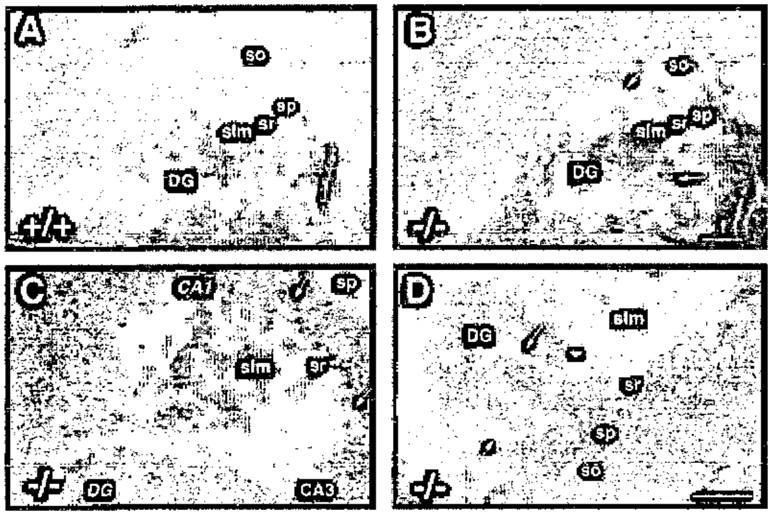

FIG. 9. Pattern of entorhino-hippocampal innervation in wild-type mouse (A) and sema3A-deficient mice (B–D). After DiI injections in the entorhinal cortex at P1–P2. In wild-type mice, entorhinal fibers are restricted to the stratum lacunosum-moleculare and the white matter (A). In sema3A-deficient mice a similar pattern of innervation was observed, but a few ectopic axons innervated the stratum radiatum in both the CA1 and CA3 regions (B, C arrows). (C) Higher magnification of the panel shown in (B) illustrating ectopic entorhinal axons (arrows) in the stratum radiatum. (D) High-magnification photomicrograph showing ectopic entorhinal axons in the hilus (arrows) and retrogradely labeled neurons in the hilus (arrowhead). Scale bar: A, B, 200 μm; C, D, 100 μm. CA1 and CA3, hippocampal regions; DG, dentate gyrus; h, hilus; slm, stratum lacunosum-moleculare; so, stratum oriens; sp, stratum pyramidale; sr, stratum radiatum.

parently normal pattern of the main hippocampal connections in neuropilin 2 (−/−) mice (Chen et al., 2000; Giger et al., 2000), suggest that the development of hippocampal connections is a multifactorial process under the control of different attractive and repulsive factors and substrate-bound molecules including Ephrins, Slits, extracellular matrix proteins, Netrins, and Semaphorins (Del Rio et al., 1997; Stein et al., 1999; Chedotal et al., 1998; Nguyen Ba-Charvet et al., 1999; Skutella et al., 1999; Barallobre et al., 2000; present results). In line with this, we observed mild layer-specific targeting errors of developing entorhinal axons in sema3A (−/−) mice, which abnormally innervate ectopic layers such as the stratum radiatum and the hilus. Since similar abnormalities have recently been described in the layer-specific targeting of commissural/associational afferents in netrin 1 (−/−) mice (Barallobre et al., 2000), the target-layer selection by developing hippocampal axons is also likely to be controlled by different signals acting at sequential developmental stages (Del Rio et al., 1997; Skutella et al., 1999; Stein et al., 1999; Super et al., 1998; Barallobre et al., 2000). The persistent expression of Semaphorins and their receptors in the adult hippocampal formation, together with the present results showing that postnatal hippocampal axons still respond to those molecules, suggest that semaphorins could play a role in the process of axonal remodeling which occur in adult brain.

EXPERIMENTAL METHODS

Animals

OF-1 mice (IFFA Credo, Lyon, France) at several embryonic (E13–E18) and postnatal (P0–P5) stages were

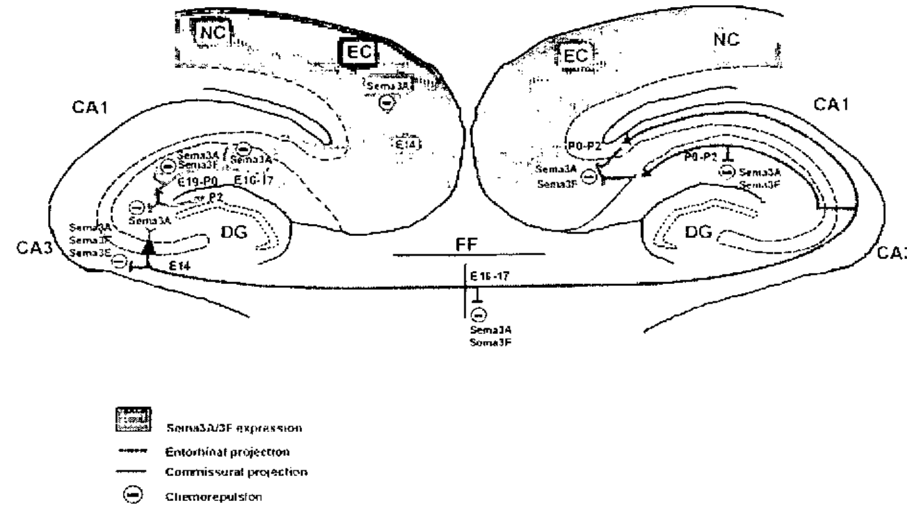

FIG. 10. Schematic diagram summarizing the main findings of the present study. At E14 entorhinal axons (EC) start to project to the ipsilateral hippocampus (orange color). At this age, a gradient of Sema3A in the neocortex (NC) chemorepels entorhinal axons. At later stages, entorhinal axons are located in the stratum lacunosum-moleculare. Sema3A chemorepels entorhinal axons at E16–18 whereas both Sema3A and Sema3F chemorepel entorhinal axons at perinatal stages (E19–P0). Finally, at postnatal stages (P2) when entorhinal fibers start to invade the dentate gyrus (DG) only Sema3A exerts chemorepulsion. Since Sema3A and Sema3F expression (violet color) are highly expressed in the NC and the EC, they may direct EC axons to the hippocampus at early embryonic stages. At later stages, moderate expression of these semaphorins in the hippocampus could restrict the target-layer termination of entorhinal axons. Commissural axons (red color) leave the hippocampus by E14 through the fimbria/fornix complex (FF). At this age, Sema3A, 3F and 3E chemorepels commissural axons. At the age when commissural fibers cross the midline towards the contralateral hippocampus (E16–E17) commissural axons retain their repulsive response to Sema3A and Sema3F. When commissural axons reach the contralateral hippocampus and invade (P0–P2) the stratum radiatum and stratum oriens, the repulsion exerted by Sema3A and Sema3F may contribute to the layer-specific termination of commissural axons. High expression of Sema3A and Sema3F in the EC may also prevent commissural axons from invading the EC, CA1 and CA3 hippocampal regions.

used for the culture experiments and binding assays. The day at which a vaginal plug was detected was considered as embryonic day 0 (E0) and the day of birth as postnatal day 0 (P0).

Stripe Assay

Cell membranes were prepared essentially as described (Nguyen Ba-Charvet et al., 1999). Briefly, transfected COS-7 cells were kept for 30 min at 4°C in a solution of 6 M urea in PBS, with 2000 KIU aprotinin, 50 μM neuraminidase inhibitor (Roche) and homogenized in a Dounce apparatus. The homogenate was centrifuged and the supernatant dialyzed overnight against PBS. The concentration of each membrane suspension was adjusted such that an aliquot, after diluting 1:15 in 2% SDS, would yield an optical density of 0.2 at 220 nm (Beckman spectrophotometer). Carpets with alternating membrane stripes on Nucleopore polycarbonate filters (Costar) were prepared according to Walter et al. (1987). Explants were stained with the vital dye fluorescein succinimidylester acetate (Molecular Probes), which labels all living cells and their processes.

Explant Cultures and Cocultures

Embryonic and postnatal brains were dissected out and sectioned at 250–350 μm using a tissue chopper.

509

Selected slices were further dissected using fine tungsten needles to extract small tissue pieces (approximately 300 μm across) from the entorhinal cortex and the CA1 and CA3 areas of the hippocampus. At postnatal ages, the EC was further halved into an upper and inner part. The marginal zone and the fimbria were taken out from the explants (see Chédotal et al., 1998; Borrell et al., 1999b). Cocultures consisted of different combinations between the entorhinal cortex and the several hippocampal subdivisions. In addition, the entorhinal cortex and the CA1 and CA3 regions were cocultured with aggregates of COS cells transfected with secreted alkaline phosphatase (AP) as a control or *human sema3A-myc* (Messersmith et al., 1995), *human sema3F AP* (Chen et al., 1997), *mouse sema3C myc* (Chen et al., 1998), or *mouse sema3E myc* (Chédotal et al., 1998) constructs. The expression of the different epitope-tagged Semaphorins was routinely assayed by Western blotting. Explants were embedded in rat tail collagen gel as previously described (Lumsden and Davies, 1986; Chédotal et al., 1998) and cultured for 72 h in Neurobasal medium supplemented with L-glutamine, $NaHCO_3$, d-glucose, and B27 supplement (all from Gibco Life Technologies). Cocultures were incubated in a 5% CO_2, 95% humidity incubator at 37°C.

Explants were then fixed with 4% paraformaldehyde in 0.1 M phosphate buffer (PB), pH 7.4. For the explant cocultures, one tissue explant in each pair was injected with a small crystal of lipophilic tracer DiI (Molecular Probes). After 4–6 days in the dark to allow the diffusion of the tracer, explants were recorded and quantified under rhodamine fluorescent optics. Explants cocultured with aggregates of transfected COS cells were processed for the immunostaining of neuronal processes with a monoclonal anti-class III β-tubulin antibody (1:2500; clone TUJ1; Babco; Moody et al., 1989), using an immunoperoxidase reaction (Chédotal et al., 1998).

For function blocking experiments, EC and hippocampal explants from E14, E16, and P0 stages were cocultured in presence of anti-NP-1 (10 μg/ml), anti-NP-2 (100 μg/ml), or control IgGs (100 μg/ml) (n = 7–12, per group). These concentrations of blocking antibodies have been previously shown to abolish the morepulsion of Semaphorins on DRG and hippocampal axons (He and Tessier-Lavigne, 1997; Chédotal et al., 1998; Gager et al., 1998).

Quantification of Fiber Growth

Analysis of the fiber growth was performed after Class III β-tubulin immunostaining or DiI tracing. The number of neurites present in 100 μm was measured in the proximal, lateral and distal quadrants (Fig. 2A) in both cases (see Chédotal et al., 1998; Borrell et al., 1999b; Bacallobre et al., 2000). For the experiments involving recombinant Semaphorins, an axonal outgrowth ratio (P/D), representing the ratio between the number of axons present in the proximal (P) and distal (D) quadrants, was used. A ratio close to 1 indicates a radial pattern of growth, and a ratio below 1 indicates chemorepulsion (Chen et al., 1998). Data were statistically analyzed using the Student's *t* test or LSD tests.

Collapse Assays

Hippocampal and entorhinal explants were placed on glass coverslips coated with Laminin (5 μg/ml) and poly-d-lysine (10 μg/ml) and were cultured as described above. After 2–3 days *in vitro*, axons emerged radially from the explants and individual fibers and their growth cones could be viewed. For the collapse assay, 5 μl of concentrated control or conditioned media containing different recombinant Semaphorins (see below) were added to the cultures for 30–45 min (Messersmith et al., 1995). Cultures were fixed with 4% paraformaldehyde, stained with phalloidin-TRICT (from Sigma), and observed by confocal microscopy. Two classes of growth cones were considered: growth cones that were large and characteristically triangular with abundant lamellipodia and filopodia, and growth cones with round tipped or pencil like forms, without lamellipodia or filopodia, which were mark as collapsed (Luo et al., 1993; Fan et al., 1993). Data were expressed as the percentage of collapsed growth cones out of the total number of growth cones, and represented the mean values from three separate experiments.

DiI Injections in Sema3A-Mutant Mice

Mutant mice were generated by replacement of the first coding exon of the *sema3A* gene with a *neo* cassette (Béhard et al., 1996). Adult heterozygous mice were mated. The genotype of the offspring was determined by PCR as described (Catalano et al., 1998). Newborn mutant mice (P0–P2) and control littermates were perfused with 4% paraformaldehyde in 0.1 M PB and used for the DiI injections. Small crystals of the lipophilic tracer DiI were placed in the EC of mutant (n = 6) and control (n = 8) littermates as described (Supèr and Soriano, 1994; Supèr et al., 1998). After several weeks in fixative, brains were cut at 80 μm, and the sections were counterstained with bisbenzimide, mounted, and photorecorded.

Binding Assay

Human sema3A AP (Messersmith et al., 1995), *human sema3F AP* (Chen et al., 1997), or control AP constructs were transfected in COS cells. After 5 days, the conditioned media were concentrated as described previously (Adams et al., 1997). Mouse brains from E16 to P5 were frozen on dry ice, sectioned on a cryostat at 20 μm and fixed in methanol at −80° for 5 min. The sections were stored at −80° until use. After rehydrating the sections in PBS, they were processed as described previously (Bagnard et al., 1998). The sections were overlaid with concentrated conditioned medium diluted in Hanks Balanced Salt Solution (HBSS) and 20% FCS for 90 min, washed and fixed in 3.7% paraformaldehyde. Endogenous phosphatase was heat inactivated at 65°C. The AP-fusion proteins were viewed through an enzymatic reaction with a solution containing 34 μM/ml of Nitro blue tetrazolium and 18 μM/ml of 5-bromo-4-chloro-3-indolylphosphate.

ACKNOWLEDGMENTS

This research was supported by grants from the Comision Interministerial de Ciencia y Tecnologia (SAF98-106), the Ramon Areces Foundation, the Fondo Europeo de Desarrollo Regional (FEDER), and the Marató TV3 to ES, the Direccion General de Ciencia y Tecnologia (PM98-0170) to J.A.D.R., the EC (BIO4-CT96-0774) to A.C., C.S., and K.P., by ARC and AFM, to A.C., and from the Fondation de France and the Institut International de Recherche en Paraplegie (Geneva, on behalf of an anonymous donation) to F.S. and K.P. [illegible] We thank Drs. [illegible] (Boston), H. Drabkin (Denver), C. K. Christensen (Copenhagen), A. L. Kolodkin (Baltimore), A. W. Püschel (Frankfurt) and M. Tessier-Lavigne (San Francisco) for providing us with different probes, expression constructs, and antibodies. We also thank Dr. [illegible] (Boston) for a generous gift of *semaphorin 3A*-deficient mice, and S. Boyrolf for editorial assistance.

REFERENCES

Adams, R. H., Lohrum, M., Klostermann, A., Betz, H., and Püschel, A. W. (1997). The chemorepulsive activity of secreted Semaphorins is regulated by furin-dependent proteolytic processing. *EMBO J.* 16: 6077–6086.

Amaral, D. G., and Witter, M. P. (1995). Hippocampal formation. In *The Rat Nervous System* (G. Paxinos, Ed.), pp. 443–493. Academic Press, San Diego.

Bagnard, D., Lohrum, M., Uziel, D., Püschel, A. W., and Bolz, J. (1998). Semaphorins act as attractive and repulsive guidance signals during the development of cortical projections. *Development* 125: 5043–5053.

Béhar, O., Golden, J. A., Mashimo, H., Schoen, F. J., and Fishman, M. C. (1996). Semaphorin III is needed for normal patterning and growth of nerves, bones and heart. *Nature* 383: 525–528.

Bacallobre, M. J., Del Rio, J. A., Alcántara, S., Borrell, V., Aguado, F., Ruiz, M., Carmona, M. A., Martín, M., Fabre, M., Yuste, R., Tessier-Lavigne, M., and Soriano, E. (2000). Aberrant development of hippocampal circuits and altered neuronal activity in netrin-1-deficient mice. *Development* 127: 4797–4810.

Borrell, V., Del Rio, J. A., Alcántara, A., Pérez, M., Martínez, A., D'Arcangelo, G., Nakajima, K., Mikoshiba, K., Derer, P., Curran, T., and Soriano, E. (1999a). Reelin regulates the development and synaptogenesis of the layer-specific entorhino-hippocampal connections. *J. Neurosci.* 19: 1345–1358.

Borrell, V., Ruiz, M., Del Rio, J. A., and Soriano, E. (1999b). Development of commissural connections in the hippocampus of reeler mice: Evidence of an inhibitory influence of Cajal-Retzius cells. *Exp. Neurol.* 156: 268–282, doi:10.1006/exnr.1999.7022.

Catalano, S., Messersmith, E. K., Goodman, C. S., Shatz, C. J., and Chédotal, A. (1998). Many major CNS axon projections develop normally in the absence of Semaphorin III. *Mol. Cell. Neurosci.* 11: 173–182, doi:10.1006/mcne.1999.0818.

Chédotal, A., Del Rio, J. A., Ruiz, M., He, Z., Borrell, V., de Castro, F., Ezan, F., Goodman, C. S., Tessier-Lavigne, M., Sotelo, C., and Soriano, E. (1998). Semaphorins III and IV repel hippocampal axons via two distinct receptors. *Development* 125: 4313–4323.

Chen, H., Bagri, A., Zupicich, J. A., Zou, Y., Stoeckli, E., Pleasure, S. J., Lowenstein, D. H., Skarnes, W. C., Chédotal, A., and Tessier-Lavigne, M. (2000). Neuropilin-2 regulates the development of selected cranial and sensory nerves and hippocampal mossy fiber projection. *Neuron* 25: 43–56.

Chen, H., Chédotal, A., He, Z., Goodman, C. S., and Tessier-Lavigne, M. (1997). Neuropilin-2, a novel member of the neuropilin family, is a high affinity receptor for the Semaphorins Sema E and Sema IV but not Sema III. *Neuron* 19: 547–559.

Chen, H., He, Z., Bagri, A., and Tessier-Lavigne, M. (1998). Semaphorin-Neuropilin interactions underlying sympathetic axon responses to class III Semaphorins. *Neuron* 21: 1283–1290.

Culotti, J. G., and Kolodkin, A. L. (1996). Functions of netrins and Semaphorins in axon guidance. *Curr. Opin. Neurobiol.* 6: [illegible]

de Castro, F., Hu, L., Drabkin, H., Sotelo, C., and Chédotal, A. (1999). Chemoattraction and chemorepulsion of olfactory bulb axons by different secreted Semaphorins. *J. Neurosci.* 19: 4428–4436.

Deller, T., Drakew, A., and Frotscher, M. (1999). Different primary target cells are important for fiber lamination in the fascia dentata: A lesson from reeler mutant mice. *Exp. Neurol.* 156: 239–253, doi:10.1006/exnr.1999.7020.

Del Rio, J. A., Heimrich, B., Borrell, V., Förster, E., Drakew, A., Alcántara, S., Nakajima, K., Miyata, T., Ogawa, M., Mikoshiba, K., Derer, P., Frotscher, M., and Soriano, E. (1997). A role for Cajal-Retzius cells and reelin in the development of hippocampal connections. *Nature* 385: 70–74.

Fan, J., Mansfield, S. G., Redmond, T., Gordon-Weeks, P. R., and Raper, J. A. (1993). The organization of F-actin and microtubules in growth cones exposed to a brain-derived collapsing factor. *J. Cell Biol.* 121: 867–878.

Feiner, L., Koppel, A. M., Kobayashi, H., and Raper, J. A. (1997). Secreted chick Semaphorins bind recombinant neuropilin with similar affinities but bind different subsets of neurons in situ. *Neuron* 19: 539–545.

Förster, E., Kaltschmidt, C., Deng, J., Cremer, H., Deller, T., and Frotscher, M. (1998). Lamina-specific cell adhesion molecules (CAMs) of hippocampus. *Development* 17: 3199–3210.

Frotscher, R., and Heimrich, B. (1993). Formation of layer-specific fiber projections to the hippocampus in vitro. *Proc. Natl. Acad. Sci. USA* 90: 10400–10403.

Gager, R. J., Dupuit, E. E., Coleman, K. H., [illegible]

510

Giger, R. J., Urquhart, E. R., Gillespie, S. K. H., Levengood, D. V., Ginty, D. D. and Kolodkin, A. L. (1998). Neuropilin-2 is a receptor for Semaphorin IV: Insight into the structural basis of receptor function and specificity. *Neuron* 21: 1079–1092.

Giger, R. J., Cloutier, J. F., Sahay, A., Prinjha, R. K., Levengood, D. V., Moore, S. E., Pickering, S., Simmons, D., Rastan, S., Walsh, F. S., Kolodkin, A. L., Ginty, D. D. and Geppert, M. (2000). Neuropilin-2 is required in vivo for selective axon guidance responses to secreted semaphorins. *Neuron* 25: 29–41.

Giger, R. J., Pasterkamp, R. J., Heijnen, S., Holtmaat, A. J. and Verhaagen, J. (1998). Anatomical distribution of the chemorepellent semaphorin III/collapsin-1 in the adult rat and human brain: Predominant expression in structures of the olfactory-hippocampal pathway and the motor system. *J. Neurosci. Res.* 52: 27–42.

Giger, R. J., Wolfer, D. P., De Wit, G. M. J. and Verhaagen, J. (1996). Anatomy of rat semaphorin III/collapsin-1 mRNA expression and relationship to developing nerve tracts during neuroembryogenesis. *J. Comp. Neurol.* 375: 378–392.

Goshima, Y., Nakamura, F., Strittmatter, P. and Strittmatter, S. M. (1995). Collapsin-induced growth cone collapse mediated by an intracellular protein related to UNC-33. *Nature* 376: 509–514.

He, Z. and Tessier-Lavigne, M. (1997). Neuropilin is a receptor for the axonal chemorepellent Semaphorin III. *Cell* 90: 739–751.

Jin, Z. and Strittmatter, S. M. (1997). Rac1 mediates collapsin-1-induced growth cone collapse. *J. Neurosci.* 17: 6256–6263.

Kapfhammer, J. P. and Raper, J. A. (1987a). Collapse of growth cone structure on contact with specific neurites in culture. *J. Neurosci.* 7: 201–212.

Kapfhammer, J. P. and Raper, J. A. (1987b). Interactions between growth cones and neurites growing from different neural tissues in culture. *J. Neurosci.* 7: 1595–1600.

Kawakami, A., Kitsukawa, T., Takagi, S. and Fujisawa, H. (1996). Developmentally regulated expression of a cell surface protein, neuropilin, in the mouse nervous system. *J. Neurobiol.* 29: 1–17.

Kolodkin, A. L. (1996). Growth cones and the cues that repel them. *Trends Neurosci.* 19: 507–513.

Kolodkin, A. L., Levengood, D. V., Rowe, E. G., Tai, Y. T., Giger, R. J. and Ginty, D. D. (1997). Neuropilin is a Semaphorin III receptor. *Cell* 90: 753–762.

Li, D., Field, P. M., Yoshioka, N. and Raisman, G. (1994). Axons regenerate with correct specificity in horizontal slice cultures of the postnatal rat entorhino-hippocampal system. *Eur. J. Neurosci.* 6: 1026–1037.

Luo, Y., Raible, D. and Raper, J. A. (1993). Collapsin: A protein in brain that induces the collapse and paralysis of neuronal growth cones. *Cell* 75: 217–227.

Linke, R., Pabst, T. and Frotscher, M. (1995). Development of the hippocampo-septal projection in the rat. *J. Comp. Neurol.* 351: 602–616.

Lumsden, A. G. S. and Davies, A. M. (1986). Chemotropic effect of specific target epithelium in the developing mammalian nervous system. *Nature* 323: 538–539.

Mark, M. D., Lohrum, M. and Püschel, A. W. (1997). Patterning neuronal connections by chemorepulsion: The Semaphorins. *Cell Tissue Res.* 290: 299–306.

Messersmith, E. K., Leonardo, E. D., Shatz, C. J., Tessier-Lavigne, M., Goodman, C. S. and Kolodkin, A. L. (1995). Semaphorin III can function as a selective chemorepellent to pattern sensory projections in the spinal cord. *Neuron* 14: 949–959.

Miyazaki, N., Furuyama, T., Amasaki, M., Sugimoto, H., Sakai, T., Takeda, N., Kubo, T. and Inagaki, S. (1999a). Mouse Semaphorin H inhibits neurite outgrowth from sensory neurons. *Neurosci. Res.* 33: 269–274.

Miyazaki, N., Furuyama, T., Sakai, T., Fujioka, S., Mori, T., Ohoka, Y., Takeda, N., Kubo, T. and Inagaki, S. (1999b). Developmental localization of Semaphorin H messenger RNA acting as a collapsing factor on sensory axons in the mouse brain. *Neuroscience* 93: 401–408.

Moody, S. A., Quigg, M. S. and Frankfurter, A. (1989). Development of the peripheral trigeminal system in the chick revealed by an isotype-specific anti-beta-tubulin monoclonal antibody. *J. Comp. Neurol.* 316: 97–118.

Nguyen Ba-Charvet, K. T., Brose, K., Marillat, V., Kidd, T., Goodman, C. S., Tessier-Lavigne, M., Sotelo, C. and Chédotal, A. (1999). Slit2-mediated chemorepulsion and collapse of developing forebrain axons. *Neuron* 22: 463–473.

Pasterkamp, R. J., Giger, R. J. and Verhaagen, J. (1998). Regulation of Semaphorin III/Collapsin-1 gene expression during peripheral nerve regeneration. *Exp. Neurol.* 153: 313–327.

Pasterkamp, R. J., De Winter, F., Holtmaat, A. J. and Verhaagen, J. (1998). Evidence for a role of the chemorepellent Semaphorin III and its receptor Neuropilin-1 in the regeneration of primary olfactory axons. *J. Neurosci.* 18: 9962–9976.

Polleux, F., Giger, R. J., Ginty, D. D., Kolodkin, A. L. and Ghosh, A. (1998). Patterning of cortical efferent projections by semaphorin-neuropilin interactions. *Science* 282: 1904–1906.

Püschel, A. W., Adams, R. H. and Betz, H. (1995). Murine Semaphorin D/Collapsin is a member of a diverse gene family and creates domains inhibitory for axonal extension. *Neuron* 14: 941–948.

Raible, S. A., Ladowski, J. M., Kuik, B., Luo, Y., Raper, J. A. and Baird, D. H. (1999). Collapsin-1/Semaphorin III/D is regulated developmentally in Purkinje cells and collapses pontocerebellar mossy fiber neuronal growth cones. *J. Neurosci.* 19: 4437–4448.

Raper, J. A. (2000). Semaphorins and their receptors in vertebrates and invertebrates. *Curr. Opin. Neurobiol.* 10: 88–94.

Reza, J. N., Gavazzi, I. and Cohen, J. (1999). Neuropilin-1 is expressed on adult mammalian dorsal root ganglion neurons and mediates semaphorin3a/collapsin-1-induced growth cone collapse by small diameter sensory afferents. *Mol. Cell. Neurosci.* 14: 317–326. doi:10.1006/mcne.1999.0786.

Rohm, B., Ottemeyer, A., Lohrum, M. and Püschel, A. W. (2000). Plexin/neuropilin complexes mediate repulsion by the axonal guidance signal semaphorin 3A. *Mech. Dev.* 93: 95–104.

Rossignol, M., Gagnon, M. L. and Klagsbrun, M. (2000). Genomic organization of human neuropilin-1 and neuropilin-2 genes: Identification and distribution of splice variants and soluble isoforms. *Genomics* 70: 211–222. doi:10.1006/geno.2000.6381.

Sakai, T., Furuyama, T., Ohoka, Y., Miyazaki, N., Fujioka, S., Sugimoto, H., Amasaki, M., Hattori, S., Matsuya, T. and Inagaki, S. (1999). Mouse Semaphorin H induces PC12 cell neurite outgrowth activating Ras-mitogen-activated protein kinase signaling pathway via Ca(2+) influx. *J. Biol. Chem.* 274: 29666–29671.

Semaphorin Nomenclature Committee (1999). Unified nomenclature for the semaphorins/collapsins. *Cell* 97: 551–552.

Shepherd, I. T., Luo, Y., Raper, J. A. and Chang, S. (1996). The distribution of collapsin-1 mRNA in the developing chicken nervous system. *Dev. Biol.* 173: 185–199. doi:10.1006/dbio.1996.0016.

Skaliora, I., Singer, W., Betz, H. and Püschel, A. W. (1998). Differential patterns of semaphorin expression in the developing rat brain. *Eur. J. Neurosci.* 10: 1215–1229.

Skutella, T., Savaskan, N. E., Ninnemann, O. and Nitsch, R. (1999). Target- and maturation-specific membrane-associated molecules determine the ingrowth of entorhinal fibers into the hippocampus. *Dev. Biol.* 211: 277–292. doi:10.1006/dbio.1999.9295.

Soriano, E., Del Río, J. A., Martínez, A. and Supèr, H. (1994). Organization of the embryonic and early postnatal murine hippocampus. I. Immunocytochemical characterization of neuronal populations in the subplate and marginal zone. *J. Comp. Neurol.* 342: 571–595.

Stein, E., Savaskan, N. E., Ninnemann, O., Nitsch, R., Zhou, R. and Skutella, T. (1999). A role for the Eph ligand ephrin-A3 in entorhino-hippocampal axon targeting. *J. Neurosci.* 19: 8885–8893.

Steup, A., Lohrum, M., Hamscho, N., Savaskan, N. E., Ninnemann, O., Nitsch, R., Fujisawa, H., Püschel, A. W. and Skutella, T. (2000). Sema3C and netrin-1 differentially affect axon growth in the hippocampal formation. *Mol. Cell. Neurosci.* 15: 141–155. doi:10.1006/mcne.1999.0818.

Steup, A., Ninnemann, O., Savaskan, N. E., Nitsch, R., Püschel, A. W. and Skutella, T. (1999). Semaphorin D acts as a repulsive factor for entorhinal and hippocampal neurons. *Eur. J. Neurosci.* 11: 729–734.

Stoppini, L., Buchs, P. A. and Muller, D. (1991). A simple method for organotypic cultures of nervous tissue. *J. Neurosci. Methods* 37: 173–182.

Supèr, H., Martínez, A., Del Río, J. A. and Soriano, E. (1998). Involvement of distinct pioneer neurons in the formation of layer-specific connections in the hippocampus. *J. Neurosci.* 18: 4616–4626.

Supèr, H. and Soriano, E. (1994). The organization of the embryonic and early postnatal murine hippocampus. II. Development of entorhinal, commissural, and septal connections studied with the lipophilic tracer DiI. *J. Comp. Neurol.* 344: 101–120.

Takahashi, T., Fournier, A., Nakamura, F., Wang, L. H., Murakami, Y., Kalb, R. G., Fujisawa, H. and Strittmatter, S. M. (1999). Plexin-neuropilin-1 complexes form functional Semaphorin-3A receptors. *Cell* 99: 59–69.

Tamagnone, L., Artigiani, S., Chen, H., He, Z., Ming, G. L., Song, H., Chedotal, A., Winberg, M. L., Goodman, C. S., Poo, M., Tessier-Lavigne, M. and Comoglio, P. M. (1999). Plexins are a large family of receptors for transmembrane, secreted, and GPI-anchored Semaphorins in vertebrates. *Cell* 99: 71–80.

Tanelian, D. L., Barry, M. A., Johnston, S. A., Le, T. and Smith, G. M. (1997). Semaphorin III can repel and inhibit adult sensory afferents in vivo. *Nature Med.* 3: 1398–1401.

Tessier-Lavigne, M. and Goodman, C. S. (1996). The molecular biology of axon guidance. *Science* 274: 1123–1133.

Varela-Echavarría, A., Tucker, A., Püschel, A. W. and Guthrie, S. (1997). Motor axon subpopulations respond differentially to the chemorepellents Netrin-1 and Semaphorin D. *Neuron* 18: 193–207.

Walter, J., Kern-Veits, B., Huf, J., Stolze, B. and Bonhoeffer, F. (1987). Recognition of position-specific properties of tectal cell membranes by retinal axons in vitro. *Development* 101: 685–696.

Received September 2, 2000
Revised April 17, 2001
Accepted April 17, 2001

511

Neoplasia • Vol. 5, No. 1, January 2003, pp. 83–92
www.neoplasia.com

Semaphorin SEMA3F and VEGF Have Opposing Effects on Cell Attachment and Spreading

Patrick Nasarre[*], *Bruno Constantin*[†], *Lydie Rouhaud*[*,‡], *Thomas Harnois*[†], *Guy Raymond*[†], *Harry A. Drabkin*[§], *Nicolas Bourmeyster*[†] *and Joëlle Roche*[*]

[*]IBMIG, EA 2224; [†]LBSC, UMR CNRS 6558, Université de Poitiers, 40 Av du Recteur Pineau, Poitiers Cédex 86022, France; [‡]Laboratoire de Génétique Cellulaire et Moléculaire, UPRES EA 2622, CHU de Poitiers, BP577, Poitiers Cédex 86021, France, [§]Division of Medical Oncology, University of Colorado Health Sciences Center, Box B171, 4200 East Ninth Avenue, Denver, CO 80262, USA

Abstract

SEMA3F, isolated from a 3p21.3 deletion, has antitumor activity in transfected cells, and protein expression correlates with tumor stage and histology. In primary tumors, SEMA3F and VEGF surface staining is inversely correlated. Coupled with SEMA3F at the leading edge of motile cells, we previously suggested that both proteins competitively regulate cell motility and adhesion. We have investigated this using the breast cancer cell line, MCF7. SEMA3F inhibited cell attachment and spreading as evidenced by loss of lamellipodia extensions, membrane ruffling, and cell–cell contacts, with cells eventually rounding-up and detaching. In contrast, VEGF had opposite effects. Although SEMA3F binds NRP2 with 10-fold greater affinity than NRP1, the effects in MCF7 were mediated by NRP1. This was determined by receptor expression and blocking of anti-NRP1 antibodies. Similar effects, but through NRP2, were observed in the C100 breast cancer cell line. Although we were unable to demonstrate changes in total GTP-bound Rac1 or RhoA, we did observe changes in the localization of Rac1-GFP using time lapse microscopy. Following SEMA3F, Rac1 moved to the base of lamellipodia and — with their collapse — to the membrane. These results support the concept that SEMA3F and VEGF have antagonistic actions affecting motility in primary tumor cell.

Neoplasia (2003) 5, 83–92

Keywords: semaphorin SEMA3F, neuropilin, VEGF, cell spreading, small GTPases.

Introduction

Semaphorins are a large family of secreted, transmembrane- and membrane-associated proteins containing a conserved, cysteine-rich 500-amino-acid Sema domain [1]. SEMA3A (Collapsin), as well as SEMA3F and other class 3 semaphorins (SEMA3B, C, D and E), are secreted proteins containing an immunoglobulin-type domain. Originally identified as repulsive molecules for nerve growth cones [2], their widespread expression suggested that they had additional functions outside the nervous system. This was confirmed by a SEMA3A knockout mouse that resulted in abnormal development of somite-derived and visceral tissues, in addition to neural abnormalities [3,4].

SEMA3F was originally isolated from a recurrent 3p21.3 homozygous deletion in small cell lung cancer cell lines, suggesting that it might be a tumor-suppressor gene [5–7]. Similarly, SEMA3B was also identified from the same 3p21.3 deletion [8]. In primary lung tumors, antibody staining against SEMA3F was shown to correlate with both tumor stage and histological subtype [8]. In a human lung cancer cell line NCI-H1299, expressing predominantly NRP1, transfection of SEMA3B and — to a lesser extent — SEMA3F inhibited *in vitro* colony formation [9]. SEMA3F also inhibited tumorigenesis of A9 cells in a nude mouse model [10]. Likewise, the tumorigenicity of HEY ovarian adenocarcinoma cells was inhibited by SEMA3B [11]. Thus, SEMA3F and SEMA3B demonstrate clear antitumor effects as judged by correlations with staging and by their effects in *in vitro* and *in vivo* model systems.

The receptors for class 3 semaphorins are two related proteins, neuropilin-1 (NRP1) and neuropilin-2 (NRP2) [12,13]. In addition, NRP1 in endothelial cells is a coreceptor for vascular endothelial growth factor $VEGF_{165}$ [14], and NRP2 binds $VEGF_{165}$ and $VEGF_{145}$ [15]. In endothelial cells, SEMA3A blocks $VEGF_{165}$-induced cell motility and lamellipodia formation [16]. In the nervous system, semaphorin signaling involves homo- and heterodimers of NRP1/NRP2, plexins, and small GTPases such as Rac1 (for reviews, see Refs. [17–21]). Other factors affecting SEMA3A signaling include collapsin response mediator protein (CRMP) [22] and the PDZ binding protein NIP [23]. In lung cancer cell lines expressing varying levels of CRMP, their invasive potential was inversely correlated with CRMP expression [24], a finding which is consistent with antitumor effects of class 3

Address all correspondence to: Prof. Joëlle Roche, IBMIG, EA 2224, Université de Poitiers, 40 Av du Recteur Pineau, Poitiers Cédex 86022, France.
E-mail: joelle.roche@univ-poitiers.fr
[‡]Present address: Institut de Biotechnologies, 123 avenue Albert Thomas, Limoges Cédex 87060, France.
Received 11 July 2002; Accepted 14 August 2002.

semaphorins. At the cellular level, COS7 cells expressing NRP1 and plexin-1 contract within 5 to 30 minutes of SEMA3A exposure [25]. Similar effects were observed with SEMA3F in COS7 cells expressing NRP2/plexin-1. Other investigators have shown that exposure to semaphorins results in rapid reorganization of actin filaments, normally present in lamellipodia and filopodia [26].

Based on the inverse staining patterns of VEGF and SEMA3F on primary lung cancer cells, SEMA3F staining at the leading edge of motile cells [8], and the reported antagonism between SEMA3A and VEGF in endothelial cells, we suggested that VEGF and SEMA3F might competitively regulate cell motility and adhesion in epithelial cancers. We have studied this in two breast cancer cell lines, MCF7 and C100, which differentially express NRP receptors. We also identified changes in Rac1 localization following exposure to SEMA3F. These results further strengthen the concept that secreted semaphorins compete with VEGF for effects on tumor cells themselves. Thus, the normal balance between VEGF and semaphorins, which is frequently and substantially disrupted in various epithelial cancers, may have important consequences on migration as it does to angiogenesis.

Materials and Methods

Plasmid Constructions

AP-SEMA3F was built by cloning SEMA3F cDNA into pSecTagA vector (Invitrogen, Cergy Pontoise, France) at the 3′ end of the alkaline phosphatase gene and was generously provided by Dr. M. Tossier-Lavigne [13]. AP-pSecTag (AP) expressed alkaline phosphatase as negative control. Rac1-GFP was a gift from Dr. Fort (CRBM, Montpellier, France).

Cell Lines and Transfections

The human mammary epithelial cell lines utilized were MCF7 and C100, a derivative of MDA-MB-435S [27]. MCF7 cells were grown in RPMI-1640 containing 10% fetal calf serum (FCS) and C100 cells were grown in 50% DMEM/50% Ham's F12 containing 10% FCS. COS7 cells were grown in DMEM plus 10% FCS. Cell lines were transfected with plasmids using Effectene (Qiagen, Courtaboeuf, France) with conditions recommended by the manufacturer. For AP-SEMA3F transfections in COS7 cells, the medium was replaced 2 days after transfection by DMEM, containing 0.5% FCS or OPTIMEM media (Invitrogen). The medium was collected 4 days after transfection and applied to MCF7 and C100 cell cultures in serum-free medium for 14 hours. SEMA3F concentration was estimated by alkaline phosphatase activity (GenHunter, Nashville, TN). Cell ruffling and spreading were measured in cells grown in OPTIMEM for 15 hours before adding AP control media, AP-SEMA3F media, or purified VEGF (Insight Biotechnology, Wembley, UK).

Quantitative RT-PCR

Total RNA and cDNA were prepared as described previously [8]. We assessed levels of *SEMA3F, NRP1, NRP2, VEGF*, and *KDR* transcription relative to *G3PDH* in lung tumors by quantitative real-time RT-PCR carried out using the GeneAmp 5700 (ABI) system with syber green chemistry as described previously [8]. The PCR cycle at which a particular sample reaches an arbitrary threshold fluorescence level (C_T) is indicative of the input quantity of that template. The PCR was carried out in 50 μl reaction volumes consisting of 1× PCR SYBR Green buffer, 0.25 μM primers, 200 μM dNTPs, and 0.03 U/μl AmpliTaq Gold (Perkin-Elmer, Wellesley, MA). cDNA was amplified as follows: 50°C for 2 minutes, 95°C for 10 minutes followed by 40 cycles at 95°C–15 seconds, 60°C–1 minute. *SEMA3F, NRP1, NRP2, VEGF, KDR*, and *FLT-1* cDNA were amplified with the following primers: SEMA3F for 5′ ACCAGACCCAGGACGTGAG 3′ and SEMA3F rev 5′ AAGACCATGCGAATATCAGCC 3′, giving a 112-bp product. $VEGF_{165}$ for 5′ CAAGACAAGAAAATCCCTGTGG 3′ and $VEGF_{165}$ rev 5′ CCTCGGCTTGTCACATCTG 3′, giving a 162-bp product; NRP2 for 5′ GGATGGCATTCCACATGTTG 3′ and NRP2 rev 5′ ACCAGGTAGTAACGCGCAGAG 3′, giving a 152-bp product; NRP1 for 5′ATCACGTGCAGCTCAAGTGG 3′ and NRP1 rev 5′ TCATGCAGTGGGCAGAGTTC 3′, giving a 167-bp product; KDR for 5′ TTCTCTTGATCTGCCCAGGC 3′ and KDR rev 5′ AGGCTCCAGTGTCATTTCCG 3′, giving a 182-bp product; FLT-1 for 5′ ATGCCACCTCCATGTTTGATG and FLT-1 rev 5′ GAGGCCTTGGGTTTGCTGTC 3′, giving a 122-bp product.

Immunostaining of Cell Lines

Immunostaining for SEMA3F was performed as described [8], except that cells were finally exposed in the dark to an Alexa488-conjugated goat antirabbit antibody for 30 minutes (1:200) (Molecular Probes, Leiden, Netherlands). Cells were mounted using Vectashield (Vector, Burlingame, CA). Immunostained samples were examined using the blue line (488 nm) of a confocal microscope. For NRP1 and NRP2 immunostaining, cell fixation was performed in 1% paraformaldehyde for 15 minutes without methanol fixation. For anti-NRP staining, we used a NRP1 rabbit polyclonal antibody (1:100) raised against amino

Table 1. Relative Expression of SEMA3F, NRP1, NRP2, VEGF, KDR, and FLT-1 for MCF7 and C100 Cells (×1000) Versus G3PDH

Cell Lines	SEMA3F	NRP1	NRP2	VEGF	KDR	FLT-1
MCF7	27	17	0.0123	9	0	0.026
C100	0.017	1.5	62.5	3	0.04	0

Quantitative real-time RT-PCR was performed. The raw data were obtained in terms of C_T values, which refer to the PCR cycle number during exponential amplification at which the product (measured in real time by SYBR green fluorescence) crosses an arbitrary threshold. To adjust for variations in the amount of RNA, the C_T values for each gene were normalized against the C_T values for the housekeeping gene, *G3PDH* (i.e., $\Delta C_T = C_{T,gene} - C_{T,G3PDH}$). While the resulting ΔC_T values are experimentally convenient, they are not readily intuitive (i.e., they reflect exponential amplification, and higher ΔC_T values represent lower expression). Instead, the results are displayed in terms of the relative expression (×1000) compared to G3PDH. Experiments were done in triplicate and all the results are within 0.5 PCR cycle.

512

acids 583 to 856 of rat NRP1 (gift from Dr. A. L. Kolodkin, Baltimore) [12] and an NRP2 rabbit polyclonal antibody (1:50) raised against amino acids 560 to 858 of human NRP2 (Santa Cruz Biotechnology, Santa Cruz, CA). Cells were exposed in the dark to a second RHX-conjugated goat anti-rabbit antibody diluted at 1:200 (Jackson Immunoresearch Laboratories, West Grove, PA). Immunostained samples were examined using the yellow line (568 nm) of the confocal microscope. NRP1 and NRP2 blocking experiments were performed with a 2-hour preincubation with 10 μg/ml anti-NRP2 polyclonal antibody (Santa Cruz Biotechnology) or/and 10 μg/ml anti-NRP1 polyclonal antibody (Oncogene, Darmstadt, Germany) as described [28].

Confocal Microscopy and Data Analysis

Labelled cells and those observed by transmission light were examined by confocal scanning microscopy using a BioRad MRC 1024 ES (BioRad, Hemel Hempstead, UK)

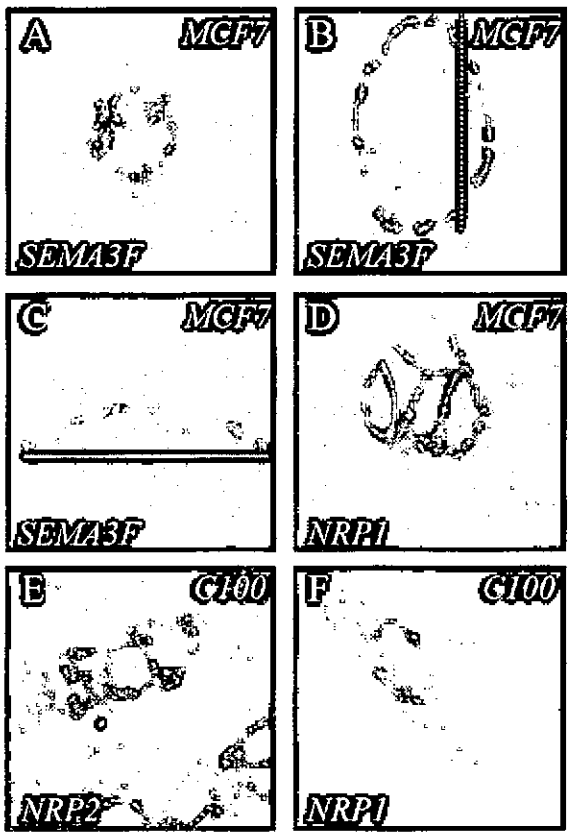

Figure 1. Immunostaining of endogenous SEMA3F and neuropilins in MCF7 and C100 cells. (A–C) MCF7 cells stained for SEMA3F with a polyclonal antibody and observed by laser scanning confocal microscopy (LSCM). (A, B) Horizontal optical sections through the surface (A) and the central part (B) of the cell islet. (C) Vertical optical section through the same cell islet obtained along the dotted line shown in (B). The plan view line represents the patch surface. (D) Horizontal optical section obtained by LSCM on MCF7 cells labelled for NRP1 with a polyclonal antibody. (E, F) C100 cells stained for NRP2 (E) and NRP1 (F) with a specific polyclonal antibody and observed by means of LSCM.

equipped with a 15-mW argon–krypton (Ar–Kr) gas laser. The confocal unit was connected to an inverted microscope (Olympus IX70; Olympus, Tokyo, Japan). Maximal resolution was obtained with Olympus plan apo ×60 water, 1.3 numerical aperture objective lens ($x-y$: 0.3 μm; z: 0.45 μm). RHX fluorochromes were excited with the 568-nm yellow line and the emission of fluorescence was collected through a photomultiplier (PMT1) through a 605-nm band pass filter. The Alexa488 fluorochrome was excited with the 488-nm blue line and the emission of fluorescence was collected through a photomultiplier (PMT2) through a 522-nm band pass filter. Fluorescence signal collection, image construction, and scaling were performed through the control software (Lasersharp 3.2; BioRad). Images and data analysis were performed through the software Lasersharp Processing (BioRad) and Origin 5.0 (Microcal Software, Northampton, MA), respectively. Results were expressed as mean ± SEM. Statistical significance between the different mean values was tested using Student's *t*-test.

GST Pull-Down Assays

The GST-PAK-CRIB domain and GST-Rhotekin-RBD were cloned into pGEX-2T fusion (gift of J. G. Collard, Netherlands Cancer Institute, Amsterdam, The Netherlands) [29]. The GST-PAK-CRIB and GST-Rhotekin-RBD recombinant peptides were prepared in *Escherichia coli* (BL21 strain) and purified using glutathione–sepharose beads (Amersham Pharmacia Biotech, Bucks, UK).

A total of $5 \cdot 10^6$ C100 and MCF7 cells were washed twice in cold PBS and then lysed in 400 μl of lysis buffer [50 mM Tris–HCl, pH 7.4, 150 mM NaCl, 5 mM $MgCl_2$, 0.05% NP-40 (vol/vol), 1% DOC (wt/vol), 1% Triton X-100, 0.1% SDS, 1.25 mM PMSF, 20 μM leupeptin, 0.8 μM aprotinin, 10 μM pepstatin]. Total amount of protein in each lysate was measured and diluted to 1 μg/μl. Lysates were repeatedly passed through a syringe followed by centrifugation at 14,000*g* for 1 minute. The supernatant was mixed with 10 to 20 μl of glutathione–sepharose beads corresponding to ~40 μg of GST fusion protein and incubated at 4°C overnight. Bead-bound complexes were washed once in lysis buffer and three times in the same buffer without DOC, Triton X-100, and SDS. Samples were boiled in Laemmli sample buffer and fractionated by a 12% SDS-PAGE electrophoresis, followed by Western blotting. The presence of RhoA was revealed using a polyclonal anti-RhoA antibody (Santa Cruz Biotechnology). The presence of Rac1 was revealed using a monoclonal anti-Rac1 antibody (Transduction Laboratories, Lexington, KY). As second antibodies, a sheep antimouse IgG, HRP-linked (Amersham Pharmacia Biotech); or a donkey antirabbit IgG, HRP-linked (Amersham Pharmacia Biotech) were used and blots were revealed by ECL detection.

Time Lapse Microscopy

C100 cells were transfected with Rac1-GFP. The medium was replaced 2 days after transfection by medium without FCS for 14 hours. Time lapse microscopy was started after AP-SEMA3F or AP media addition and recorded every 30 seconds for 30 minutes. The GFP was excited with the 488-nm blue line and the emission of fluorescence was collected through a 522-nm band pass filter.

Results

Expression of SEMA3F, Neuropilins, VEGF, KDR, and FLT-1 in MCF7 and C100 Adenocarcinoma Cell Lines

The effects of SEMA3F were investigated in two breast cancer cell lines, which exhibited different biologic phenotypes. MCF7 cells, which grow in islets and exhibit numerous intercellular contacts, provide a model of low metastatic potential. In contrast, C100 cells are highly motile and metastatic. Quantitative RT-PCR demonstrated that MCF7 cells express SEMA3F and NRP1 (Table 1), but barely

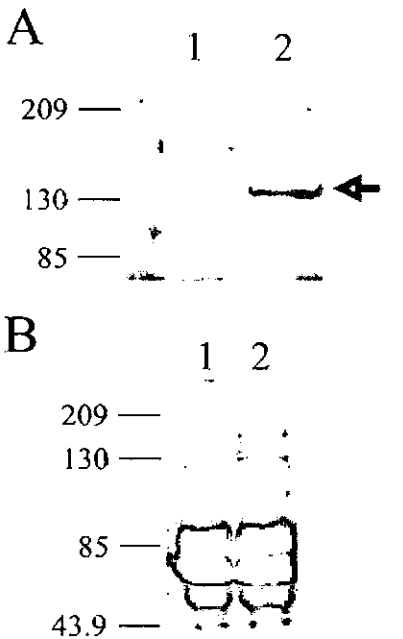

Figure 2. Western blot analysis of AP-SEMA3F expression. Media from transfected AP (−) or AP-SEMA3F (+) COS7 cells were concentrated on Microcon 10 (Amicon, Guyancourt, France) and subjected to SDS-polyacrylamide on a 12% polyacrylamide gel. Immunodetection was performed with a polyclonal AP antibody (1:2500) (GeneHunter) in (A) and loading controls stained by Coomassie blue are shown in (B).

undetectable NRP2. Immunostaining of MCF7 cells confirmed these results. Using a specific polyclonal antibody raised against SEMA3F [30], cytoplasmic SEMA3F was detected. By laser confocal microscopy, the major distribution of SEMA3F was in near-membrane domains of cells delineating the periphery of the islets (Figure 1, *A* and *B*). In a vertical section through the islets, SEMA3F is apically located (Figure 1*C*). Staining with anti-NRP polyclonal antibodies showed that NRP1 was localized at the plasma membrane of all cells within the islets (Figure 1*D*), whereas NRP2 staining was negative (not shown), consistent with the RT-PCR results. The membranous pattern of staining in MCF7 islets for SEMA3F was reminiscent of that obtained in normal bronchial epithelial cells *in situ*, as well as in cultured adenocarcinoma Calu-3 cells [8].

In contrast, the C100 cells contain very low levels of SEMA3F transcripts, about 1600 times less than MCF7 (Table 1), and immunostaining with the polyclonal antibody was negative (not shown). Quantitative RT-PCR showed that C100 cells had high levels of NRP2 receptor mRNA, and immunostaining against NRP2 showed a cytoplasmic vesicular pattern together with a significant distribution of NRP2 at the surface membrane (Figure 1E). NRP1 was also expressed in C100, but at levels that were approximately one-third that in MCF7 (Table 1, Figure 1*F*). Both C100 and MCF7 expressed moderate levels of VEGF (compared to various other cell lines not shown) and low to absent levels of the VEGF receptor, KDR. In addition, FLT-1 was barely detectable in MCF7 and absent in C100 cells.

Rapid Effects of Extracellular SEMA3F on Cell Morphology

Previous studies have shown that class 3 semaphorins have a repulsive effect on developing axons and in COS7 cells transfected with neuropilins and plexins [25]. To explore the effects of SEMA3F in MCF7 and C100 cells, we transfected COS7 cells with alkaline phosphatase–tagged SEMA3F (AP-SEMA3F), and the cultured supernatant was used as a source of SEMA3F. As a negative control, COS7 cells were transfected with the AP vector only. This approach was first described by two groups [12,31], and further widely used by others because bacterial or Baculovirus-produced semaphorins are insoluble, presumably due to their highly disulfide-linked nature. Secretion of AP-SEMA3F was confirmed by Western blot (Figure 2) and

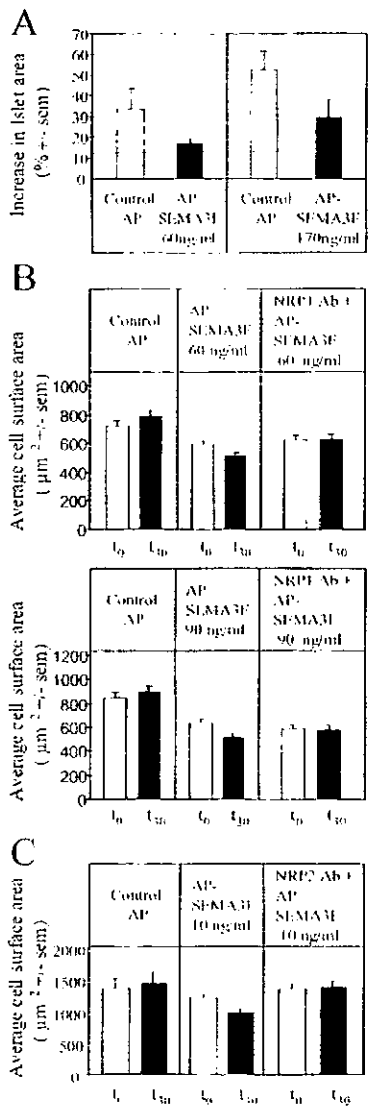

Figure 3. *AP-SEMA3F reduces the islets of MCF7 cell islets and C100 cells to variant. (A) Total MCF7 islets areas were measured before and after 60 minutes of treatment at 37°C with COS7 cells culture media containing 0.5% FCS and secreted AP (white columns, control) or AP-SEMA3F (black columns), at two different concentrations (60 and 170 ng/ml). A volume of AP media equivalent to that of AP-SEMA3F media is added for the control. The percentage of increase in islet areas was calculated and reported on bar graph. Error bars, SEM. (B) Changes in cell surface area when MCF7 cells are cultured for 15 minutes with control AP or AP-SEMA3F, 60 and 90 ng/ml, with and without a blocking anti-NRP1 antibody. (C) Mean C100 cells areas were calculated before (white columns) and after treatment for 30 minutes (black columns) with COS7 cells media containing 0.5% FCS and control AP (left panel) or AP-SEMA3F at 10 ng/ml (middle panel). AP-SEMA3F was added in the presence of an anti-NRP2 antibody (right panel). Error bars, SEM.*

the enzymatic alkaline phosphatase activity was used to determine the amount of SEMA3F protein applied to cells.

After a 60-minute incubation with control AP medium, MCF7 cells were observed to spread and form membrane ruffles and lamellipodia, which resulted in an increase in the average surface area of cell islets and individual cells (Figure 3, *A* and *B*). This cell spreading was significantly inhibited after incubation with 60, 90, and 170 ng/ml AP-SEMA3F (Figure 3, *A* and *B*). The ruffling activity of MCF7 cells was recorded by microcinematography (Figure 4*A*). The number of ruffles was increased over a 45-minute period by the AP control medium, suggesting that COS7 cells secrete one or more factors that positively affect membrane ruffling. Alternatively, the effect of the AP control medium could be due to the 0.5% serum from the transfected COS cells because the MCF7 cells were placed in serum-free medium before treatment (Figure 4*B*). This background effect was also dose-dependent (Figure 3*A*). Nevertheless, membrane ruffling was strongly inhibited by AP-SEMA3F (Figure 4*B*). When 100 ng/ml VEGF was added to control AP medium, the ruffling activity was promoted (Figure 4*C*). AP-SEMA3F at 60 ng/ml was able to block the positive effect of VEGF (Figure 4*C*). These results are consistent with competing actions of SEMA3A and VEGF on endothelial cells [16].

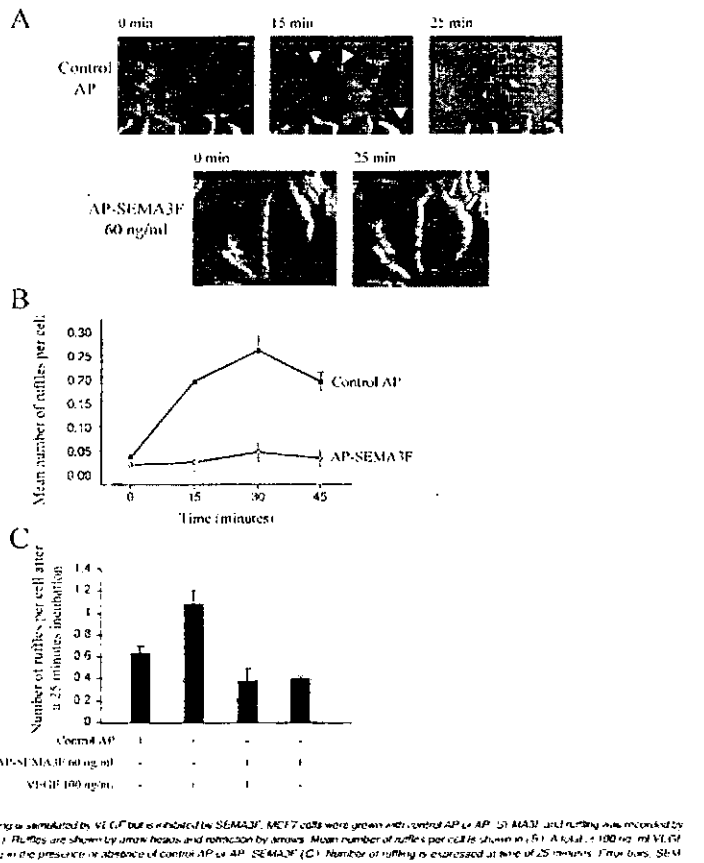

Figure 4. *MCF7 cell ruffling is stimulated by VEGF but is inhibited by SEMA3F. MCF7 cells were grown with control AP or AP-SEMA3F and ruffling was recorded by microcinematography (A). Ruffles are shown by arrow heads and retraction by arrows. Mean number of ruffles per cell is shown in (B). A total of 100 ng/ml VEGF was tested on cell ruffling in the presence or absence of control AP or AP-SEMA3F (C). Number of ruffling is expressed at time of 25 minutes. Error bars, SEM.*

5/14

Retraction of the cell body and extensions could be observed in MCF7 cells that had separated from the islet. After exposure to SEMA3F for 30 minutes, these cells rounded-up and eventually detached from adjacent cells. This resulted in an overall decrease in the number of cells within a microscope field, whereas with control COS7 supernatant, the number of cells increased from cell division.

Responses in C100 cells were more complex because of morphologic heterogeneity. These cells could be divided in three groups representing small round cells with few extensions, spindle-shaped cells with neurite-like cell processes, and extended cells with large lamellipodia. Whereas the first and second groups of cells did not appear to respond to SEMA3F, cell spreading was significantly inhibited after 30 minutes by 10 ng/ml AP-SEMA3F in the third subset of cells having an extended morphology. Thus, the average cell surface area decreased as a result of lamellipodia retraction (Figure 3C), and other cells were observed to round-up and detach from the substrate.

SEMA3F Signal Transduction

As MCF7 and C100 cells exhibited different patterns of NRP1 and NRP2 expression, we tested antibodies for their ability to block SEMA3F action. In MCF7, the SEMA3F effects on cell spreading were inhibited by anti-NRP1 antibodies (Figure 3B), whereas in C100 cells (Figure 3C), anti-NRP2 blocked SEMA3F inhibition of cell spreading and anti-NRP1 had no effect. These results are consistent with the levels of NRP1 and NRP2 expression in MCF7 and C100 cells (Table 1) and also demonstrate that NRP1 can function in SEMA3F signalling.

As neuropilin signal transduction has been shown to involve small GTPases in neural cells, we looked for changes in the amount of active GTP-bound Rac1 and RhoA using GST fusion proteins expressing either the GST-PAK-CRIB domain or GST-Rhotekin-RBD. In a pull-down experiment using extracts of C100 and MCF7 cells treated with AP-SEMA3F, we did not identify any difference in levels of GTP-bound Rac1 and RhoA (Figure 5). Also, we did not find any difference in the amount of total Rac1 and RhoA upon AP-SEMA3F treatment. As this negative result might have been due to insufficient sensitivity, we examined the subcellular distribution of Rac1 using C100 cells transfected with Rac1-GFP. Time lapse analysis by confocal laser scanning microscopy showed that Rac1 was predominant at intercellular junctions before the addition of AP-SEMA3F. Upon addition of AP-SEMA3F, Rac1 was observed first at the base of lamellipodia and subsequently at the membrane (Figure 6*A*). Isolated cells became spherical at the end of the retraction process and were decorated with Rac1 around the membrane (Figure 6*B*). These results indicate that SEMA3F induces changes in Rac1 activation, at least at a local level, and that the presence of Rac1 at the membrane is associated with the retraction.

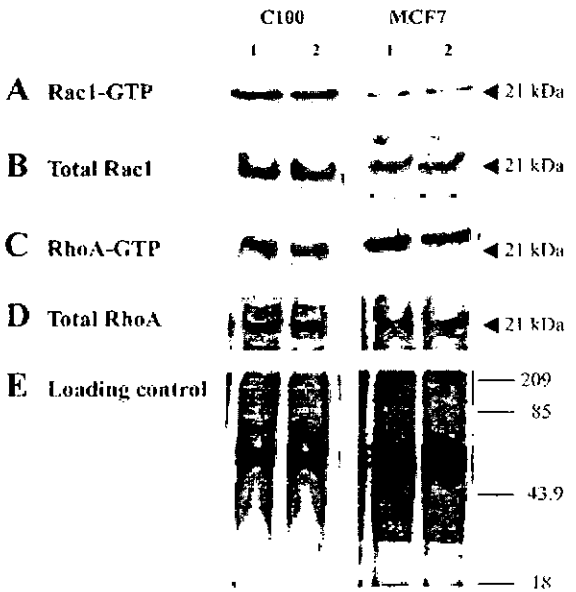

Figure 5. Levels of Rac1-GTP and RhoA-GTP were not affected by AP-SEMA3F. Levels of active Rac1-GTP (A) and RhoA-GTP (C) were estimated by GST pull-down assay in C100 and MCF7 cells after treatment with AP-1 (1) or AP-SEMA3F (2). Total amount of total Rac1 (B) and RhoA (D) was determined by Western blot after electrophoresis on a 12% SDS polyacrylamide gel, and a loading control is shown in (E).

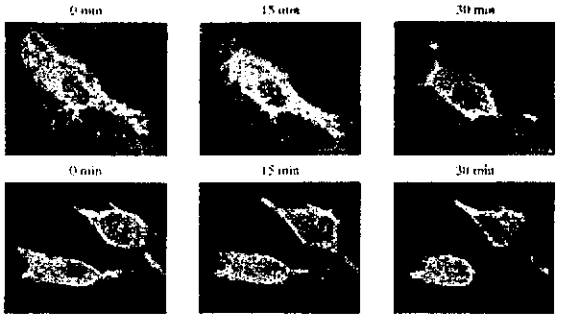

Figure 6. Rac1 moved to the base of lamellipodia and later to the membrane upon AP-SEMA3F treatment. Time lapse analysis by confocal laser scanning microscopy showed Rac-GFP localization in connected (A) and in isolated C100 cells (B) at time 0, 15, and 30 minutes after AP-SEMA3F addition.

Discussion

Semaphorins were initially identified on the basis of their inhibition of nerve growth cone migration; however, they clearly affect non-neural tissues. On the basis of its localization at 3p21.3, a region that undergoes frequent loss of heterozygosity in lung tumors, and because of the activity of genomic clones containing SEMA3F in suppressing tumorigenicity of mouse fibrosarcoma A9 cells [32], SEMA3F was hypothesized to be a tumor-suppressor gene. Subsequent studies demonstrated that SEMA3F protein expression was decreased or absent in high-grade lung cancers [8]. These studies also suggested, based on complementary staining patterns, that SEMA3F might compete with VEGF for binding to their common neuropilin receptors. More recent experiments using single gene transfectants have confirmed that SEMA3F has tumor-suppressor gene activity [10].

Our results demonstrate that SEMA3F and VEGF have opposing actions on primary tumor cells. Whereas VEGF promotes cell spreading and membrane ruffling, activities associated with increased cell migration and metastasis, SEMA3F inhibits these changes and is able to block the effects of VEGF. During a brief treatment with AP-SEMA3F, MCF7 cell spreading and lamellipodia extension were inhibited and membrane ruffling was reduced. Even though MCF7 cells do not express NRP2 (or express very little), they express NRP1 and responded to the cultured supernatant of AP-SEMA3F expressing COS7 cells. These effects were mediated by NRP1, as shown by the use of an anti-NRP1 antibody, which blocked the activity. In contrast, C100 cells express NRP2 at high levels, and anti-NRP2 (but not anti-NRP1) antibodies were able to block the SEMA3F effects. These results demonstrate that both NRP1 and NRP2 are capable of binding and transmitting SEMA3F signals. Although MCF7 cells express SEMA3F, they still responded to exogenous SEMA3F. This may simply represent a dosage effect in the presence of excess NRP1 receptor. As noted, anti-SEMA3F staining was detected predominantly at the periphery of the islets whereas NRP1 staining was detected throughout. Also, SEMA3F may have been in competition with VEGF present in the cultured supernatant.

Initially considered as an endothelial-specific mitogen, there is now evidence that VEGF stimulates nonendothelial cell types. For example, VEGF stimulates osteoblast migration [33,34] and positively influences melanoma cell migration *in vitro* through an integrin-dependent mechanism [35]. We have not investigated whether SEMA3F affects integrin activation. However, our findings do suggest that SEMA3F affects cell adhesion as evidenced by the separation of cells, their rounding-up, and subsequent detachment from the substrate. These responses are likely comparable to the effects seen in NP/plexin-transfected COS7 cells following exposure to SEMA3A or SEMA3F [25]. In these cells, SEMA3F led to cytoskeleton perturbations similar to those described in nerve growth cones. This suggests that SEMA3F has a common action on different cell types that may involve small GTP binding proteins like Rho family GTPases because lamellipodia were generally affected. Although we were unable to detect changes in total GTP-bound Rac1 or Rho, we did detect changes in Rac1-GFP localization. The Rho family of small GTPases is the central regulator of cytoskeletal dynamics and controls the organization of actin filaments and cellular morphology [36]. In growth cones, SEMA3A (Collapsin) has been shown to initiate clustering of neuropilin and plexin receptors. This occurred in a CRMP-dependent manner and was Rac1-

dependent (for review, see Ref. [20]). Similarly, plexin-A1, a coreceptor for class 3 semaphorins, interacts not only with Rnd1 but also with RhoD, and those GTPases have antagonistic effects on the activity of plexin-A1 [37]. These authors suggested that interaction of Rnd1 results in a conformational change that ultimately activates downstream signal transduction cascades, including Rac1, RhoA, LIM kinase 1, and cofilin that mediate growth cone collapse [38]. Indeed, we demonstrated in epithelial tumor cells a clear recruitment of Rac1 to retraction fibers upon AP-SEMA3F treatment.

Finally, we have some additional observations regarding the viability of the detached cells following SEMA3F exposure. These cells were not able to reattach and the number of cells decreased over time, suggesting that they underwent apoptosis or anoikis. An apoptotic effect was reported for SEMA3A in sensory neurons [39] and in neural progenitors [40]. This apoptotic effect was shown to be mediated by NRP1 and was antagonized by $VEGF_{165}$ [40]. We also performed additional experiments showing that C100 cells undergo apoptosis in response to transfected SEMA3F as evidenced by annexin and propidium iodine staining (data not shown).

In summary, we have shown that mammary adenocarcinoma cells stimulated with SEMA3F lose lamellipodia extensions and cell-cell contacts, and eventually detach with subsequent apoptosis or anoikis. These effects can be mediated by either NRP1 or NRP2 receptors and appear to involve Rac1 redistribution.

Acknowledgements

We are very grateful to M. Tessier-Lavigne and Kolodkin for providing us with the AP-SEMA3F construct and neuropilin antibodies, respectively. We thank P. Fort for the Rac-GFP vector and J. Collard for GST-Rhotekin-RBD and GST-PAK-CRIB constructs. We thank A. Cantereau for technical assistance in the confocal microscopy studies performed in the confocal microscopy core of the Federative Research Institute IFR59 at the University of Poitiers. We thank J. Habrioux and J. P. Poindessault for edition of the figures.

References

[1] Semaphorin Nomenclature Committee (1999). Unified nomenclature for the semaphorins/collapsins. *Cell* 97, 551–52.

[2] Luo Y, Raible D, and Raper A (1993). Collapsin: a protein in brain that induces the collapse and paralysis of neuronal growth cones. *Cell* 75, 217–27.

[3] Behar O, Golden JA, Mashimo H, Schoen FJ, and Fishman MC (1996). Semaphorin III is needed for normal patterning and growth of nerves, bones and heart. *Nature* 383, 525–28.

[4] Taniguchi M, Yuasa S, Fujisawa H, Naruse I, Saga S, Mishina M, and Yagi T (1997). Disruption of semaphorin III/D gene causes severe abnormality in peripheral nerve projection. *Neuron* 19, 519–30.

[5] Roche J, Boldog F, Robinson M, Robinson L, Varella-Garcia M, Swanton M, Waggoner B, Fishel R, Franklin W, Gemmill R, and Drabkin H (1996). Distinct 3p21.3 deletions in lung cancer and identification of a new human semaphorin. *Oncogene* 12, 1289–97.

[6] Sekido Y, Bader S, Latif F, Chen JY, Duh FM, Wei MH, Albanesi JP, Lee CC, Lerman MI, and Minna JD (1996). Human semaphorins A(V) and (IV) reside in the 3p21.3 small cell lung cancer deletion region and demonstrate distinct expression patterns. *Proc Natl Acad Sci USA* 93, 4120–25.

[7] Xiang R, Hensel C, Garcia D, Carlson H, Kok K, Daly M, Kerbacher K, Van Den Berg A, Veldhuis P, Buys C, and Naylor S (1996). Isolation of the human semaphorin III/F gene (SEMA3F) at chromosome 3p21, a region deleted in lung cancer. *Genomics* 32, 39–48.

[8] Brambilla E, Constantin B, Drabkin H, and Roche J (2000). Semaphorin SEMA3F localization in malignant human lung and cell lines: a suggested role in cell adhesion and cell migration. *Am J Pathol* 156, 939–50.

[9] Tomizawa Y, Sekido Y, Kondo M, Gao B, Yokota J, Roche J, Drabkin H, Lerman M, Gazdar A, and Minna J (2001). Inhibition of lung cancer cell growth and induction of apoptosis following re-expression of 3p21.3 candidate tumor suppressor gene SEMA3B. *Proc Natl Acad Sci USA* 98, 13954–59.

[10] Xiang R, Davalos AR, Hensel CH, Zhou XJ, Tse C, and Naylor SL (2002). Semaphorin 3F gene from human 3p21.3 suppresses tumor formation in nude mice. *Cancer Res* 62, 2637–43.

[11] Tse C, Xiang RH, Bracht T, and Naylor SL (2002). Human semaphorin 3B (SEMA3B) located at chromosome 3p21.3 suppresses tumor formation in an adenocarcinoma cell line. *Cancer Res* 62, 542–46.

[12] Kolodkin A, Levengood D, Rowe E, Tai Y, Giger R, and Ginty D (1997). Neuropilin is a semaphorin III receptor. *Cell* 90, 753–62.

[13] Chen H, Chedotal A, He Z, Goodman CS, and Tessier-Lavigne M (1997). Neuropilin-2, a novel member of the neuropilin family, is a high affinity receptor for the semaphorins Sema E and Sema IV but not Sema III. *Neuron* 19, 547–59.

[14] Soker S, Takashima S, Miao H, Neufeld G, and Klagsbrun M (1998). Neuropilin-1 is expressed by endothelial and tumor cells as an isoform-specific receptor for vascular endothelial growth factor. *Cell* 92, 735–45.

[15] Gluzman-Poltorak Z, Cohen T, Herzog Y, and Neufeld G (2000). Neuropilin-2 and neuropilin-1 are receptors for $VEGF_{165}$ and PLGF-2, but only neuropilin-2 functions as a receptor for $VEGF_{145}$. *J Biol Chem* 275, 18040–45.

[16] Miao HQ, Soker S, Feiner L, Alonso JL, Raper JA, and Klagsbrun M (1999). Neuropilin-1 mediates collapsin-1/semaphorin III inhibition of endothelial cell motility: functional competition of collapsin-1 and vascular endothelial growth factor-165. *J Cell Biol* 146, 233–42.

[17] Nakamura F, Kalb RG, and Strittmatter SM (2000). Molecular basis of semaphorin-mediated axon guidance. *J Neurobiol* 44, 219–29.

[18] Goshima Y, Sasaki Y, Nakayama T, Ito T, and Kimura T (2000). Functions of semaphorins in axon guidance and neuronal regeneration. *Jpn J Pharmacol* 82, 273–79.

[19] Tamagnone L and Comoglio PM (2000). Signalling by semaphorin receptors: cell guidance and beyond. *Trends Cell Biol* 10, 377–83.

[20] Liu BP and Strittmatter SM (2001). Semaphorin-mediated axonal guidance via Rho-related G proteins. *Curr Opin Cell Biol* 13, 619–26.

[21] He Z, Wang KC, Koprivica V, Ming G, and Song HJ (2002). Knowing how to navigate: mechanisms of semaphorin signaling in the nervous system. *Sci STKE* 2002, RE1.

[22] Gu Y and Ihara Y (2000). Evidence that collapsin response mediator protein-2 (CRMP-2) is involved in the dynamics of microtubules. *J Biol Chem* 275, 17917–20.

[23] Cai H and Reed RR (1999). Cloning and characterization of neuropilin-1-interacting protein: a PSD-95/Dlg/ZO-1 domain-containing protein that interacts with the cytoplasmic domain of neuropilin-1. *J Neurosci* 19, 6519–27.

[24] Shih JY, Yang SC, Hong TM, Yuan A, Chen JJ, Yu CJ, Chang YL, Lee YC, Peck K, Wu CW, and Yang PC (2001). Collapsin response mediator protein-1 and the invasion and metastasis of cancer cells. *J Natl Cancer Inst* 93, 1392–400.

[25] Takahashi T, Fournier A, Nakamura F, Wang LH, Murakami Y, Kalb RG, Fujisawa H, and Strittmatter SM (1999). Plexin-neuropilin-1 complexes form functional semaphorin-3A receptors. *Cell* 99, 59–69.

[26] Fan J and Raper R (1995). Localized collapsing cues can steer growth cones without inducing their full collapse. *Neuron* 14, 263–74.

[27] Kantor JD, McCormick B, Steeg PS, and Zetter BR (1993). Inhibition of cell motility after nm23 transfection of human and murine tumor cells. *Cancer Res* 53, 1971–73.

[28] Hernandez-Farina S, Beck KW, and Püschel A (2001). Differential responsiveness to the chemorepellent semaphorin 3A distinguishes ipsi- and contralaterally projecting axons in the chick midbrain. *Dev Biol* 237, 381.

[29] Sander EE, van Delft S, ten Klooster JP, Reid T, van der Kammen RA, Michiels F, and Collard JG (1998). Matrix-dependent Tiam1/Rac signaling in epithelial cells promotes either cell–cell adhesion or cell migration and is regulated by phosphatidylinositol 3-kinase. *J Cell Biol* 143, 1385–98.

[30] Hirsch E, Hu LJ, Prigent A, Constantin B, Agid Y, Drabkin H, and Roche J (1999). Distribution of semaphorin IV in adult human brain. *Brain Res* 823, 67–79.

[31] He Z and Tessier-Lavigne M (1997). Neuropilin is a receptor for the axonal chemorepellent semaphorin III. *Cell* 90, 739–51.

[32] Todd M, Xiang R, Garcia D, Kerbacher K, Moore S, Hensel C, Liu P, Siciliano M, Kok K, van den Berg A, Veldhuis P, Buys C, Killary A, and Naylor S (1996). An 80 Kb P1 clone from chromosome 3p21.3 suppresses tumor growth in vivo. *Oncogene* 13, 2387–96.

[33] Deckers MM, Karperien M, van der Bent C, Yamashita T, Papapoulos SE, and Lowik CW (2000). Expression of vascular endothelial growth factors and their receptors during osteoblast differentiation. *Endocrinology* 141, 1667–74.

[34] Midy V and Plouet J (1994). Vasculotropin/vascular endothelial growth factor induces differentiation in cultured osteoblasts. *Biochem Biophys Res Commun* 199, 380–86.

[35] Byzova TV, Goldman CK, Pampori N, Thomas KA, Bett A, Shattil SJ, and Plow EF (2000). A mechanism for modulation of cellular responses to VEGF: activation of the integrins. *Mol Cell* 6, 851–60.

[36] Hall A (1998). Rho GTPases and the actin cytoskeleton. *Science* 279, 509–14.

[37] Zanata SM, Hovatta I, Rohm B, and Puschel AW (2002). Antagonistic effects of Rnd1 and RhoD GTPases regulate receptor activity in Semaphorin 3A-induced cytoskeletal collapse. *J Neurosci* 22, 471–77.

[38] Aizawa H, Wakatsuki S, Ishii A, Moriyama K, Sasaki Y, Ohashi K, Sekine-Aizawa Y, Sehara-Fujisawa A, Mizuno K, Goshima Y, and Yahara I (2001). Phosphorylation of cofilin by LIM-kinase is necessary for semaphorin 3A-induced growth cone collapse. *Nat Neurosci* 4, 367–73.

[39] Gagliardini V and Fankhauser C (1999). Semaphorin III can induce death in sensory neurons. *Mol Cell Neurosci* 14, 301–16.

[40] Bagnard D, Vaillant C, Khuth ST, Dufay N, Lohrum M, Puschel AW, Belin MF, Bolz J, and Thomasset N (2001). Semaphorin 3A-vascular endothelial growth factor-165 balance mediates migration and apoptosis of neural progenitor cells by the recruitment of shared receptor. *J Neurosci* 21, 3332–41.

Neoplasia • Vol. 5, No. 1, 2003

516

Pancreatic Carcinoma Cells Express Neuropilins and Vascular Endothelial Growth Factor, but Not Vascular Endothelial Growth Factor Receptors

Min Li, PhD.
Hui Yang, M.D., Ph.D.
Hong Chai, M.D., PhD.
William E. Fisher, M.D.
Xiaoping Wang, Ph.D.
F. Charles Brunicardi, M.D.
Qizhi Yao, M.D., Ph.D.
Changyi Chen, M.D., Ph.D.

Molecular Surgeon Research Center, Michael E. DeBakey Department of Surgery, Baylor College of Medicine/Methodist Hospital, Houston, Texas.

Supported in part by Grants R01 HL61943, R01 HL60135, R01 HL65916, and R01 HL72716 from the National Institutes of Health (NIH) (to C.C.), by NIH Grants R01 DK46441, R01 CA95731, and R21 CA101889 (to F.C.B.); by NIH Grants R21 AI491116 and R01 DE015543 (to Q.Y.); by Grant 30935 from the Methodist Hospital Foundation (to M.L.); and by Grant R18 CA85827 from the National Cancer Institute (to W.E.F.).

The authors thank Dr. Ming-Sound Tsao (Ontario Cancer Institute, Princess Margaret Hospital, University Health Network, Toronto, Ontario, Canada) for generously providing the human pancreatic ductal epithelial cells used in the current study.

Address for reprints: Changyi Chen, M.D., Ph.D., Michael E. DeBakey Department of Surgery, Baylor College of Medicine, One Baylor Plaza, Mail Stop NAB 2010, Houston, TX 77030; Fax: (713) 798-5613; E-mail: cchen@bcm.tmc.edu

Received April 13, 2004; revision received July 12, 2004; accepted August 3, 2004

BACKGROUND. Neuropilin (NRP)-1 and -2 are characterized as coreceptors for vascular endothelial growth factor (VEGF). In the current study, the authors assessed the expression of NRPs, VEGF, and vascular endothelial growth factor receptors (VEGFRs), as well as VEGF-induced cell proliferation, in pancreatic carcinoma cell lines and tissue specimens.

METHODS. Human pancreatic carcinoma cell lines (Panc-1 and MIA PaCa-2), normal human pancreatic ductal epithelial cells (HPDE), and human umbilical vein endothelial cells (HUVECs) were cultured. Human pancreatic adenocarcinoma tissue specimens were also studied. Expression levels of NRPs, VEGFRs, and VEGF were determined by real-time polymerase chain reaction analysis and immunostaining. Cell proliferation was examined using a [^{3}H]thymidine incorporation assay.

RESULTS. Both NRP-1 and NRP-2 were expressed in Panc-1 cells, HPDE cells, and HUVECs but were expressed minimally in MIA PaCa-2 cells. Panc-1 expressed 30 times more NRP-1 mRNA than NRP-2 mRNA. NRP-1 levels in Panc-1 cells were 63 times higher than in HPDE cells but were similar to NRP-1 levels in HUVECs. NRP-2 levels in Panc-1 cells were similar to NRP-2 levels in HPDE cells but lower than NRP-2 levels in HUVECs. Expression of all three VEGFRs was observed only in HUVECs. However, VEGF mRNA was detected in all cell types except for HUVECs. NRP-1 immunoreactivity levels were much higher than NRP-2 immunoreactivity levels in Panc-1 and human pancreatic adenocarcinoma tissue specimens, whereas VEGFRs were not detected in either of these two settings. In response to VEGF$_{165}$, [^{3}H]thymidine incorporation in Panc-1 cells increased significantly (by 65%; $P < 0.01$). A monoclonal antibody against human NRP-1 significantly blocked VEGF-induced cell proliferation in Panc-1 cells.

CONCLUSIONS. The pancreatic carcinoma cell line Panc-1 and adenocarcinoma tissue specimens expressed high levels of NRP-1 and VEGF, but not VEGFRs, and exogenous VEGF significantly increased NRP-1-mediated, but not VEGFR-mediated, Panc-1 cell proliferation. These data suggested that NRP-1 may be involved in the pathogenesis of pancreatic carcinoma. *Cancer* 2004;101:2341–50.
© 2004 American Cancer Society.

KEYWORDS: neuropilins, vascular endothelial growth factor, vascular endothelial growth factor receptors, pancreatic carcinoma, cell proliferation.

Neuropilins (NRPs), are type I transmembrane glycoproteins with a molecular weight of 130–140 kilodaltons (kD). They were originally identified in neuronal cells as receptors for the class 3 semaphorin subfamily, which is involved in neuronal cell guidance and axonal growth in the development of the nervous system.[1] Recently, they also have been characterized as receptors or coreceptors for specific isoforms of vascular endothelial growth factors (VEGFs). VEGF is a dominant stimulant of angiogenesis and also functions as a potent permeability-inducing agent and an endothelial cell survival factor. Alternative splicing of the eight exons of the VEGF gene generates five isoforms of the VEGF-A protein (VEGF$_{121}$, VEGF$_{145}$, VEGF$_{165}$, VEGF$_{189}$, and VEGF$_{206}$). VEGF$_{121}$ and VEGF$_{165}$ are the most abundant isoforms of VEGF.[2] VEGF binds to three VEGF receptors (VEGFRs) with high affinity. VEGFR-1 (Flt-1, 180 kD) and VEGFR-2 (KDR/Flk-1, 200 kD) are associated with tyrosine kinase activity. All VEGF-A splice forms bind to VEGFR-1 and VEGFR-2.[3] VEGFR-3, a member of the same family of receptor-associated tyrosine kinases, is a receptor for VEGF-C and VEGF-D (but not for VEGF-A).[4] VEGFR-3 has been shown to be essential for lymphangiogenesis and has been implicated in angiogenesis in both embryos and adults.[5,6]

Several studies suggest that NRPs play an important role in tumor growth and angiogenesis and may serve as markers for the progression of prostate carcinoma, breast carcinoma, and pancreatic carcinoma.[7] Many prostate and breast carcinoma cell lines have been found to overexpress NRP-1 proteins while not expressing any of the VEGFRs.[7] Clinically, overexpression of NRP-1 appears to be correlated with the metastatic potential of prostate carcinoma cells and with advanced disease stage and grade.[8,9] NRP-1 is also expressed in pituitary tumors,[10] astrocytoma,[11] neuroblastoma,[12] and lung carcinoma.[13] In addition, NRP-2 expression has been reported in osteosarcoma,[14] neuroblastoma,[15] bladder carcinoma,[16] and lung carcinoma.[13] Two recent reports have demonstrated that NRPs may play a role in pancreatic carcinoma. Cohen et al.[17] documented moderate-to-strong NRP-2 expression in 27 of 30 endocrine pancreatic tumor specimens, whereas staining for this protein was found only in a distinct subset of islet cells situated primarily at the islet periphery in normal pancreatic tissue specimens. However, the biologic role of NRP-2 in endocrine pancreatic tumors is not clear. At present, NRP-2 is used as a diagnostic marker for such tumors. An immunohistochemical analysis conducted by Parikh et al.[18] revealed that NRP-1 was expressed in 12 of 12 human pancreatic adenocarcinoma specimens but was absent in nonmalignant pancreatic tissue specimens. Furthermore, NRP-1 mRNA was detected in 8 of 11 human pancreatic adenocarcinoma cell lines by Northern blot analysis. Nonetheless, the specific role of NRP-1 in pancreatic adenocarcinoma and other malignancies remains to be elucidated.

At present, data regarding the expression and quantitation of NRPs in pancreatic carcinoma are limited, and data on the role of NRPs in regulating pancreatic carcinoma growth are even more scarce. In the current study, we investigated the expression of NRP-1, NRP-2, VEGFR-1, VEGFR-2, VEGFR-3, and VEGF-C in human pancreatic carcinoma cell lines (Panc-1 and MIA PaCa-2), normal human pancreatic ductal epithelial cells (HPDE), human umbilical vein endothelial cells (HUVECs), and surgical human adenocarcinoma specimens using a quantitative real-time reverse transcription polymerase chain reaction (RT-PCR) and immunohistochemical staining. Proliferation of pancreatic carcinoma cells expressing high levels of NRP-1 also was examined after these cells were treated with VEGF at various doses. These studies should add to our understanding of the progression and control of pancreatic carcinoma, potentially leading to the development of novel diagnostic markers and effective treatment strategies.

MATERIALS AND METHODS

Chemicals and Reagents

The IQ SYBR Green supermix and iScript cDNA synthesis kits were purchased from Bio-Rad (Hercules, CA), and RNAqueous-4PCR and DNA removal kits were obtained from Ambion (Austin, TX). [^{3}H]-labeled thymidine was purchased from Perkin Elmer (Boston, MA). EGM-2 Bulletkit media, trypsin-ethylenediaminetetra acetic acid, and trypsin neutralization solution were obtained from Clontech (Walkersville, MD). Finally, recombinant human VEGF$_{165}$ was purchased from Sigma (St. Louis, MO).

Cell and Tissue Cultures

The human pancreatic carcinoma cell lines Panc-1 and MIA PaCa-2 were purchased from the American Type Culture Collection (ATCC; Rockville, MD), and primary HUVECs were obtained from Clontech. HPDE cells were a kind gift from Dr. Ming-Sound Tsao (University of Toronto, Toronto, Ontario, Canada), and were described previously.[19,20] Panc-1 cells were cultured in Dulbecco modified Eagle medium (DMEM) with 10% fetal bovine serum (FBS) at 37 °C with 5% CO_2. MIA PaCa-2 cells were grown in DMEM with 10% FBS and 2.5% horse serum at 37 °C with 5% CO_2. Cells were passed up to 20 times after they were obtained from the ATCC, with their media being refreshed every 2–3 days. HUVECs were grown in EGM-2 Bulletkit media (basic endothelial cell media containing hydrocortisone, fibroblast growth factor-B, VEGF, long R3 insulin-like growth factor-1, ascorbic acid, epidermal growth factor [EGF], gentamicin/amphotericin, and heparin) supplemented with 10% FBS. HUVECs were passed no more than 1 of 5 times in all experiments. HPDE cells were cultured in keratinocyte serum-free culture medium (SFM) supplemented with 5 ng/mL

DOI 10.1002/cncr.20634
Published online 8 October 2004 in Wiley InterScience (www.interscience.wiley.com)

Bad" and 50 μg/mL bovine pituitary extract (Invitrogen, Carlsbad, CA). Cells were passed up to 30 times. Human pancreatic adenocarcinoma specimens and normal surrounding tissue specimens were collected from patients undergoing surgery according to an approved human protocol (H7091) at the Baylor College of Medicine (Houston, TX). Tissue specimens were stored at −80 °C before processing.

RNA Extraction from Cells

Total RNA samples were extracted from two pancreatic carcinoma cell lines (Panc-1 and MIA PaCa-2), HPDE cells, and HUVECs using the Ambion RNAqueous-PCR kit in accordance with the manufacturer's instructions. In brief, cells with 90% confluence were lysed with Ambion lysis buffer for 20 minutes, and the resulting cell lysates were mixed with an equal volume of 64% ethanol. The lysates then were transferred to an Ambion minicolumn in a 2 mL collection tube and centrifuged at 10,000 × g for 1 minute. The column was washed once with 700 μL of Wash Buffer 1 and twice with 500 μL of Wash Buffer 2/3. After incubation with 50 μL of prewarmed elution buffer, the eluted fluid was collected using a new tube, and another 50 μL of elution buffer was added, after which a second centrifugation was performed. The Ambion DNA removal kit was used to remove the trace amount of genomic DNA contamination present in the RNA solution. In brief, 1 μL DNase I, along with the appropriate DNase I buffer, was added to 20 μL RNA solution, which then was incubated at 37 °C for 2 hours. DNase I was removed by adding 0.1–0.2 volumes of DNase-removing agent, and the purified RNA sample was collected by centrifugation at 10,000 × g for 1 minute.

Primer Design

Specific primers for NRP-1, NRP-2, VEGFR-1, VEGFR-2, VEGFR-3, and VEGF were designed using Beacon Designer 2.1 software (PREMIER Biosoft International, Palo Alto, CA). The primer sequences are listed in Table 1. Homologies between the various subtypes and the template secondary structure were carefully considered, and primers were chosen so as to avoid such homologies. The lengths of all primers ranged from 75 to 150 base pairs. The primer sequence for PCR amplification of the housekeeping gene β-actin was as follows: sense, 5′ CTGGAACGGTGAAGGTGACA 3′, and antisense, 5′ AAGGGACTTCCTGTAACAATGCA-3′.

RT-PCR

Levels of NRP-1, NRP-2, VEGFR-1, VEGFR-2, VEGFR-3, and VEGF mRNA in pancreatic carcinoma cells, HPDE cells, and HUVECs were analyzed via real-time RT-PCR using the iCycler system (Bio-Rad). The mRNA sample was reverse-transcribed into cDNAs by using the iScript cDNA synthesis kit. Primer specificity was tested by running a regular PCR for 40 cycles of 95 °C for 20 seconds and 60 °C for 1 minute, after which products were visualized via agarose gel electrophoresis. Real-time PCR was performed using the SYBR supermix kit (the PCR reaction included the following components: each primer at a concentration of 100 nM, diluted cDNA templates, and iQ SYBR Green supermix [which contained each deoxynucleotide at a concentration of 0.2 mM, iTaq DNA polymerase at a concentration of 25 units per mL, SYBR Green I, 10 nM fluorescein, 3 mM $MgCl_2$, 50 mM KCl, and 20 mM Tris-HCl]) and running for 40 cycles of 95 °C for 20 seconds and 60 °C for 1 minute. PCR efficiency was examined by serially diluting the template cDNA, and melting curve data were collected so that PCR specificity could be assessed. Each cDNA sample was run in triplicate, and a corresponding mRNA sample that had not been subjected to reverse transcription was included as a negative control in each case. β-actin primers were included in every plate to correct for sample-to-sample variation. For each experimental sample, mRNA levels were normalized to β-actin mRNA levels. The relative mRNA level was presented as $2^{(\text{threshold cycle for } \beta\text{-actin} - \text{threshold cycle for gene of interest})}$.

TABLE 1
Real-Time PCR Primer Sequences for NRP-1, NRP-2, VEGFR-1, VEGFR-2, VEGFR-3, and VEGF Genes

	Primer sequence	Primer position (nt)
NRP-1	[illegible]	[illegible]
NRP-2	[illegible]	[illegible]
VEGFR-1	[illegible]	[illegible]
VEGFR-2	[illegible]	[illegible]
VEGFR-3	[illegible]	[illegible]
VEGF	[illegible]	[illegible]

[illegible]

[³H]Thymidine Incorporation Assay

Panc-1 cells and HUVECs were seeded in 96-well plates (2×10^3 cells per well) for 24 hours. The cells

were subjected to serum starvation (0% FBS for Panc-1 or 2% FBS for HUVECs) for 24 hours before the addition of VEGF$_{165}$ (0.4, 2, and 10 ng/mL) for both Panc-1 cells and HUVECs or, for control samples, phosphate-buffered saline (PBS). After 6 hours, [³H]thymidine (1 microcurie [μCi] per mL) was added to each well. Cells were incubated further for another 18 hours, after which [³H]thymidine incorporation was measured in scintillation solution using a microplate scintillation and luminescence counter (Packard Biosciences, Meriden, CT). For the blocking assay, Panc-1 cells were seeded in 96-well plates (2×10^3 cells per well). After being grown to 80% confluence, cells were starved in SFM for 24 hours. Cells then were incubated with 1 μg/mL anti-NRP-1 monoclonal antibody (MoAb; Santa Cruz Biotechnology, Santa Cruz, CA) for 1 hour at 37 °C, before the addition of VEGF$_{165}$ (2 ng/mL) or PBS. After 6 hours, 1 μCi/mL [³H]thymidine was added to each well and incubated for another 18 hours. Incorporation of [³H]thymidine was measured as described earlier in the text.

Immunofluorescence and Immunohistochemical Assays

Clinical pancreatic adenocarcinoma ($n = 11$) and surrounding normal tissue specimens were collected and processed into 5-μm sections using a Cryostat (Meyer Instruments, Houston, TX). Tissue specimens were fixed and stained with hematoxylin and eosin according to standard protocol. For immunofluorescence and immunohistochemical analyses, fixed cells or tissue slides were incubated with anti-NRP-1, anti-NRP-2 (Santa Cruz Biotechnology), or anti-VEGFR-2 antibodies (R&D Systems, Minneapolis, MN) for 30 minutes at 4 °C, washed 3 times with PBS, and incubated with secondary antibodies conjugated with Texas Red or fluorescein isothiocyanate (Vector Laboratories, Burlingame, CA) for another 30 minutes at 4 °C. After three washes with PBS, slides were mounted with 4′,6-diamidino-2-phenylindole or Texas Red mounting medium and observed under an Olympus BX41 microscope (Olympus USA, Melville, NY). Images were captured with an attached SPOT RT digital camera (Diagnostic Instruments, Sterling Heights, MI). For diaminobenzidine (DAB) visualization, slides were incubated with avidin-biotin-peroxidase solution (Vectastain ABC Elite kit, Vector Laboratories, Burlingame, CA) at room temperature for 1 hour, followed by 0.1% DAB and 0.003% H_2O_2 in Tris-buffered saline for 5–10 minutes. The reaction was terminated by rinsing in tap water, and sections were then mounted and observed under a microscope.

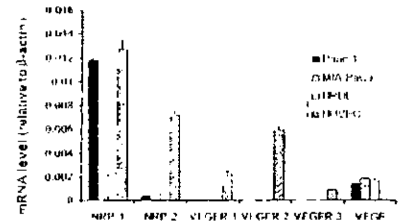

FIGURE 1. Levels of neuropilin (NRP)-1, NRP-2, vascular endothelial growth factor receptor (VEGFR), and vascular endothelial growth factor (VEGF) mRNA in Panc-1, MIA PaCa-2, and HPDE cells and in HUVECs. Total RNA was extracted from two pancreatic carcinoma cell lines (Panc-1 and MIA PaCa-2), HPDE cells, and HUVECs. All mRNA levels were assessed via the real-time polymerase chain reaction using the Bio-Rad iCycler system (Bio-Rad, Hercules, CA). Each cDNA sample was subjected to triplicate assays, and a corresponding mRNA sample that had not been subjected to reverse transcription was included as a negative control in each case. Primers for the amplification of β-actin were included in every plate to correct for sample-to-sample variations; in all cases, mRNA levels for genes of interest were normalized to β-actin mRNA levels. Relative mRNA levels are presented as 2^(threshold cycle for β-actin − threshold cycle for gene of interest). Mean values ± standard deviations from three separate experiments are shown.

Statistical Analysis

Data from real-time PCR and [³H]thymidine incorporation assays were expressed as mean values ± standard deviations. Comparisons were analyzed using the Student t test. $P < 0.05$ was considered indicative of statistical significance.

RESULTS

mRNA Levels of NRPs, VEGF, and VEGFRs in Human Pancreatic Carcinoma Cells, HPDE Cells, and HUVECs

To investigate the role of NRPs in human pancreatic carcinoma, we assessed the expression of NRPs, VEGFRs, and VEGF in human pancreatic carcinoma cell lines as well as in control samples (normal HPDE cells and HUVECs). mRNA levels were evaluated via real-time RT-PCR using specifically designed primers (Table 1) for the NRP-1, NRP-2, VEGFR-1, VEGFR-2, VEGFR-3, and VEGF genes. mRNA levels of the housekeeping gene β-actin served as a reference against which mRNA levels in experimental samples could be normalized. Threshold cycle values, which represent relative amounts of mRNA molecules, were compared across cell lines. As shown in Figure 1, NRP-1 and NRP-2 both were expressed in Panc-1 cells, HPDE cells, and HUVECs but were expressed minimally in MIA PaCa-2 cells. NRP-1 mRNA levels in Panc-1 cells

518

were 5.7 times higher than in normal HPDE cells but were similar to NRP-1 mRNA levels in HUVECs. In contrast, Panc-1 and HPDE cells exhibited similar NRP-2 mRNA levels, which were approximately 18.4 and 13.0 times lower, respectively, than NRP-2 mRNA levels in HUVECs. Furthermore, NRP-1 mRNA levels were 29.7 times higher than NRP-2 mRNA levels in Panc-1 cells and approximately 4.0 times higher than NRP-2 mRNA levels in HPDE cells, whereas NRP-1 mRNA levels were only 1.7 times higher than NRP-2 mRNA levels in HUVECs. Thus, increased expression of NRP-1 in Panc-1 cells may play a role in malignant progression.

Also noteworthy is that VEGFR mRNA was not detected in pancreatic carcinoma cells or in HPDE cells, whereas VEGFR mRNA was present in HUVECs. Levels of VEGFR-2, the most abundant VEGFR, were 2.3 times higher than VEGFR-1 levels and 6.5 times higher than VEGFR-3 levels in HUVECs. Furthermore, VEGF mRNA was detected at similar levels in Panc-1, MIA PaCa-2, and HPDE cells, but not in HUVECs.

NRP-1, NRP-2, and VEGFR-2 Immunoreactivity in Panc-1 Cells

To confirm the expression and localization of NRP-1 and NRP-2 proteins in Panc-1 cells, staining of these cells with anti-NRP-1 and anti-NRP-2 antibodies was performed, followed by immunofluorescence staining. As shown in Figure 2, NRP-1 was expressed on the surface of Panc-1 cells, whereas NRP-2 was only weakly expressed in the Panc-1 cell line. Aside from NRP-1 and NRP-2, scant VEGFR-2 expression was observed in Panc-1 cells, a finding that was consistent with real-time RT-PCR results.

Effect of VEGF on the Proliferation of Panc-1 Cells

VEGF is a multifunctional cytokine that plays an important role in angiogenesis and endothelial cell proliferation. To examine whether VEGF stimulates the proliferation of pancreatic carcinoma cells, we incubated Panc-1 cells with $VEGF_{165}$ at various concentrations for 24 hours, with HUVEC samples run concurrently as controls. Cell proliferation was detected using a [^{3}H]thymidine incorporation assay. As shown in Figure 3, a low concentration of $VEGF_{165}$ (2 ng/mL) increased cell proliferation by up to 61%, and 10 ng/mL $VEGF_{165}$ increased Panc-1 cell proliferation by 43% relative to control samples ($P < 0.01$). In addition, 2 ng/mL and 10 ng/mL $VEGF_{165}$ stimulated cell proliferation approximately 22% and 41% more, respectively, in HUVECs compared with control samples. Considering the absence of VEGFR and the elevated expression of NRP-1 in Panc-1 cells, our results indicate that NRP-1 may serve as an alternative receptor for VEGF in pancreatic carcinoma cells.

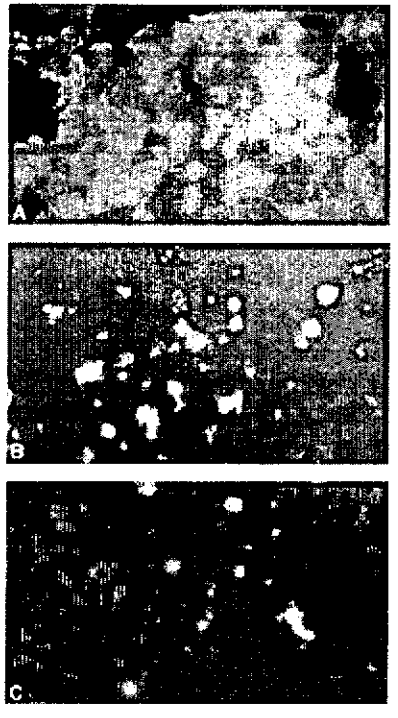

FIGURE 2. Neuropilin (NRP)-1, NRP-2, and vascular endothelial growth factor receptor (VEGFR)-2 immunoreactivity in Panc-1 cells. Panc-1 cells were seeded on chamber slides and incubated with anti-NRP-1, anti-NRP-2, and anti-VEGFR-2 antibodies, respectively. Cells then were stained with phycoerythrin (PE) or fluorescein isothiocyanate (FITC)-conjugated secondary antibodies. Nuclei were counterstained with 4′,6-diamidino-2-phenylindole (DAPI) or Texas Red. (A) NRP-1 staining. Red (PE) indicates NRP-1-positive staining (strong). Blue (DAPI) indicates nuclear staining. (B) NRP-2 staining. Green (FITC) indicates NRP-2-positive staining (weak). Red (Texas Red) indicates nuclear staining. (C) VEGFR-2 staining. Green (FITC) indicates VEGFR-2 positive staining (very weak). Red (Texas Red) indicates nuclear staining. Panc-1 cells strongly expressed NRP-1, weakly expressed NRP-2, and did not express or minimally expressed VEGFR-2. Original magnification × 400 (A–C).

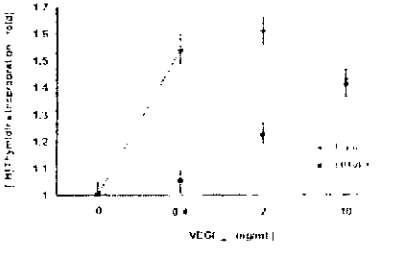

FIGURE 3. Effect of vascular endothelial growth factor ($VEGF_{165}$) on cell proliferation in Panc-1 and human umbilical vascular endothelial cells (HUVECs). Subconfluent Panc-1 cells or HUVECs were subjected to serum starvation for 24 hours and then treated with $VEGF_{165}$ at various concentrations for a total of 24 hours. At the 6-hour mark, [^{3}H]thymidine (1 microcurie per mL) was added to the cells. [^{3}H]thymidine incorporation was measured using a Top Count microplate scintillation and luminescence counter (Packard Instrument Co., Meriden, CT). Treatment with VEGF significantly increased Panc-1 cell proliferation ($P < 0.01$). Data are expressed as mean values ± standard deviations from triplicate experiments.

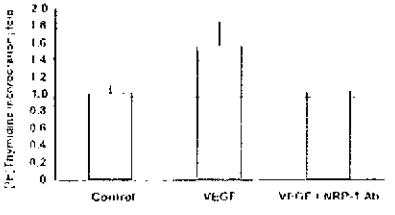

FIGURE 4. Inhibition of vascular endothelial growth factor (VEGF)-induced cell proliferation by a neuropilin (NRP)-1 specific antibody (Ab). Subconfluent Panc-1 cells were subjected to serum starvation for 24 hours and then incubated with 1 μg/mL anti-NRP-1 Ab (Santa Cruz Biotechnology, Santa Cruz, CA) before being treated with $VEGF_{165}$ for 24 hours. At the 6-hour mark, [^{3}H]thymidine (1 microcurie per mL) was added to the cells. [^{3}H]thymidine incorporation was measured using a Top Count microplate scintillation and luminescence counter (Packard Instrument Co., Meriden, CT). Data were expressed as mean values ± standard deviations from triplicate experiments.

NRP-1 Antibody Blocks VEGF-Induced Cell Proliferation

To examine whether NRP-1 antibody blocked VEGF-induced cell proliferation, 1 μg/mL anti-NRP-1 antibody was incubated with Panc-1 cells for 1 hour at 37 °C, before treatment with $VEGF_{165}$. As shown in Figure 4, cells treated with VEGF exhibited significantly increased cell proliferation compared with negative controls ($P < 0.05$). However, VEGF-induced cell proliferation was blocked to a significant extent by NRP-1-specific antibodies, and similar levels of [^{3}H]thymidine incorporation were noted in the VEGF/NRP-1-specific antibody group and the control group. Thus, NRP-1, but not VEGFRs, appears to mediate VEGF-induced cell proliferation in Panc-1 cells.

NRP and VEGFR Immunoreactivity in Pancreatic Adenocarcinoma Tissue Specimens

To investigate the expression of NRPs and VEGFRs in pancreatic carcinoma tissue specimens, we collected clinical specimens of pancreatic adenocarcinoma tissue and surrounding normal tissue from patients undergoing surgery and ascertained the presence of NRPs and VEGFRs using immunohistochemical methods. As shown in Figure 5, NRP-1 was expressed significantly in pancreatic carcinoma tissue specimens, but not in samples of normal surrounding tissue. In contrast, NRP-2 was weakly expressed in pancreatic carcinoma tissue or in normal surrounding tissue. These findings indicate that NRP-1 may be a valuable marker for the diagnosis of pancreatic carcinoma. It also is noteworthy that no VEGFRs were detected in pancreatic tissue specimens (data not shown). Overall, our findings in tissue specimens were consistent with our observations in Panc-1 cells.

DISCUSSION

The current study represents a detailed analysis of the expression status of NRPs, VEGF, and VEGFRs in human pancreatic carcinoma cells and clinical specimens and of the involvement of NRPs in VEGF-induced pancreatic carcinoma cell proliferation. We have examined both mRNA and protein levels of NRP-1, NRP-2, VEGFR-1, VEGFR-2, VEGFR-3, and VEGF in human pancreatic carcinoma cell lines (Panc-1 and MIA PaCa-2) and in surgical specimens using quantitative real time RT-PCR and immunohistochemical analysis. Panc-1 cells expressed high levels of NRP-1 compared with normal HPDE cells, but similar levels of NRP-2 were observed in Panc-1 and HPDE cells. No pancreatic carcinoma or HPDE cells expressed any of the VEGFRs, but these cells did express VEGF mRNA. Exogenous VEGF stimulated Panc-1 cell proliferation by up to 61%, and this stimulation of growth was blocked by an NRP-1-specific antibody, indicating that NRP-1 may be involved in regulating pancreatic carcinoma growth in the absence of VEGFRs.

The VEGF family and VEGFRs have been involved

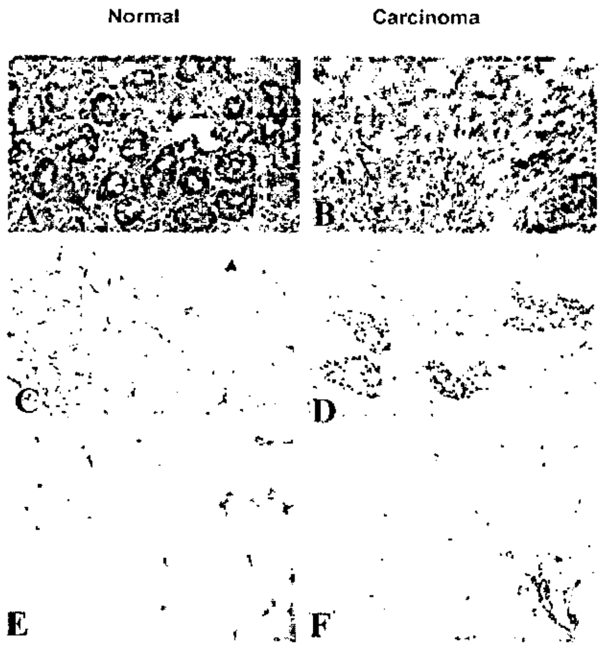

FIGURE 5. Neuropilin (NRP)-1 and NRP-2 immunoreactivity in pancreatic carcinoma tissue specimens. Human pancreatic adenocarcinoma specimens and normal surrounding tissue specimens were collected and processed into 5-μm thick slices using a Cryostat (Meyer Instruments, Houston, TX) at −20 °C. (A,B) Fixed tissue specimens were stained with hematoxylin and eosin according to standard protocol. (C,D) Parallel slides were incubated with anti-NRP-1 antibodies, after which immunohistochemical staining and visualization with diaminobenzidine (DAB) were performed. (E,F) Parallel slides were incubated with anti-NRP-2 antibodies, after which immunohistochemical staining and visualization with DAB were performed. Dark brown coloration corresponds to positive staining for NRP-1 or NRP-2. Pancreatic carcinoma tissue specimens strongly expressed NRP-1 but weakly expressed NRP-2. Original magnification ×400.

in the formation of new blood vessels in both malignant and nonmalignant conditions.[1,2] VEGF is a multifunctional cytokine that is secreted by a wide variety of tissue types, including premalignant lesions, invasive tumors, and cell lines, in breast carcinoma, colon carcinoma, melanoma, lung carcinoma, and pancreatic carcinoma.[21–27] It remains unknown as to whether overexpressed VEGF acts in an autocrine manner to regulate the proliferation of cells that contain VEGFRs or binds to VEGFRs on endothelial cells and enhances their proliferation and migration in a paracrine manner. Itakura et al.[28] reported concomitant overexpression of VEGF and VEGFRs in some, but not all, pancreatic carcinoma tissue specimens and cell lines (e.g., Capan 1 cells), indicating that an autocrine pathway that involves VEGF and VEGFR and promotes cell proliferation may exist in certain pancreatic carcinoma cell types. Von Marschall et al.[29] also detected VEGF in all pancreatic tumor cell lines investigated, as well as VEGFRs in two cell lines. VEGF treatment stimulated the growth of VEGFR-bearing cells, which was blocked by a VEGF antagonist, suggesting a possible autocrine mitogenic loop in pancreatic carcinoma cells that is mediated by VEGF and VEGFRs. VEGF overexpression is believed to be associated with increased vascularization, poor prognosis, and high-grade tumor metastasis in several tumor types, including lung carcinoma and pancreatic carcinoma.[21,30,31] One of the most notable discoveries of the current study is that VEGF stimulates pancreatic carcinoma cell proliferation without VEGFRs. Although pancreatic carcinoma cells expressed higher levels of VEGF than did HUVECs, they did not express VEGFRs. Alternative receptors such as NRP-1 may play a role in the activity of VEGF and may induce cell proliferation via signal transduction pathways. The current study provides evidence suggesting the existence of an autocrine pathway in pancreatic carcinoma cells that is mediated by the interaction between VEGF and NRP-1. Parikh et al.[18] also found evidence indicating that VEGF plays an important role in pancreatic carcinoma growth and metastasis; however, data on VEGFR expression was not reported by those investigators.

NRPs were recently shown to bind to certain isoforms of VEGF, such as $VEGF_{165}$ and $VEGF_{145}$, in addition to their natural ligand, semaphorin. The binding domain for VEGF is located in the b1/b2 region of NRPs, and the exon 7-encoded peptide of VEGF is responsible for its interaction with NRPs.[32] Many studies have investigated the role of NRPs in tumor progression. Overexpression of NRP-1 and NRP-2 has been observed in pancreatic carcinoma, prostate carcinoma, and lung carcinoma.[33] In addition, differential expression of NRP-1 has been observed in myoepithelial and vascular smooth muscle cells in preneoplastic and neoplastic human breast, and consequently, NRP-1 may serve as a marker for the progression of breast carcinoma. Furthermore, NRP-2 is believed to be a novel marker in pancreatic islet cells and endocrine pancreatic tumors,[17] and NRP-1 and NRP-2 coexpression were found to be significantly correlated with increased vascularity and poor prognosis in nonsmall cell lung carcinoma.[11] The current study demonstrated that NRP-1 was expressed at high levels in Panc-1 cells and clinical pancreatic carcinoma specimens, a finding that is consistent with previous studies. Fukahi et al.[12] reported aberrant expression of NRP-1 and NRP-2, but not VEGFRs, in human pancreatic carcinoma cells. Those investigators also documented elevated expression of VEGF ligands in pancreatic carcinoma cells. The potential functions of NRP-1 were not investigated in that study. We found that treatment of Panc-1 cells with VEGF led to increased cell proliferation in a dose-dependent manner. This is a noteworthy finding, because VEGFRs are not present in Panc-1 cells, whereas NRP-1 is. VEGF may interact with NRP-1 to induce cell proliferation in human pancreatic carcinoma cells. Thus, the VEGF-NRP-1 system may play an important role in pancreatic carcinoma tumorigenesis. In fact, interruption of the binding of VEGF to NRPs led to decreased mitogenic activity in human endothelial cells and less binding of VEGF to VEGFRs, indicating that NRPs may serve as important coreceptors for VEGF in VEGFR-positive cells.[9,12] The current study clearly demonstrates that VEGF can stimulate the proliferation of pancreatic carcinoma cells in a VEGFR-independent manner and that MoAbs against NRP-1 can successfully block the mitogenic activity of VEGF, indicating the significant role of NRP-1 in pancreatic carcinoma growth.

NRPs have a short cytoplasmic tail (40 amino acids) that is not sufficient for triggering downstream signal transduction.[34] In VEGFR-positive cells, NRPs may form complexes with VEGF to cause or bring it into proximity with VEGFRs on single cells, bridging. Thus, NRPs could enhance the binding of VEGF to VEGFRs, which induce downstream signal transduction pathways. In VEGFR-negative cells, other receptor molecules may play a role in signal transduction through their interactions with NRPs. Two candidate receptors are plexin A and L1, which is a cell adhesion molecule belonging to the immunoglobulin superfamily (L1-CAM). Plexin A, a member of the plexin family, has been shown to form complexes with both NRPs and acts as a signal-transducing subunit when NRPs function as ligand-binding subunits in semaphorin-induced signal transduction pathways.[35] In addition, NRP-1 can form stable complexes with L1-CAM via their extracellular domains.[36,37] L1 may be required for the modulation of the semaphorin signal in NRP/plexin/L1 complexes. L1-deficient axons do not respond to semaphorin 3A stimulation.[38] Further studies aimed at ascertaining the presence of plexin A and L1-CAM or other candidate receptors on the surface of pancreatic carcinoma cells are underway. Lipid rafts, which are specialized microdomains on the cell surface that contain high concentrations of cholesterol and sphingolipids, may also play a role in NRP signal transduction by concentrating signal transducing receptors and NRPs in a microenvironment and bringing them into proximity with one another to trigger the downstream signal pathway. However, Wang et al.[44] reported that NRP-1 can promote cell migration in endothelial cells without assistance from other molecules and demonstrated the importance of the three C-terminal amino acids (SEA-COOH) of NRP-1 with regard to this molecule's cell signaling ability. Whether NRP-1 can independently mediate cell proliferation in pancreatic carcinoma cells remains unclear, and more detailed studies involving chimeric NRP-1 mutants are warranted to elucidate the mechanism by which the NRP-1 signal transduction pathway operates.

In summary, pancreatic carcinoma is a clinically significant condition that carries a poor prognosis. Furthermore, the molecular mechanisms underlying pancreatic carcinoma tumorigenesis are poorly understood. The current study demonstrated that NRP-1 expression was substantially elevated in the pancreatic carcinoma cell line Panc-1 and in pancreatic adenocarcinoma tissue specimens compared with normal pancreatic epithelial cells and pancreatic tissue specimens. VEGFRs were not expressed in any pancreatic carcinoma cell lines or tissue specimens, whereas relatively high levels of VEGF expression were documented in these settings. More notable was the

520

finding that exogenous V[illegible] induced pan[illegible] cell proliferation in the absence of VEGF-[illegible] stimulation of proliferative activity was [illegible] NRP-1-specific antibody, indicating that [illegible] may play a role in the activity of VEGF. Thus VEGF and NRP-1 may participate in a unique autocrine mechanism that mediates pancreatic cell growth and tumor progression. However, the molecular mechanism underlying the interaction between VEGF and NRP-1 remain unknown. Further investigation is warranted to elucidate the mechanisms associated with pancreatic carcinoma progression and to develop more specific diagnostic markers and more effective treatment strategies.

REFERENCES

1. Luo Y, Raible D, Raper JA. Collapsin: a protein in brain that induces the collapse and paralysis of neuronal growth cones. *Cell.* 1993;75:217–227.
2. He Z, Tessier-Lavigne M. Neuropilin is a receptor for the axonal chemorepellent semaphorin III. *Cell.* 1997;90:739–751.
3. Houck KA, Leung DW, Rowland AM, Winer J, Ferrara N. Dual regulation of vascular endothelial growth factor bioavailability by genetic and proteolytic mechanisms. *J Biol Chem.* 1992;267:26031–26037.
4. Neufeld G, Cohen T, Gengrinovitch S, Poltorak Z. Vascular endothelial growth factor (VEGF) and its receptors. *FASEB J.* 1999;13:9–22.
5. Karkkainen MJ, Makinen T, Alitalo K. Lymphatic endothelium: a new frontier of metastasis research. *Nat Cell Biol.* 2002;4:E2–E5.
6. Lymboussaki A, Olofsson B, Eriksson U, Alitalo K. Vascular endothelial growth factor (VEGF) and VEGF-C show overlapping binding sites in embryonic endothelia and distinct sites in differentiated adult endothelia. *Circ Res.* 1999;85:992–999.
7. Witmer AN, van Blijswijk BC, Dai J, et al. VEGFR-3 in adult angiogenesis. *J Pathol.* 2001;195:490–497.
8. Stephenson JM, Banerjee S, Saxena NK, Cherian R, Banerjee SK. Neuropilin-1 is differentially expressed in myoepithelial cells and vascular smooth muscle cells in preneoplastic and neoplastic human breast: a possible marker for the progression of breast cancer. *Int J Cancer.* 2002;101:409–414.
9. Soker S, Takashima S, Miao HQ, Neufeld G, Klagsbrun M. Neuropilin-1 is expressed by endothelial and tumor cells as an isoform-specific receptor for vascular endothelial growth factor. *Cell.* 1998;92:735–745.
10. Latil A, Bieche I, Pesche S, et al. VEGF overexpression in clinically localized prostate tumors and neuropilin-1 overexpression in metastatic forms. *Int J Cancer.* 2000;89:167–171.
11. Banerjee SK, Zoubine MN, Tran TM, Weston AP, Campbell DR. Overexpression of vascular endothelial growth factor 164 and its co-receptor neuropilin-1 in estrogen-induced rat pituitary tumors and GH3 rat pituitary tumor cells. *Int J Oncol.* 2000;16:253–260.
12. Ding H, Wu X, Roncari L, et al. Expression and regulation of neuropilin-1 in human astrocytomas. *Int J Cancer.* 2000;88:584–592.
13. Fakhari M, Pullirsch D, Abraham D, et al. Selective upregulation of vascular endothelial growth factor receptors neu[illegible] and [illegible] in human neuroblastoma [illegible]
14. Kawakami T, Tokunaga T, Hatanaka H, et al. Neuropilin 1 and neuropilin 2 co-expression is significantly correlated with increased vascularity and poor prognosis in nonsmall cell lung carcinoma. *Cancer.* 2002;95:2196–[illegible]
15. Handa A, Tokunaga T, Tsuchida T, et al. Neuropilin-2 expression affects the increased vascularization and is a prognostic factor in osteosarcoma. *Int J Oncol.* 2000;17:291–[illegible]
16. Sanchez-Carbayo M, Socci ND, Lozano JJ, et al. Gene discovery in bladder cancer progression using cDNA microarrays. *Am J Pathol.* 2003;163:505–516.
17. Cohen T, Herzog Y, Brodzky A, et al. Neuropilin-2 is a novel marker expressed in pancreatic islet cells and endocrine pancreatic tumours. *J Pathol.* 2002;198:[illegible]
18. Parikh AA, Liu WB, Fan F, et al. Expression and regulation of the novel vascular endothelial growth factor receptor neuropilin-1 by epidermal growth factor in human pancreatic carcinoma. *Cancer.* 2003;98:720–729.
19. Furukawa T, Duguid WP, Rosenberg L, Viallet J, Galloway DA, Tsao MS. Long-term culture and immortalization of epithelial cells from normal adult human pancreatic ducts transfected by the E6E7 gene of human papilloma virus 16. *Am J Pathol.* 1996;148:1763–1770.
20. Ouyang H, Mou LJ, Luk C, et al. Immortal human pancreatic duct epithelial cell lines with near normal genotype and phenotype. *Am J Pathol.* 2000;157:1623–1631.
21. Lantuejoul S, Constantin B, Drabkin H, Brambilla C, Roche J, Brambilla E. Expression of VEGF, semaphorin SEMA3F, and their common receptors neuropilins NP1 and NP2 in preinvasive bronchial lesions, lung tumours, and cell lines. *J Pathol.* 2003;200:336–347.
22. Kerbel RS, Viloria-Petit A, Okada F, Rak J. Establishing a link between oncogenes and tumor angiogenesis. *Mol Med.* 1998;4:286–295.
23. Veikkola T, Karkkainen M, Claesson-Welsh L, Alitalo K. Regulation of angiogenesis via vascular endothelial growth factor receptors. *Cancer Res.* 2000;60:203–212.
24. Veikkola T, Alitalo K. VEGFs, receptors and angiogenesis. *Semin Cancer Biol.* 1999;9:211–220.
25. Tian X, Song S, Wu J, Meng L, Dong Z, Shou C. Vascular endothelial growth factor: acting as an autocrine growth factor for human gastric adenocarcinoma cell MGC803. *Biochem Biophys Res Commun.* 2001;286:505–512.
26. Decaussin M, Sartelet H, Robert C, et al. Expression of vascular endothelial growth factor (VEGF) and its two receptors (VEGF-R1-Flt1 and VEGF-R2-Flk1/KDR) in non-small cell lung carcinomas (NSCLCs): correlation with angiogenesis and survival. *J Pathol.* 1999;188:369–377.
27. Herold-Mende C, Steiner HH, Andl T, et al. Expression and functional significance of vascular endothelial growth factor receptors in human tumor cells. *Lab Invest.* 1999;79:1573–1582.
28. Itakura J, Ishiwata T, Shen B, Kornmann M, Korc M. Concomitant over-expression of vascular endothelial growth factor and its receptors in pancreatic cancer. *Int J Cancer.* 2000;85:27–34.
29. von Marschall Z, Cramer T, Hocker M, et al. De novo expression of vascular endothelial growth factor in human pancreatic cancer: evidence for an autocrine mitogenic loop. *Gastroenterology.* 2000;119:1358–1372.
30. Ellis LM, Takahashi Y, Fenoglio CJ, Cleary KR, Bucana CD, Evans DB. Vessel counts and vascular endothelial growth factor expression in pancreatic adenocarcinoma. *Eur J Cancer.* 1998;34:337–340.

31. Fujimoto K, Hosotani R, Wada M, et al. Expression of two angiogenic factors, vascular endothelial growth factor and platelet-derived endothelial cell growth factor, in human pancreatic cancer, and its relationship to angiogenesis. *Eur J Cancer.* 1998;34:[illegible]
32. Soker S, Fidder H, Neufeld G, Klagsbrun M. Characterization of novel vascular endothelial growth factor (VEGF) receptors on tumor cells that bind VEGF165 via its exon 7-encoded domain. *J Biol Chem.* 1996;271:5761–5767.
33. Fukahi K, Fukasawa M, Neufeld G, Itakura J, Korc M. Aberrant expression of neuropilin-1 and -2 in human pancreatic cancer cells. *Clin Cancer Res.* 2004;10:581–590.
34. Takahashi T, Fournier A, Nakamura F, et al. Plexin-neuropilin-1 complexes form functional semaphorin-3A receptors. *Cell.* 1999;99:59–69.
35. Neufeld G, Kessler O, Herzog Y. The interaction of neuropilin-1 and neuropilin-2 with tyrosine-kinase receptors for VEGF. *Adv Exp Med Biol.* 2002;515:81–90.
36. Rohm B, Ottemeyer A, Lohrum M, Puschel AW. Plexin [illegible] semaphorin [illegible] *Mech Dev.* [illegible]
37. [illegible]agnoux I, Artigiani S, Chen H, et al. Plexin[illegible] semaphorin [illegible] *Cell.* 1999;99:[illegible]
38. Puschel AW. The function of neuropilin/plexin complexes. *Adv Exp Med Biol.* 2002;515:71–80.
39. Castellani V, Chedotal A, Schachner M, Faivre-Sarrailh C, Rougon G. Analysis of the L1-deficient mouse phenotype reveals cross-talk between Sema3A and L1 signaling pathways in axonal guidance. *Neuron.* 2000;27:237–249.
40. Castellani V, Falk J, Rougon G. Semaphorin3A-induced receptor endocytosis during axon guidance responses is mediated by L1 CAM. [illegible] *Dev.* 2004;[illegible]
41. Wang L, Zeng H, Wang P, Soker S, Mukhopadhyay D. Neuropilin-1-mediated vascular permeability factor/vascular endothelial growth factor-dependent endothelial cell migration. *J Biol Chem.* 2003;278:48848–48860.

521

Developmental Cell, Vol. 5, 45–57, July, 2003, Copyright ©2003 by Cell Press

Neuropilin-1 Conveys Semaphorin and VEGF Signaling during Neural and Cardiovascular Development

Chenghua Gu,[1,2] E. Rene Rodriguez,[3] Dorothy V. Reimert,[1,4] Tianzhi Shu,[4] Bernd Fritzsch,[5] Linda J. Richards,[4] Alex L. Kolodkin,[1,*] and David D. Ginty[2,*]
[1]Department of Neuroscience
[2]Howard Hughes Medical Institute
[3]Department of Pathology
The Johns Hopkins University School of Medicine
725 North Wolfe Street
Baltimore, Maryland 21205
[4]Department of Anatomy and Neurobiology
School of Medicine
The University of Maryland, Baltimore
Baltimore, Maryland 21201
[5]Department of Biomedical Sciences
Creighton University
Omaha, Nebraska 68178

Summary

Neuropilin-1 (Npn-1) is a receptor that binds multiple ligands from structurally distinct families, including secreted semaphorins (Sema) and vascular endothelial growth factors (VEGF). We generated *npn-1* knockin mice, which express an altered ligand binding site variant of Npn-1, and *npn-1* conditional null mice to establish the cell-type- and ligand specificity of Npn-1 function in the developing cardiovascular and nervous systems. Our results show that VEGF-Npn-1 signaling in endothelial cells is required for angiogenesis. In striking contrast, Sema-Npn-1 signaling is not essential for general vascular development but is required for axonal pathfinding by several populations of neurons in the CNS and PNS. Remarkably, both Sema-Npn-1 signaling and VEGF-Npn-1 signaling are critical for heart development. Therefore, Npn-1 is a multifunctional receptor that mediates the activities of structurally distinct ligands during development of the heart, vasculature, and nervous system.

Introduction

During development, many distinct processes contribute to organ morphogenesis including cell proliferation, migration, differentiation, and neural innervation and vascularization. These developmental events are under the control of numerous cues present in the extracellular environment. One cell surface receptor whose function has been implicated in development of both the cardiovascular and nervous systems is neuropilin-1 (Npn-1), yet the cell-type- and ligand specificity of Npn-1 signaling during development of these interdependent organ systems is not clear.

Npn-1 is a type I transmembrane protein with a small cytoplasmic domain and multiple extracellular domains capable of mediating a variety of protein/protein interactions (Fujisawa et al., 1997). While Npn-1 can mediate heterophilic cell adhesion (Fujisawa et al., 1997; Shimizu et al., 2000), it is also the ligand binding subunit of the semaphorin 3A/collapsin-1 (Sema3A) receptor complex (He and Tessier-Lavigne, 1997; Kolodkin et al., 1997). Semaphorins comprise a large family of proteins first described as regulators of axon pathfinding (Luo et al., 1993). Class 3 semaphorins, including Sema3A, are secreted vertebrate semaphorins that can act as potent axon repellents for specific populations of neurons. These ligands appear to exert their chemorepulsive effects via receptor complexes which include the ligand binding subunit Npn-1, or its close family member Npn-2, and a signal transducing subunit consisting of one of four class A plexin proteins (He et al., 2002). Six class 3 secreted semaphorins have been identified, Sema3A, 3B, 3C, 3D, 3E, and 3F, and each of these ligands can bind with high affinity to either Npn-1, Npn-2, or to both. Moreover, Npn-1 is necessary for Sema3A-mediated chemorepulsion, whereas Npn-2 is necessary for Sema3F-mediated chemorepulsion.

Interestingly, Npn-1 is also expressed in endothelial cells and can bind with high affinity to select isoforms of vascular endothelial growth factor (VEGF) (Soker et al., 1998). VEGFs, including $VEGF_{165}$, are critical regulators of vasculogenesis, angiogenesis, and vascular remodeling. Likewise, Npn-2 binds to a distinct but overlapping set of VEGF family ligands (Neufeld et al., 2002). The biological effects of VEGFs are mediated by their signaling receptors, the receptor tyrosine kinases Flt-1 (VEGFR-1), Flk-1/KDR (VEGFR-2), and VEGFR-3 (Ferrara, 2001; Neufeld et al., 1999). Thus, VEGF holoreceptors are likely comprised of VEGFR alone or VEGFR complexes with Npn-1 and/or Npn-2. Indeed, overexpression of Npn-1 in vascular endothelial cells enhances both the affinity labeling of $VEGF_{165}$ to VEGFR-2 and also $VEGF_{165}$-induced cell chemotaxis (Soker et al., 1998).

Despite these in vitro findings, how Npn-1 and Npn-2 function in vivo as requisite coreceptors for VEGF ligands during development remains poorly understood. Analysis of *npn-1* and *npn-2* null mice has, however, provided some insight into neuropilin functions in vivo. *npn-1* null mice die midway through gestation, ~E10.5–E12.5, and exhibit defects in the heart, vasculature, and nervous system (Kawasaki et al., 1999; Kitsukawa et al., 1997). Furthermore, a genetic interaction between VEGF and Npn-1 has been observed in zebrafish (Lee et al., 2002). In contrast to *npn-1* null mice, *npn-2* null mice are viable but exhibit multiple nervous system defects and have a paucity of lymphatic vessels (Chen et al., 2000; Giger et al., 2000; Yuan et al., 2002). *npn-1/npn-2* double mutant null mice die early in gestation, around E8, because of severe vascular anomalies in both the embryo and placenta (Takashima et al., 2002). The various defects in *neuropilin* mutant mice could be due to deficiencies of Sema-Npn signaling, VEGF-Npn signaling, or both. In fact, mouse genetic analyses have revealed that, like VEGFs, two secreted semaphorins,

*Correspondence: kolodkin@jhmi.edu (A.L.K.), dginty@jhmi.edu (D.D.G.)

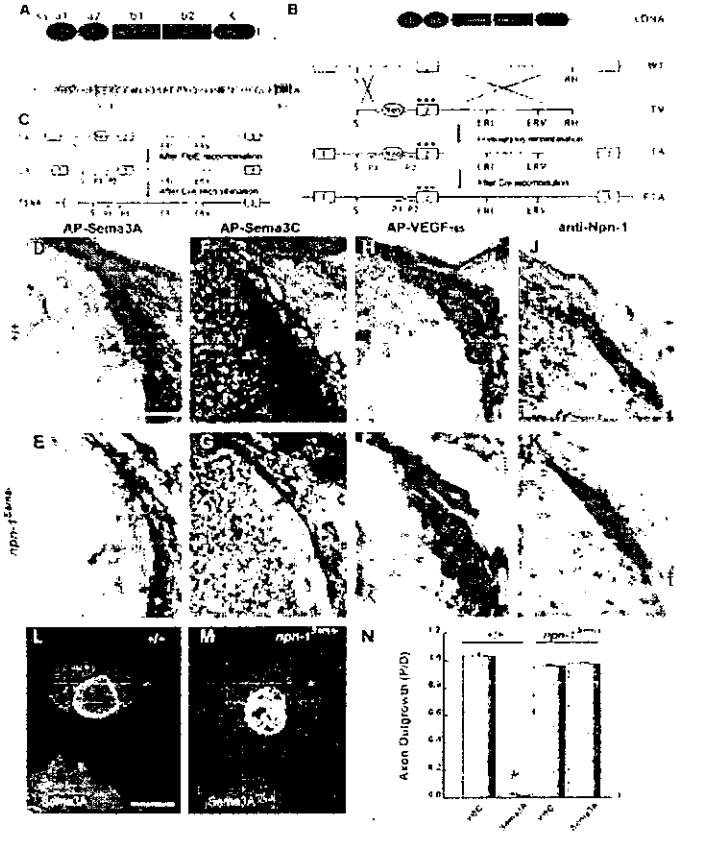

Figure 1. Generation and Characterization of *npn-1*$^{a/a}$ Mice

(A) Extracellular domain structure of the Npn-1 protein and a 7 amino acid substitution in the N terminus of the Npn-1 a1 CUB domain (Gu et al., 2002).

(B) Gene targeting strategy used to generate *npn-1*$^{a/a}$ mice. The boxes represent *npn-1* exons 1–3. The targeting vector (TV) contains a mutated exon 2 encoding a 7 amino acid substitution (three stars) and a *pgk-neo* cassette flanked by loxP sites (triangles) placed within the intron upstream of exon 2. The *pgk-neo* cassette was excised upon crossing mice with an FA with mice expressing germline Cre recombinase. The final targeted allele (FTA) contains the mutated *npn-1* exon 2 and one loxP site within the upstream intron.

(C) Gene targeting strategy for generation of *npn-1* null and conditional mutant mice. The targeted allele (TA) contains an *FRT* (squares) flanked neo cassette and loxP sites (triangles) flanking exon 2. After crossing mice harboring the TA with germline FlpE recombinase mice, the *pgk-neo* cassette was removed and the conditional targeted allele (CA) contained two loxP sites flanking exon 2. After crossing with mice carrying Cre recombinase under the control of the *Tie-2* promoter, exon 2 was excised to generate a tissue specific *npn-1* null allele (TSNA). *Npn-1* null mice were obtained by crossing mice harboring the CA with mice expressing Cre recombinase in the germline.

(D–I) Alkaline phosphatase (AP)-tagged ligand binding to sections of the DREZ (arrowhead in [D] and [E]) from wild-type littermate controls

Sema3A and Sema3C, control specific aspects of cardiovascular development (Behar et al., 1996; Feiner et al., 2001). Likewise, in addition to their prominent roles as regulators of vascular and heart development, VEGFs may serve as potent trophic factors for motor, sensory, and sympathetic neurons (Oosthuyse et al., 2001; Sondell et al., 1999, 2000). Moreover, both secreted semaphorins and VEGFs are widely expressed within both the nervous system and cardiovascular primordium throughout development. Thus, many secreted semaphorin and VEGF proteins are implicated in both neural and cardiovascular development. *Npn-1* null mice die midway through gestation, very early in the development of the cardiovascular and nervous systems, and therefore how Npn-1 mediates semaphorin and/or VEGF signaling in the heart, vasculature, and nervous system is not known.

To unravel Npn-1's ligand- and cell-type-specific functions and thereby shed light on the regulation of cardiovascular and neuronal development, we sought to selectively disrupt Npn-1 interactions with semaphorins while retaining interactions with VEGFs. Guided by the structure of the bovine Spermadhesin CUB domain (Romero et al., 1997), we identified 7 amino acids located on two adjacent hydrophilic loops of the amino-terminal Npn-1 CUB domain that are critical for binding to the Sema domain of class 3 semaphorins. Substitution of these 7 amino acids completely disrupts Sema-Npn-1 binding but does not affect $VEGF_{165}$-Npn-1 binding or $VEGF_{165}$'s ability to associate with and activate its signaling receptor, VEGFR2 (Gu et al., 2002). Here, we describe a mouse mutant (*npn-1*$^{Sema-}$) that was generated by altering the coding determinants of these 7 amino acids within the *npn-1* locus by homologous recombination in ES cells. The *npn-1*$^{Sema-}$ mouse expresses normal levels of Npn-1 protein, but Sema-Npn-1 signaling is abolished while VEGF-Npn-1 signaling is retained. For complementary analyses, we also used a Cre-loxP strategy to generate a conditional *npn-1* null mouse. Furthermore, we crossed *npn-1*$^{Sema-}$ mice and *npn-2* null mice to generate double mutant mice in which all secreted semaphorin signaling is abolished. Analyses of these mutant mice allow us to determine the ligand- and cell-type specificity of Npn-1 function in vivo. Our findings indicate that Npn-1 coordinates the activities of structurally distinct ligands that control the development of the heart, vasculature, and nervous system.

Results

Generation of *npn-1*$^{Sema-}$ Mice

We first sought to delineate the ligand specificity of Npn-1 function during neural and cardiovascular development. Our recent structure function analysis revealed that substitution of 7 amino acids located in three regions of the amino-terminal Npn-1 CUB domain completely disrupts Sema-Npn-1 binding but does not affect $VEGF_{165}$-Npn-1 binding or the ability of $VEGF_{165}$ to associate with or activate its signaling receptor, VEGFR2 (Gu et al., 2002). Therefore, we used a gene replacement strategy to generate a knockin mouse, which we call *npn-1*$^{Sema-}$, that expresses only this variant Npn-1 protein (Figure 1). Homozygous *npn-1*$^{Sema-}$ knockin mice express normal levels of Npn-1^{Sema-} protein (Figures 1J and 1K). Moreover, alkaline phosphatase (AP) section binding experiments show that *npn-1*$^{Sema-}$ mice display normal AP-$VEGF_{165}$ binding (Figures 1H and 1I), but little or no AP-Sema3A or AP-Sema3C binding, to endogenous receptors on axons within the dorsal root entry zone (DREZ; Figures 1D–1G). Importantly, neurons from *npn-1*$^{Sema-}$ mice are completely unresponsive to Sema3A. In a three-dimensional collagen matrix, wild-type dorsal root ganglia (DRG) sensory axons were robustly repelled by Sema3A-transfected COS cell aggregates, whereas sensory axons from *npn-1*$^{Sema-}$ mutant mice were not repelled by Sema3A and often grew directly into Sema3A-expressing cell aggregates (Figures 1L–1N).

Interestingly, unlike *npn-1* null mice, which die around E12.5 (Kitsukawa et al., 1997), homozygous *npn-1*$^{Sema-}$ mice survive until birth. This suggests that VEGF-Npn-1 signaling, but not Sema-Npn-1 signaling, is critical for embryonic viability. Approximately 25% of P0 mice from *npn-1*$^{Sema-}$ intercrosses are *npn-1*$^{Sema-}$; however, only 60% of these *npn-1*$^{Sema-}$ mice are alive at P7. Seventy percent of P7 survivors are growth retarded, and at least some of these can survive into adulthood. The viability of *npn-1*$^{Sema-}$ mice allowed us to investigate semaphorin-dependent and -independent Npn-1 signaling events during both embryonic and postnatal development. To define the role of Sema-Npn-1 signaling in development of the nervous system, we assessed the integrity of both PNS and CNS projections in *npn-1*$^{Sema-}$ mice and, for comparison, in *npn-1* null embryos when feasible.

Npn-1 and Neural Development

Embryonic Cranial and Spinal Nerves

As observed previously (Kitsukawa et al., 1997), whole-mount neurofilament immunostaining revealed that both cranial and spinal nerves are severely defasciculated and abnormally extended in both E11.5 and E12.5 *npn-1* null embryos (Figures 2B and 2F). Abnormal projections of cranial and spinal nerves, including defasciculation and exuberant axon arborizations, were also observed in *npn-1*$^{Sema-}$ mice (Figures 2D and 2H). Interestingly, some of these neural defects appear qualitatively different between *npn-1* null and *npn-1*$^{Sema-}$ mice. For example, distal axons of the ophthalmic nerve in *npn-1* null mice appear considerably more defasciculated and disorganized than those observed in *npn-1*$^{Sema-}$ mice (Figures 2F and 2H). Axon branches from the ophthalmic nerve extend much further in the *npn-1*$^{Sema-}$ mouse than in either *npn-1* null or wild-type mice, and these branches exhibit a more regular and equally spaced distribution in the region surrounding the developing eye (n = 7). The differences between *npn-1* null and *npn-1*$^{Sema-}$ trigeminal projections may be due to semaphorin-independent Npn-1 functions in these neurons, including axon fasciculation mediated through Npn-1 heterophilic adhesive events (Shimizu et al., 2000; Takagi et al., 1987). Therefore, Sema-Npn-1 signaling is indeed required for cranial and spinal nerve projections, and additional Sema-independent Npn-1 functions may promote fasciculation of some peripheral nerves.

Vestibulocochlear Projections

We next assessed the role of Sema-Npn-1 signaling during development of the vestibulocochlear nerve (nVIII), which conveys sensory information from hair cells of the ear to the brain stem. Lipophilic dye placed into the brainstem shows that afferent fibers of nVIII innervate each of the sensory end organs of the ear by E12.5 (Figure 3A). The E12.5 *npn-1*$^{Sema-}$ mutant mice have additional smaller fiber bundles that extend beyond their normal termination zones within the sensory end organs (Figures 3B and 3C) to form at least three types of defects (four out of four). In most *npn-1*$^{Sema-}$ mice (three out of four), aberrant fibers course between the sensory epithelia of the anterior and horizontal semicircular canal cristae, piercing through the otic capsule to reach the skin above the ear (Figure 3B). In other *npn-1*$^{Sema-}$ mice (three out of four), fibers emanate from the utricle, run anteriorly around the ear, and terminate at or near the posterior canal crista. One *npn-1*$^{Sema-}$ mouse had fibers that formed a loop around the forming cochlea (Figure 3C). Errant projections were not observed in any of the wild-type mice; however, a few errant fibers projecting to the posterior crista were observed in some heterozygous mice (two out of three; data not shown).

These vestibular nerve projection defects persisted in E14.5 (one out of one) and E15.5 (three out of five) *npn-1*$^{Sema-}$ mice but not in either wild-type or heterozygous mice (two out of two). Errant afferent projections extended beyond the anterior and horizontal canal epithelium (Figure 3E), pierced the otocyst wall, and extended toward the auricular branch of the trigeminal nerve (data not shown). Dye injection into auriculotemporal nerve in three separate animals resulted in retrograde labeling of vestibular fibers and neurons in the rostral part of the vestibular ganglion (Figures 3F–3G). Apparently, a subset of afferent fibers of the vestibular nerve project beyond their normal termination fields in the absence of Sema-Npn-1 signaling to innervate areas of the skin normally innervated exclusively by the trigeminal nerve. Nevertheless, these fibers maintain their central projections and terminate in the vestibular nuclei in the brain stem rather than in the nearby trigeminal sensory nuclei (data not shown). Therefore, Sema-Npn-1 signaling is required for guidance of peripheral projections of bipolar neurons of the vestibular ganglion, presumably providing a stop signal near the sensory epithelium.

Sensory Afferent Projections to the Spinal Cord

We next examined the projections of DRG sensory axons into spinal cord gray matter of E14.5 and postnatal day 2 (P2) *npn-1*$^{Sema-}$ mice. Normally, cutaneous afferent

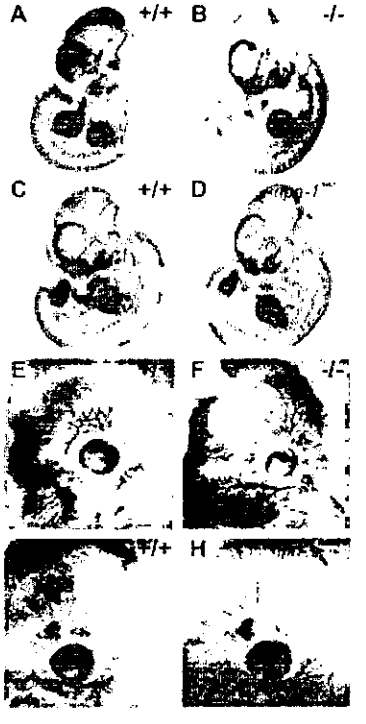

Figure 2. Peripheral Projections of Cranial and Spinal Nerves Are Severely Disorganized in Both *npn-1* Null and *npn-1*$^{Sema-}$ Mice

(A–D) Whole-mount anti-neurofilament staining of E11.5 *npn-1* null (B), wild-type littermate (A), homozygous *npn-1*$^{Sema-}$ (D), and wild-type littermate (C) embryos. The ophthalmic branch of the trigeminal nerve (upper arrowhead in [D]) and spinal nerves (lower arrowhead in [D]) are disorganized in both *npn-1* null (B) and *npn-1*$^{Sema-}$ mice (D).

(E–H) Whole-mount anti-neurofilament staining of the ophthalmic nerve at E12.5 homozygous *npn-1* null (F), wild-type littermate (E), homozygous *npn-1*$^{Sema-}$ (H), and wild type littermate (G) embryos. Note the exuberant extension and more regular distribution of ophthalmic nerve branches in *npn-1*$^{Sema-}$ as compared to *npn-1* null ophthalmic projections. Scale bar: (A–D) 0.5 mm; (E–H), 0.2 mm.

(D, F, and H) and *npn-1*$^{Sema-}$ mice (E, G, and I) with AP-Sema3A (D and E), AP-Sema3C (F and G), or AP-VEGF (H and I).

(J–K) Expression of Npn-1 protein in *npn-1*$^{Sema-}$ mice (K) and wild type littermate control mice (J).

(L–M) DRG sensory neuron axons from wild-type embryos are repelled by Sema3A-expressing COS cells (L) while DRG axons from *npn-1*$^{Sema-}$ embryos are not repelled (M).

(N) Quantitation of repulsion experiments. The repulsive activity is measured by the axon outgrowth ratio P/D, where P is the extent of axon outgrowth on the side proximal to the cell aggregate, and D is the extent of axon outgrowth distal to the cell aggregate. Shown are means ± SEM of 22 (wild-type) and 39 (*npn-1*$^{Sema-}$) explants from three independent experiments ($p < 0.001$, two-way ANOVA). Vec, vector-transfected COS cells; Sema3A, Sema3A-expressing COS cells. Scale bars: (D–I), 50 μm; (J–K), 40 μm; (L–M), 45 μm.

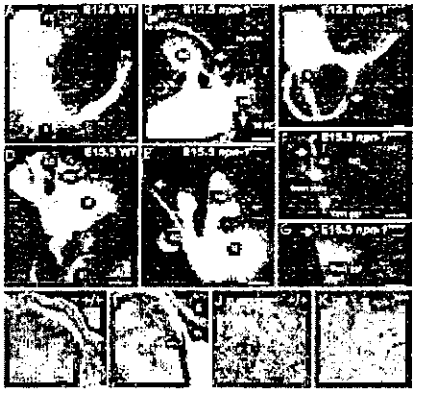

Figure 3. Sema-Npn-1 Signaling Is Required for Sensory Afferent Innervation of the Inner Ear and Spinal Cord

(A–C) In E12.5 *npn-1*$^{lacZ/-}$ mice, vestibular nerve fibers extend beyond the anterior and horizontal cristae (AC, HC) and reach the skin above the ear ([B], top arrow). In addition, fiber bundles extend from the utricle (U) to the posterior crista (PC) where they may leave the ear through the round window ([B], bottom arrow; data not shown). In some animals, vestibular fibers are observed projecting around the forming cochlea without innervating any target (CC, arrow).

(D–G) E15.5 *npn-1*$^{lacZ/-}$ mutants form inner ear afferent fibers to the skin. These fibers extend beyond the anterior cristae (E), pass through the otic capsule, and run together with the auriculotemporal nerve to the skin anterior to the auricle (arrow). Injection of dye into this area of the skin labels nVIII fibers that pass through the lateral otic wall (F) and pass underneath the canal cristae where some fibers branch and provide afferents to these epithelia (arrow). These fibers come from vestibular ganglion neurons (G) which project centrally into vestibular nuclei (data not shown).

(H–K) Abnormal central projections of spinal sensory afferents. TrkA immunohistochemistry of E14 (H and I) and P2 (J and K) lumbar spinal cord in *npn-1*$^{lacZ/-}$ (I and K) and wild-type littermates (H and J), examined by confocal microscopy. Dorsal spinal cord is at the top. Scale bars: (A–G), 100 μm; (H–K), scale bar in (G) is equal to 200 μm in (H)–(K).

axons project to the DREZ and then stall during a "waiting period," which in the mouse extends from ~E11 until ~E15, before innervating the spinal cord. As shown in Figure 3H, TrkA-positive fibers in wild-type embryos are restricted to the DREZ at E14.5 (n = 3). In contrast, many TrkA-positive fibers in *npn-1*$^{lacZ/-}$ mice have already entered the gray matter at E14.5, and a subset of these errant projections extends into the most ventral regions of the spinal cord (Figure 3I and data not shown; n = 3). At a later time, P2, TrkA-positive fibers in wild-type mice have invaded the spinal cord and are completely restricted to their target fields within the dorsal laminae (Figure 3J, n = 7). In contrast, in *npn-1*$^{lacZ/-}$ mice, some axons were observed outside of their normal termination zones, traveling along the midline and into the medial-ventral spinal cord (Figure 3K, n = 7). Similar aberrant projections were reported in *sema3A* null mice (Behar et al., 1996). Thus, Sema3A signaling through Npn-1 is indeed required for guiding the central projections of a subset of TrkA-positive axons of cutaneous sensory neurons during development.

Corpus Callosum

Other later developing CNS fiber tracts were also disrupted in *npn-1*$^{lacZ/-}$ mice including axons of the corpus callosum, which project to the contralateral cortical hemisphere. This fiber tract normally binds avidly to the AP-Sema3A fusion protein (Figure 1I). DiI labeling experiments revealed callosal defects in all E17.5 *npn-1*$^{lacZ/-}$ embryos examined (Figures 4B, 4C, and 4E–4H, n = 10). Corpus callosum phenotypes varied from mild, in which some callosal axons deviated from the main bundle into the glial wedge and septum but most crossed the midline (Figures 4B and 4E), to more severe phenotypes where the main callosal bundle was highly defasciculated and few, if any, callosal axons crossed the midline (Figures 4C and 4F). In the most extreme cases we observed complete agenesis of the corpus callosum, resulting in the formation of Probst bundles (Figures 4G and 4H). Callosal defects were not observed in any wild-type or heterozygote littermate controls (n = 10; Figures 4A and 4D).

Entorhinohippocampal Projections

To determine whether Sema-Npn-1 signaling is required for the generation of layer-specific connections in the hippocampus, we next analyzed the development of entorhinohippocampal connections in the *npn-1*$^{lacZ/-}$ mice. At E18–P2, entorhinal fibers terminate in the stratum lacunosum-moleculare whereas commissural/associational fibers terminate in the stratum radiatum and stratum oriens (Super and Soriano, 1994). For these experiments, DiI was injected into the entorhinal cortex of P2 *npn-1*$^{lacZ/-}$ mice and wild-type littermate controls to visualize entorhinohippocampal projections. As in previous studies, entorhinohippocampal fibers were restricted in wild-type mice to the ipsilateral stratum lacunosum-moleculare, with no labeled axons present in either the stratum radiatum or stratum oriens (Figure 4J, n = 7). In contrast, in *npn-1*$^{lacZ/-}$ mice, entorhinohippocampal axons were no longer restricted in the stratum lacunosum-moleculare of the ipsilateral hippocampus. Many fibers had innervated ectopic layers, mostly the stratum radiatum of the CA1 field (Figure 4K, n = 9). An entorhinohippocampal projection defect was also observed in *sema3A* null mice (Pozas et al., 2001), but that phenotype appeared much less severe since most fibers were observed to correctly innervate the stratum lacunosum-moleculare and only a few fibers were found to innervate ectopic hippocampal layers such as the

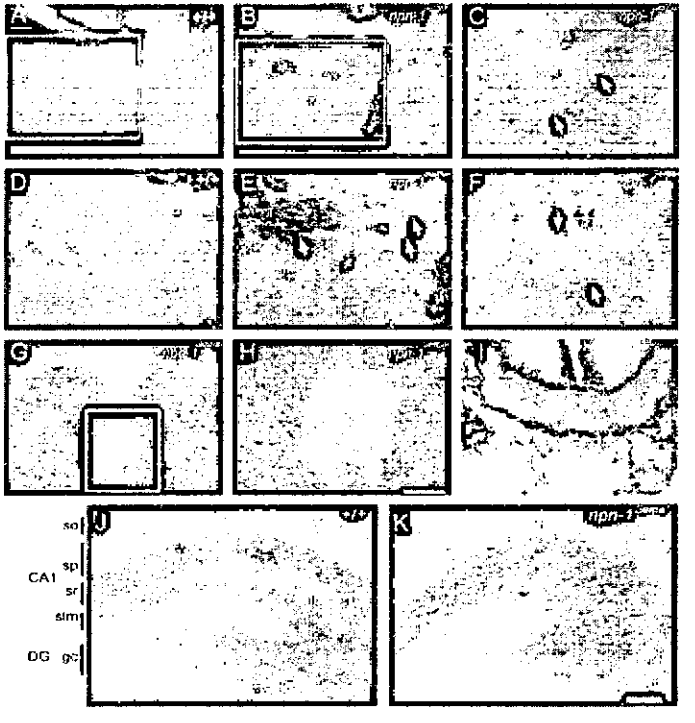

Figure 4. Axonal Projection Defects in the Corpus Callosum and Hippocampus in *npn-1*$^{lacZ/-}$ Mice

(A–H) DiI labeling at E17.5 was used to investigate development of the corpus callosum in wild-type (A and D) and *npn-1*$^{lacZ/-}$ mice (B, C, and E–H). The corpus callosum developed normally in all wild-type littermate embryos analyzed (n = 10), whereas in all *npn-1*$^{lacZ/-}$ embryos examined (n = 10) callosal axons (red) displayed varying degrees of defasciculation from more mild phenotypes (arrows in [E]) to more severe phenotypes (arrows in [C] and [F]). In the most extreme cases, callosal axons formed Probst bundles (G and H). Sections were double labeled with GFAP immunohistochemistry to label midline glial structures (A–H). In some cases, axons grew through the glial wedge (green labeling in [E]) and into the septum.

(I) AP-Sema3A section binding reveals a high level of Sema3A binding to axons of the E17.5 corpus callosum in wild-type mice. (D), (E), and (H) are high-magnification views of the boxed regions in (A), (B), and (G), respectively.

(J–K) Sema-Npn-1 signaling is crucial for layer-specific targeting of entorhinohippocampal projections. Coronal sections of brains of P2 wild-type (J) and *npn-1*$^{lacZ/-}$ littermate mice (K) showing DiI-labeled (red) entorhinohippocampal axons. The sections were counterstained with bisbenzimide (blue) to reveal the hippocampal architecture. In wild-type mice, entorhinal fibers (red) are restricted to the stratum lacunosum-moleculare (slm) (J). In contrast, entorhinal fibers of *npn-1*$^{lacZ/-}$ mice are found in the slm layer and also ectopic layers such as the stratum radiatum (sr) of the CA1 field (K). DG, dentate gyrus; slm, stratum lacunosum-moleculare; sp, stratum pyramidale; sr, stratum radiatum. Scale bars: (A–C, F, and I), 150 μm; (D), 200 μm; (H), 60 μm; (J and K), 100 μm.

stratum radiatum and the hilus (Pozas et al., 2001). Therefore, we conclude that Sema3A, and probably additional secreted semaphorins in the hippocampus, act through Npn-1 to restrict axonal projections of entorhinohippocampal neurons to their specific targets within the stratum lacunosum-moleculare.

524

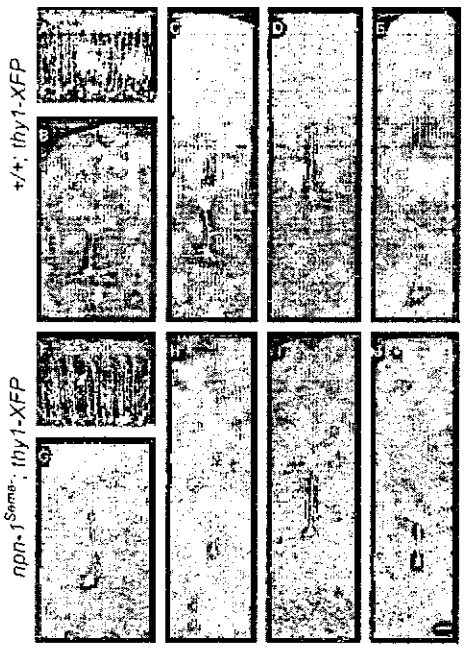

Figure 5. Sema-Npn-1 Signaling Is Required for Growth of Basal Dendrites, but Not for Apical Dendrite Orientation

(A and F) Orientation of apical dendrites of layer 5 pyramidal neurons from neocortex of P2 mutant (*npn-1Sema- ;thy1-YFP*) (F) and control littermates (*+/+;thy1-YFP*) (A).

(B and G) Similar dendritic morphologies of cingulate cortical neurons from P14 mutant (*npn-1Sema- ;thy1-GFP-m*) (G) and control littermates (*+/+;thy1-GFP-m*) (B).

(C–E and H–J) Dendritic morphologies of individual GFP-positive pyramidal neurons from P14 mutant (*npn-1Sema- ;thy1-GFP-m*) (H–J) and control littermates (*+/+;thy1-GFP-m*) (C–E). While apical dendrite and axon orientation appears similar in mutants (H–J) and littermate controls (C–E), basal dendrites are less elaborate in mutants (H–J) compared to controls (C–E). Scale bar: 50 μm.

Cortical Neuron Dendrites

In addition to their roles as axonal chemorepellents, secreted semaphorins have also been implicated in dendrite formation (Behar et al., 1996; Polleux et al., 1998, 2000). Therefore, we next assessed the integrity of both apical and basal dendrites of layer 5 pyramidal neurons of *npn-1Sema-* mice. Since many *npn-1Sema-* mice are viable, our analysis was carried out with P2 (n = 4), P6 (n = 2), and P14 (n = 3) brains, times at which dendrites of layer 5 pyramidal neurons are elaborated. To examine cortical neuron morphology, we crossed *npn-1Sema-* mice with mice that express YFP in all layer 5 neurons (*npn-1Sema- ;thy1-YFP* mice, Figures 5A and 5F) or in mice expressing GFP in a small subset of neurons (*npn-1Sema- ;thy1-GFP-m* mice, Figures 5B–5E and 5G–5J) (Feng et al., 2000). Although Sema3A can serve as an attractant for apical dendrites and a repellent for axons of cortical neurons in vitro (Polleux et al., 1998, 2000), we did not observe apical dendrite or axon orientation defects in cortical neurons of either the *npn-1Sema- ;thy1-YFP* mice (Figure 5F) or the *npn-1Sema- ;thy1-GFP-m* mice (Figures 5G–5J, and data not shown). We did, however, observe that the basal dendrites of layer 5 cortical neurons within the neocortex (compare Figures 5C–5E and 5H–5J), but not neurons in the cingulate cortex (compare Figures 5B and 5G), of *npn-1Sema- ;thy1-GFP-m* mice were markedly diminished in both length and complexity. Thus, Sema-Npn-1 signaling contributes to basal, but not apical, cortical neuron dendrite development.

Npn-1 and Development of the Cardiovascular System

While our results support a model in which Sema-Npn-1 signaling is necessary for the establishment of PNS and CNS projections during both early and late embryonic development, the ligand dependence of Npn-1 signaling for cardiovascular system development is more complex. *npn-1* is expressed in multiple cell types that contribute to development of the cardiovascular system including cardiac neural crest cells (Brown et al., 2001; Feiner et al., 2001) and endothelial cells (Soker et al., 1998). Moreover, mice with null mutations in *npn-1*, or in the genes encoding Npn-1 ligands VEGF-A, VEGF-B, PLGF-2, Sema3A, and Sema3C, exhibit heart and/or

vasculature defects (Behar et al., 1996; Brown et al., 2001; Feiner et al., 2001; Kawasaki et al., 1999; Neufeld et al., 1999; Takashima et al., 2002). Thus, to understand how VEGF-Npn-1 signaling and Sema-Npn-1 signaling contribute in vivo to cardiovascular development, we first determined whether Npn-1 is required in endothelial cells for vasculature development.

Npn-1 Signaling and Angiogenesis

Endothelial cell-specific *npn-1* null mice were generated by crossing homozygous "floxed" *npn-1* conditional mice (Figure 1C) with *Tie-2-Cre* transgenic mice (Kisanuki et al., 2001), which express Cre recombinase only in endothelial cells (*C/C;Cre* mice). For some analyses, we employed compound heterozygous mice (one floxed *npn-1* allele, one null *npn-1* allele, and one *Tie-2-Cre* transgenic allele; called *C/- ;Cre* mice), which allowed for more efficient Cre-mediated removal of Npn-1. We first examined vasculature integrity in *C/- ;Cre* and control littermate mice by whole-mount PECAM immunostaining and isolectin staining. Whole-mount PECAM staining revealed dramatic systemic vascular deficiencies in E12.5 *C/- ;Cre* mice which probably account for the mid-to-late embryonic lethality of these mice. For example, the abdominal wall contains only distended vessels and lacks the medium and small-diameter branched vessels readily observed in littermate controls (Figures 6A–6D; n = 4). In addition, isolectin staining of horizontal brain sections from E13.5 *C/- ;Cre* mice revealed dramatic defects in the vasculature of the developing brain. While vessels are evenly distributed and normally branched in the developing diencephalon and telencephalon of control embryos (Figures 6G and 6I), vessels in brains from *C/- ;Cre* littermates are large, dramatically underdeveloped, and not branched (Figures 6H and 6J, and data not shown). Interestingly, none of these vascular defects were observed in *npn-1Sema-* embryos (Figures 6E, 6F, 6K, and 6L; n = 4). These results show that VEGF-Npn-1 signaling, and not Sema-Npn-1 signaling, within endothelial cells is essential for general development of the vasculature.

Npn-1 Signaling in Heart Development

We next examined the cell-type- and ligand dependence of Npn-1 signaling for development of the heart. For this analysis we used *C/C;Cre* mice, which were found to die perinatally (25 out of 25 animals). These mice exhibit multiple cardiac defects, including persistent truncus arteriosus (Figure 7D; Table 1; 17 out of 17 mice), which results from a failure of septation of the cardiac outflow tract. Thus, *C/C;Cre* mice share common pulmonary artery and aortic roots. Some *C/C;Cre* mutant mice also exhibited misplacement (anomalous origin) of the coronary arteries (Figure 7C and arrow in Figure 7D; Table 1, four out of ten mice) and ventricular septal defects (three out of eight mice, data not shown). Truncus arteriosus was also observed in experiments using *C/- ;Cre* embryos (four out of four mice; data not shown). In contrast, truncus arteriosus was not observed in *npn-1Sema-* mice (Figure 7F; Table 1). Thus, Sema-independent Npn-1 signaling in endothelial cells is essential for septation of the cardiac outflow tract and heart development.

While the precise mechanism of outflow tract septation remains to be described, cardiac neural crest cells have been implicated in this process (Creazzo et al., 1999). Interestingly, a previous report showed that one of the secreted semaphorins, Sema3C, is required for septation of the outflow tract, possibly because it guides the migration of cardiac neural crest cells into the proximal outflow tract during heart development (Feiner et al., 2001). While the nature of the Sema3C receptor in vivo is not known, this secreted semaphorin binds with high affinity to both Npn-1 and its close relative Npn-2, and a Npn-1/Npn-2 heterodimer may serve as a Sema3C receptor in sympathetic neurons (Chen et al., 1997, 1998; Takahashi et al., 1998). Since impaired VEGF and/or Sema3C signaling may result in the septation defects observed in *C/C;Cre* mice, we next examined the cardiac outflow tracts in *npn-1Sema-* mice, *npn-2* null mice (Giger et al., 2000), and in *npn-1Sema- ;npn-2 -/-* double mutant mice to distinguish between these possibilities. Both *npn-1Sema-* mice and *npn-2* null mice have normal cardiac outflow tracts and great vessels (11 out of 11 mice and 8 out of 8 mice, respectively; Figures 7E and 7F; Table 1). Interestingly, 66% of *npn-1Sema- ;npn-2 -/-* double mutant mice displayed a persistent truncus arteriosus (six out of nine; Figures 7H and 7J; Table 1). Some *npn-1Sema- ;npn-2 -/-* double mutant mice also exhibited ventricular septal defects (Figure 7K). Since in certain genetic backgrounds a similar outflow tract phenotype was observed in *sema3C* null mice, these results taken together suggest that the Sema3C receptor is either Npn-1 or Npn-2 (either receptor alone being sufficient). Thus, at least two distinct ligands, Sema3C and a VEGF family member, each act through Npn-1 to coordinate outflow tract septation. Finally, nearly all of the *npn-1Sema-* mice (10 out of 11) and *npn-1Sema- ;npn-2 -/-* double mutant mice (8 out of 9) exhibited bilateral atrial enlargement (Figure 7; Table 1), a defect also noted in the *sema3A* null mice (Behar et al., 1996). It is interesting that we also observed atrial enlargement in *C/- ;Cre* mice, raising the intriguing possibility that Sema3A-Npn-1 signaling in endothelial cells contributes to atrial development. These observations indicate that Npn-1 serves as a receptor for both secreted semaphorins and VEGFs to coordinate cardiac development.

Discussion

Our results show that Npn-1 is a receptor for members of structurally and functionally distinct ligand families in vivo. In the nervous system, Npn-1 functions as a receptor for secreted semaphorins, promoting fasciculation and proper targeting of several populations of PNS and CNS projections. Because of the extended viability of *npn-1Sema-* mice compared to *npn-1* null mice, we have uncovered several neural functions of Sema-Npn-1 signaling. Remarkably, we have so far observed no defects in the vasculature of either *npn-1Sema-* (Figure 6) or *npn-1Sema- ;npn-2 -/-* double mutant mice (data not shown), which is in dramatic contrast to the devastation of the vasculature observed in both *npn-1* null mice and in mice lacking *npn-1* exclusively in endothelial cells. These findings support the idea that VEGF-Npn-1 signaling, but not Sema-Npn-1 signaling, is critical for general vasculature development. Finally, and surprisingly, both VEGF-Npn-1 and Sema-Npn-1 and/or -Npn-2 signaling coordinate septation of the cardiac outflow tract, while

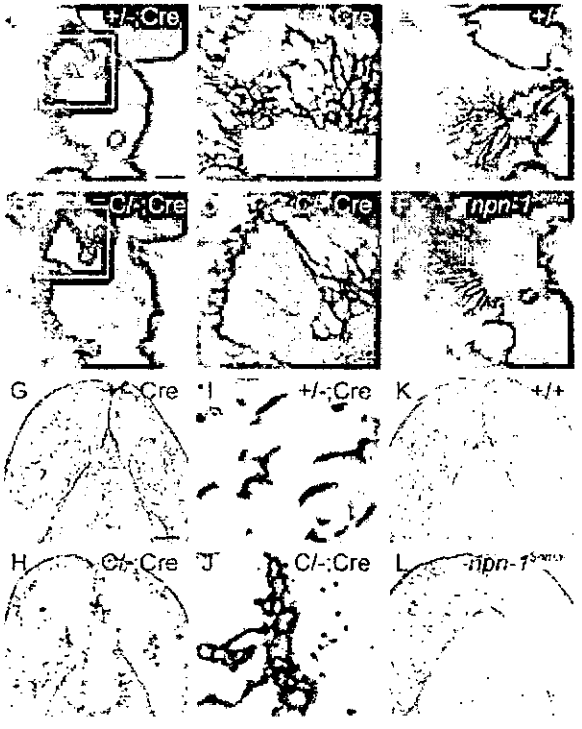

Figure 6. Severe Vasculature Disruption in Endothelial-Specific *npn-1* Null Mice, but Not in *npn-1*$^{Sema-}$ Mice

(A–F) Whole-mount anti-PECAM staining of a endothelial cell-specific *npn-1* null mutant (*C/*$^{-}$*; Cre*) (B), a heterozygous littermate control (*+/*$^{-}$*; Cre*) (A), homozygous *npn-1*$^{Sema-}$ (F), and a wild type littermate control embryo (E), all at E12.5. Boxed regions from (A) and (B) are displayed at higher magnification in (C) and (D), respectively.

(G–L) Isolectin staining of E13.5 horizontal brain sections from a endothelial cell-specific *npn-1* null mutant embryo (*C/*$^{-}$*; Cre*) (H), a heterozygous littermate control embryo (*+/*$^{-}$*; Cre*) (G), a homozygous *npn-1*$^{Sema-}$ embryo (L), and a wild type littermate control embryo (K). Select regions from (G) and (H) are displayed at higher magnification in (I) and (J), respectively. Note the decrease in endothelial branching in *C/*$^{-}$*; Cre* mice compared to controls. Scale bars: (A, B, E, and F), 0.5 mm; (C and D), 0.2 mm; (G, H, K, and L), 750 μm; (I and J), 50 μm.

Sema3A-Npn-1 signaling in endothelial cells appears to control growth of the atria. Thus, Npn-1 is a versatile, multifunctional receptor for distinct families of ligands that coordinate heart, vasculature, and nervous system development.

Npn-1 and Nervous System Development

The chemorepellant Sema3A was the first identified ligand for Npn-1, and several lines of evidence indicate that Npn-1 is an obligate coreceptor for Sema3A, while Npn-2 is a coreceptor for Sema3F. Indeed, a comparison of the phenotypes of *Npn-1*$^{Sema-}$ mice and *sema3A* null mice indicates that these mutants partially phenocopy one another. For example, spinal and cranial nerves are defasciculated and abnormally extended in both mutant mice (Behar et al., 1996; Kitsukawa et al., 1997; Taniguchi et al., 1997). Moreover, entorhinal cortical axons are mistargeted in both *npn-1*$^{Sema-}$ mice and *sema3A* null mice (Pozas et al., 2001), although this phenotype is more dramatic in *npn-1*$^{Sema-}$ mice. This suggests that

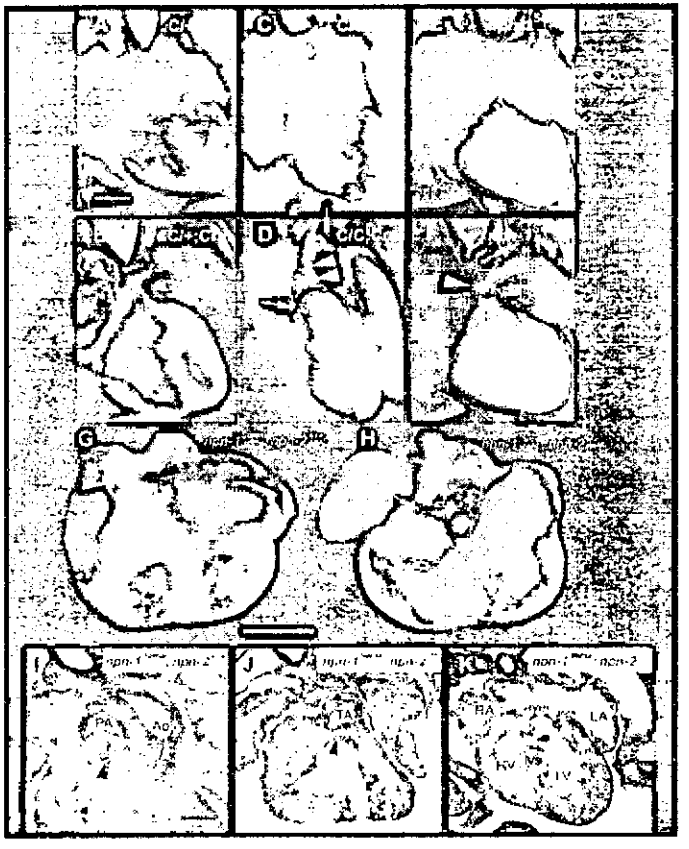

Figure 7. Cardiac Defects in Endothelial Cell-Specific *npn-1* Null Mice, *npn-1*$^{Sema-}$ Mice, and *npn-1*$^{Sema-}$ *npn-2*$^{-/-}$ Double Mutant Mice

(A–F) Gross examination of the hearts of wild-type (A and B), endothelial cell-specific *npn-1* null mice (*C/C;Cre*) (C and D), and *npn-1*$^{Sema-}$ mice (E and F). (A and B) Ventral view of a wild type heart in which normal atria, ventricles, and vessels of the aortic arch can be seen (A). After removal of the anterior half of the atria (B), the right ventricular outflow tract can be clearly seen giving rise to the pulmonary trunk (black arrowhead). The aorta (white arrowhead) is distinctly visible interio posterior to the pulmonary trunk (B). The left anterior descending coronary artery (lair-l) courses normally through the interventricular sulcus. (C and D) Ventral view of the heart from a *C/C;Cre* mutant. There is marked right atrial enlargement (C). The ventricular outflow tract shows a common trunk (double arrowhead in (D)) giving rise to both the aorta and the pulmonary trunk (truncus arteriosus). Upon removal of the anterior half of the atria (D) an anomalous origin of the left coronary artery from the right side of the truncus arteriosus can be seen (white arrow), and this misplaced coronary artery crosses over the outflow tract to become the left anterior descending artery. (E and F) Ventral view of the heart of a *npn-1*$^{Sema-}$ mouse. There is bilateral atrial enlargement (E), but, upon removal of the atria, it is clear that the aorta, pulmonary arteries, and coronary arteries arise normally.

(G–K) Persistent truncus arteriosus in E14.5 *npn-1*$^{Sema-}$ *;npn-2*$^{-/-}$ double mutant mice. (G and H) Gross examination of the heart. (G) Ventral view of a heart from an E11.5 *npn-1*$^{Sema-}$ mouse exhibiting a normal outflow tract. The aorta (white arrowhead) arises from its normal position

Table 1. Cardiac Defects in C/C;Cre, npn-1^Sema-, npn-2^-/-, and npn-1^Sema-;npn-2^-/- Double Mutant Mice

Genotype	PTA	BAE	AOC	VSD
C/C;Cre	17/17	17/17	4/10	3/8
npn-1^Sema-	0/11	10/11	0/11	1/11
npn-2	0/8	0/4	0/4	0/4
npn-1^Sema-;npn-2^-/-	6/9	8/9	3/9	2/6

Numbers show mice with defect/total mice examined. PTA, persistent truncus arteriosus; BAE, bilateral atrial enlargement; AOC, anomalous origin of the coronary arteries, VSD, ventricular septal defect.

Sema3A and one or more additional secreted semaphorins act through Npn-1 to instruct the layer-specific targeting of entorhinohippocampal projections. We have also observed several axon guidance defects in *npn-1^Sema-* mice that have not been reported in *sema3A* mutant mice. These include precocious entry of the TrkA-positive fibers into the spinal cord, defects in the formation of the corpus callosum, and aberrant projections of vestibular ganglion neurons within the inner ear. Sema3A, Sema3C, Sema3D, and Sema3E can each bind to Npn-1, and, therefore, these neuronal defects may be due to a lack of signaling by any or all of these four secreted semaphorins. Furthermore, while we have not observed defects in orientation of apical dendrites and axons of layer 5 cortical neurons in P2, P6, or P14 *npn-1^Sema-* mice, we have noted striking differences in both the length and complexity of their basal dendrites. Additional comparisons between *npn-1^Sema-* mice and mice lacking one or more genes encoding each of the class 3 semaphorins will be necessary to establish which of these ligands might instruct the fasciculation and targeting of axons and the growth of dendrites of Npn-1–expressing cortical neurons during development.

Npn-1 and Cardiovascular Development

To investigate Npn-1 function in vasculature development, we generated mice in which Npn-1 was specifically deleted in endothelial cells. We found that the vasculature is severely disrupted in *C/-;Cre* mice, indicating that Npn-1 is indeed required within endothelial cells for angiogenesis. These defects are likely due to a deficiency in VEGF-Npn-1 signaling since the vasculature of *npn-1^Sema-* mice appears normal.

Compared to the relatively simple cell-type- and ligand specificities of Npn-1 signaling requirements in the nervous system and vasculature, we found that heart development requires a remarkable degree of coordination between the families of ligands that signal through their common Npn-1 receptor. Taken together with previous reports, our observations support a model in which Npn-1 confers responsiveness of multiple cell types to both VEGF and semaphorin ligands and functions within endothelial cells to coordinate heart development. Our findings also indicate that VEGF-Npn-1 signaling in endothelial cells controls septation of the outflow tract and topographic origin of the coronary arteries. These results also support a model in which Sema3C signaling, through either Npn-1 or Npn-2, instructs outflow tract septation; however, the cell-type dependence of this signaling event is less clear. Indeed, Sema3C signaling is required for outflow tract development (Feiner et al., 2001), and this ligand can bind with high affinity to both Npn-1 and Npn-2. Interestingly, while a Npn-1/Npn-2 heterodimer was previously suggested to be a Sema3C receptor in sympathetic neurons (Chen et al., 1997, 1998; Takahashi et al., 1998), we observed outflow tract defects in the *npn-1^Sema-* mice only in a *npn-2* null background, strongly supporting a distinct model in which either Npn-1 or Npn-2 can serve as a Sema3C receptor in the developing heart. It has been suggested that Sema3C guides migrating cardiac neural crest cells as they take up residence in the proximal outflow tract, where they play a crucial role in outflow tract septation (Brown et al., 2001; Feiner et al., 2001). While our results are consistent with this possibility, they are also consistent with a Sema3C signaling requirement in another cell type, possibly endothelial cells, for outflow tract septation. In any case, our results indicate that a secreted semaphorin, Sema3C, and one or more members of the VEGF family of ligands signal through a common receptor, Npn-1, to coordinate septation of the cardiac outflow tract. Lastly, a Sema3A-Npn-1 signal is required for proper development of the atria, and this signal is likely propagated within endothelial cells since atrial enlargement was observed in *Sema3A* null mice (Behar et al., 1996) and in both the *C/C;Cre* mice and *npn-1^Sema-* mice reported here.

In summary, our findings show that members of distinct ligand families, semaphorins and VEGFs, act through a common receptor, Npn-1, to instruct axonal pathfinding in neurons and growth of the vasculature, respectively. Remarkably, through Npn-1, members of these same ligand families collaborate to orchestrate development of the heart. Thus, neuropilins have the unique capacity to mediate functional interactions between distinct families of ligands to coordinate complex morphogenic events during development.

Experimental Procedures

Generation of npn-1^Sema-, npn-1 Conditional, and npn-1 Null Mice

A bacterial artificial chromosome (BAC) containing *npn-1* exon 2 was obtained from Incyte genomics (Palo Alto, CA). A 9 kb BamHI/SalI fragment containing 1.4 kb of upstream intron sequence, exon 2, and 7 kb of downstream intron sequence was subcloned into pBluescript, and this plasmid served as a template for the construction of the targeting vectors. To generate the *npn-1^Sema-* targeting vector, a loxP-flanked neo cassette was inserted into the SacI site, which is 330 bp upstream of exon2. Exon 2 was replaced with a mutated exon 2 encoding a 7 amino acid substitution (see Gu et al., 2002) using standard cloning techniques (Figure 1B). For generation of the conditional *npn-1* targeting vector, a *neo FRT/loxP* cassette (kindly provided by Kogo Takamiya and Richard Huganir, Johns Hopkins School of Medicine) was cloned into the SacI site of the BamHI/SalI fragment (Figure 1C). The targeting vectors were linearized with NotI, electroporated into 129.1 mouse strain embryonic stem (ES) cells, and ES cell clones were selected with G418 (300 μg/ml). ES cell clones were screened by PCR, and the results were confirmed by Southern blotting. Two conditional or four *npn-1^Sema-* clones that successfully underwent homologous recombination were injected into C57B/6 blastocysts that were then introduced into pseudopregnant females. Chimeric animals were mated with C57B/6 to produce agouti heterozygous animals, and these mice were subsequently crossed with mice expressing either Cre recombinase (Schwenk et al., 1995) or FlpE recombinase (Rodriguez et al., 2000) in germ cells (kindly provided by Susan Dymecki, Harvard University) to excise the neo cassettes. *Npn-1* null mice were obtained by crossing conditional *npn-1* mice with mice expressing Cre recombinase in germ cells. Mice with the genotype *C/C; Cre* shown in Figures 7A–7D were produced by mating *C/C* mice with *C/+; Tie-2-Cre* mice. Offspring were genotyped by PCR using primers that detect both the Cre transgene and the *npn-1* conditional alleles. Mice with the genotype *C/-; Cre* (Figure 6) were produced by mating *C/-* mice (harboring one *C* allele and one *npn-1* null allele) with *C/+; Tie-2-Cre* mice. Offspring were genotyped by PCR using primers that detect the Cre allele, the *npn-1* conditional allele, and the *npn-1* null allele. Germline chimeras were crossed into a pure C57/B6 background, and all subsequent breeding was done in a C57/B6 background. All the analyses were performed on the F2–F5 generations.

AP Fusion Protein Binding to Tissue Sections

Fresh-frozen E12.5 and E17.5 embryos were sectioned using a cryostat, and AP fusion protein binding to tissue sections was performed as previously described (Giger et al., 1998).

DRG Repulsion Assay

DRG were dissected from E14.5 wild-type or mutant embryos, and collagen repulsion assays were performed essentially as previously described (Kolodkin et al., 1997). Statistical analysis was performed using a two-way ANOVA.

Whole-Mount Immunostaining and Immunohistochemical Procedures

Embryos were fixed in PBS containing 4% PFA, and whole-mount staining was performed as described (Giger et al., 2000) using primary monoclonal antibodies against either PECAM-1 (clone MEC13.3, isotype rat, 1:500 dilution; Pharmingen, San Diego, CA) or neurofilament 2H3 (supernatant from hybridoma cells; 1:50 dilution; Developmental Studies Hybridoma Bank, Iowa City, IA) and peroxidase-conjugated secondary antibodies. Immunocytochemistry of cryosections (20 μm) using rabbit anti-Npn-1 (Kolodkin et al., 1997), rabbit anti-TrkA antibody (1:1000; kindly provided by L. Reichardt, University of California, San Francisco), and 2H3 neurofilament antibody was performed as described (Giger et al., 2000).

DiI Labeling of Callosal and Entorhinohippocampal Projections

DiI labeling of callosal projections was performed on E17.5 embryos as described (Shu and Richards, 2001). 45 μm vibratome sections of DiI-labeled brains were immunostained with antibodies against glial fibrillary acidic protein (GFAP) as described (Shu and Richards, 2001). DiI labeling of entorhinohippocampal projections was performed on newborn mice (P0–P2) as described (Super et al., 1998; Super and Soriano, 1994).

Anterograde and Retrograde Labeling of Vestibulocochlear Projections

A fluorescent lipophilic tracer (PKH26) was used to label the peripheral and central projections of the vestibulocochlear nerve as previously described (Maklad and Fritzsch, 2002; Wilm and Fritzsch, 1993).

Visualization of Cortical Dendrites

The *thy1-GFP-m* mouse line was obtained from Joshua Sanes (Washington University School of Medicine) and *thy1-YFP-15Jrs* mice were obtained from Jackson Labs (Bar Harbor, MA). Both reporter lines were crossed with *npn-1^Sema/+* mice to obtain double heterozygous mice, which were then bred to obtain mutant mice (*npn-1^Sema-;thy1-GFP-m*, and *npn-1^Sema-;thy1-YFP*) and control littermates. P2, P6, and P14 mutant and littermate control mice were anesthetized and perfused with 4% paraformaldehyde. 100 μm (P14) and 40 μm (P2 and P6) coronal brain sections were made, mounted, and analyzed by confocal microscopy.

Acknowledgments

We thank members of the Kolodkin and Ginty laboratories, Jan Rosenbaum, Daniel Leahy, and Anirvan Ghosh for helpful discussions and comments on the manuscript. We thank Mitra Cowan and the Johns Hopkins Transgenic Facility for blastocyst injections and advice with ES cells, Guo Huang for help with the TrkA staining experiments, Sarah Lowson and Todd Hippe for excellent technical assistance, Naren Ramanan for help with preparation of the figures, Kogo Takamiya and Richard Huganir for advice with targeting vectors, Susan Dymecki for the germline FlpE mice, and Masashi Yanagisawa for the *Tie-2-Cre* mice. This work was supported by NIH/NRSA-5F32NS11016, NIH/NHLBI P01-HL70295, NIH/NIDCD R01-DC 005530, the Robert Packard Center for ALS Research at Johns Hopkins, NIH/NIMH R01MH59199, the Kirsch Foundation, and the Howard Hughes Medical Institute.

Received: January 27, 2003
Revised: April 29, 2003
Accepted: May 7, 2003
Published: July 7, 2003

References

Behar, O., Golden, J.A., Mashimo, H., Schoen, F.J., and Fishman, M.C. (1996). Semaphorin III is needed for normal patterning and growth of nerves, bones, and heart. Nature 383, 525–528.

Brown, C.B., Feiner, L., Lu, M.M., Li, J., Ma, X., Webber, A.L., Jia, L., Raper, J.A., and Epstein, J.A. (2001). PlexinA2 and semaphorin signaling during cardiac neural crest development. Development 128, 3071–3080.

Chen, H., Chedotal, A., He, Z., Goodman, C.S., and Tessier-Lavigne, M. (1997). Neuropilin-2, a novel member of the neuropilin family, is a high affinity receptor for the semaphorins Sema E and Sema IV but not Sema III. Neuron 19, 547–559.

Chen, H., He, Z., Bagri, A., and Tessier-Lavigne, M. (1998). Semaphorin-neuropilin interactions underlying sympathetic axon responses to class III semaphorins. Neuron 21, 1283–1290.

Chen, H., Bagri, A., Zupicich, J.A., Zou, Y., Stoeckli, E., Pleasure, S.J., Lowenstein, D.H., Skarnes, W.C., Chedotal, A., and Tessier-Lavigne, M. (2000). Neuropilin-2 regulates the development of selective cranial and sensory nerves and hippocampal mossy fiber projections. Neuron 25, 43–56.

Creazzo, T.L., Godt, R.E., Leatherbury, L., Conway, S.J., and Kirby, M.L. (1998). Role of cardiac neural crest cells in cardiovascular development. Annu. Rev. Physiol. 60, 267–286.

Feiner, L., Webber, A.L., Brown, C.B., Lu, M.M., Jia, L., Feinstein, P., Mombaerts, P., Epstein, J.A., and Raper, J.A. (2001). Targeted disruption of semaphorin 3C leads to persistent truncus arteriosus and aortic arch interruption. Development 128, 3061–3070.

Feng, G., Mellor, R.H., Bernstein, M., Keller-Peck, C., Nguyen, Q.T., Wallace, M., Nerbonne, J.M., Lichtman, J.W., and Sanes, J.R. (2000).

behind the pulmonary trunk. (H) Ventral view of the heart from a *npn-1^Sema-;npn-2^-/-* double mutant mouse showing truncus arteriosus (white arrowheads) and an abnormal vascular proliferation (arrow) similar to that seen in (D). (I–J) Hematoxylin and Eosin-stained paraffin sections (5 μM) through the heart of a E14.5 control littermate showing the right ventricular outflow tract and endocardial cushions forming the pulmonic valve (concave black arrowhead) (I). The endocardial cushions forming the aortic valve are caudal to this level of section but the root of the aorta is clearly formed (white arrowhead). The *npn-1^Sema-;npn-2^-/-* double mutant embryos (J) showed a single common root to the aorta and pulmonary artery (truncus arteriosus; concave black arrowhead). Some double mutant embryos also showed ventricular septal defects (arrow) (K). RA, right atrium; LA, left atrium; RV, right ventricle; LV, left ventricle; ivs, interventricular septum; AVEC, atrioventricular endocardial cushions (black arrowheads). Scale bars, (A–F) 500 μm, (G and H) 1 mm, (I and J) 50 μm, (K) 100 μm.

Imaging neuronal subsets in transgenic mice expressing multiple spectral variants of GFP. Neuron 28, 41–51.

Ferrara, N. (2001). Role of vascular endothelial growth factor in regulation of physiological angiogenesis. Am. J. Physiol. Cell Physiol. 280, C1358–C1366.

Fujisawa, H., Kitsukawa, T., Kawakami, A., Takagi, S., Shimizu, M., and Hirata, T. (1997). Roles of a neuronal cell-surface molecule, neuropilin, in nerve fiber fasciculation and guidance. Cell Tissue Res. 290, 465–470.

Giger, R.J., Urquhart, E.R., Gillespie, S.K.H., Levengood, D.V., Ginty, D.D., and Kolodkin, A.L. (1998). Neuropilin-2 is a receptor for semaphorin IV: insight into the structural basis of receptor function and specificity. Neuron 21, 1079–1092.

Giger, R.J., Cloutier, J.F., Sahay, A., Prinjha, R.K., Levengood, D.V., Moore, S.E., Pickering, S., Simmons, D., Rastan, S., Walsh, F.S., et al. (2000). Neuropilin-2 is required in vivo for selective axon guidance responses to secreted semaphorins. Neuron 25, 29–41.

Gu, C., Limberg, B.J., Whitaker, G.B., Perman, B., Leahy, D.J., Rosenbaum, J.S., Ginty, D.D., and Kolodkin, A.L. (2002). Characterization of neuropilin-1 structural features that confer binding to semaphorin 3A and vascular endothelial growth factor 165. J. Biol. Chem. 277, 18069–18076.

He, S., and Tessier-Lavigne, M. (1997). Molecular basis of axonal chemorepulsion: neuropilin is a semaphorin/collapsin receptor. Cell 90, 739–751.

He, Z., Wang, K.C., Koprivica, V., Ming, G., and Song, H.J. (2002). Knowing how to navigate: mechanisms of semaphorin signaling in the nervous system. Sci. STKE 2002, RE1.

Huber, A.B., Kolodkin, A.L., Ginty, D.D., and Cloutier, J.F. (2003). Signaling at the growth cone: ligand-receptor complexes and the control of axon growth and guidance. Annu. Rev. Neurosci., in press. Published online June 16, 2003. 10.1146/annurev.neuro.26.010302.081139.

Kawasaki, T., Kitsukawa, T., Bekku, Y., Matsuda, Y., Sanbo, M., Yagi, T., and Fujisawa, H. (1999). A requirement for neuropilin-1 in embryonic vessel formation. Development 126, 4895–4902.

Kisanuki, Y.Y., Hammer, R.E., Miyazaki, J., Williams, S.C., Richardson, J.A., and Yanagisawa, M. (2001). Tie2-Cre transgenic mice: a new model for endothelial cell-lineage analysis in vivo. Dev. Biol. 230, 230–242.

Kitsukawa, T., Shimizu, M., Sanbo, M., Hirata, T., Taniguchi, M., Bekku, Y., Yagi, T., and Fujisawa, H. (1997). Neuropilin-semaphorin III/D-mediated chemorepulsive signals play a crucial role in peripheral nerve projection in mice. Neuron 19, 995–1005.

Kolodkin, A.L., Levengood, D.V., Rowe, E.G., Tai, Y.-T., Giger, R.J., and Ginty, D.D. (1997). Neuropilin is a semaphorin III receptor. Cell 90, 753–762.

Lee, P., Goishi, K., Davidson, A.J., Mannix, R., Zon, L., and Klagsbrun, M. (2002). Neuropilin-1 is required for vascular development and is a mediator of VEGF-dependent angiogenesis in zebrafish. Proc. Natl. Acad. Sci. USA 99, 10470–10475.

Maklad, A., and Fritzsch, B. (2002). The developmental segregation of posterior crista and saccular vestibular fibers in mice: a carbocyanine tracer study using confocal microscopy. Brain Res. Dev. Brain Res. 135, 1–17.

Neufeld, G., Cohen, T., Gengrinovitch, S., and Poltorak, Z. (1999). Vascular endothelial growth factor (VEGF) and its receptors. FASEB J. 13, 9–22.

Neufeld, G., Cohen, T., Shraga, N., Lange, T., Kessler, O., and Herzog, Y. (2002). The neuropilins: multifunctional semaphorin and VEGF receptors that modulate axon guidance and angiogenesis. Trends Cardiovasc. Med. 12, 13–19.

Oosthuyse, B., Moons, L., Storkebaum, E., Beck, H., Nuyens, D., Brusselmans, K., Van Dorpe, J., Hellings, P., Gorselink, M., Heymans, S., et al. (2001). Deletion of the hypoxia-response element in the vascular endothelial growth factor promoter causes motor neuron degeneration. Nat. Genet. 28, 131–138.

Polleux, F., Giger, R.J., Ginty, D.D., Kolodkin, A.L., and Ghosh, A. (1998). Patterning of cortical efferent projections by semaphorin-neuropilin interactions. Science 282, 1904–1906.

Polleux, F., Morrow, T., and Ghosh, A. (2000). Semaphorin 3A is a chemoattractant for cortical apical dendrites. Nature 404, 567–573.

Porcs, E., Pascual, M., Nguyen Ba-Charvet, K.T., Guijarro, P., Sotelo, C., Chedotal, A., Del Rio, J.A., and Soriano, E. (2001). Age-dependent effects of secreted Semaphorins 3A, 3F, and 3E on developing hippocampal axons: in vitro effects and phenotype of Semaphorin 3A (−/−) mice. Mol. Cell. Neurosci. 18, 26–43.

Rodriguez, C.I., Buchholz, F., Galloway, J., Sequerra, R., Kasper, J., Ayala, R., Stewart, A.F., and Dymecki, S.M. (2000). High-efficiency deleter mice show that FLPe is an alternative to Cre-loxP. Nat. Genet. 25, 139–140.

Romero, A., Romao, M.J., Varela, P.F., Kolen, E., Dias, J.M., Carvalho, A.L., Sanz, L., Topfer-Petersen, E., and Calvete, J.J. (1997). The crystal structures of two spermadhesins reveal the CUB domain fold. Nat. Struct. Biol. 4, 783–788.

Schwenk, F., Baron, U., and Rajewsky, K. (1995). A cre-transgenic mouse strain for the ubiquitous deletion of loxP-flanked gene segments including deletion in germ cells. Nucleic Acids Res. 23, 5080–5081.

Shimizu, M., Murakami, Y., Suto, F., and Fujisawa, H. (2000). Determination of cell adhesion sites of neuropilin-1. J. Cell Biol. 149, 1283–1293.

Shu, T., and Richards, L.J. (2001). Cortical axon guidance by the glial wedge during the development of the corpus callosum. J. Neurosci. 21, 2749–2758.

Soker, S., Takashima, S., Miao, H.-Q., Neufeld, G., and Klagsbrun, M. (1998). Neuropilin-1 is expressed by endothelial and tumor cells as an isoform-specific receptor for vascular endothelial growth factor. Cell 92, 735–745.

Sondell, M., Lundborg, G., and Kanje, M. (1999). Vascular endothelial growth factor has neurotrophic activity and stimulates axonal outgrowth, enhancing cell survival and Schwann cell proliferation in the peripheral nervous system. J. Neurosci. 19, 5731–5740.

Sondell, M., Sundler, F., and Kanje, M. (2000). Vascular endothelial growth factor is a neurotrophic factor which stimulates axonal outgrowth through the flk-1 receptor. Eur. J. Neurosci. 12, 4243–4254.

Super, H., and Soriano, E. (1994). The organization of the embryonic and early postnatal murine hippocampus. II. Development of entorhinal, commissural, and septal connections studied with the lipophilic tracer DiI. J. Comp. Neurol. 344, 101–120.

Super, H., Martinez, A., Del Rio, J.A., and Soriano, E. (1998). Involvement of distinct pioneer neurons in the formation of layer-specific connections in the hippocampus. J. Neurosci. 18, 4616–4626.

Takagi, S., Tsuji, T., Amagai, T., Takamatsu, T., and Fujisawa, H. (1987). Specific cell surface labels in the visual center of Xenopus laevis tadpole identified using monoclonal antibodies. Dev. Biol. 122, 90–100.

Takahashi, T., Nakamura, F., Jin, Z., Kalb, R., and Strittmatter, S. (1998). Semaphorins 4A and 4D act as antagonists of neuropilin-1 and agonists of neuropilin-2 receptors. Nat. Neurosci. 1, 487–493.

Takashima, S., Kitakaze, M., Asakura, M., Asanuma, H., Sanada, S., Tashiro, F., Niwa, H., Miyazaki, J.-I., Hirota, S., Kitamura, Y., et al. (2002). Targeting of both mouse neuropilin-1 and neuropilin-2 genes severely impairs developmental yolk sac and embryonic angiogenesis. Proc. Natl. Acad. Sci. USA 99, 3657–3662.

Taniguchi, M., Yuasa, S., Fujisawa, H., Naruse, I., Saga, S., Mishina, M., and Yagi, T. (1997). Disruption of semaphorin III/D gene causes severe abnormality in peripheral nerve projection. Neuron 19, 519–530.

Wilm, C., and Fritzsch, B. (1993). Regenerating retinal fibers display error-free homing along undamaged normal fibers. J. Neurobiol. 24, 895–902.

Yuan, L., Moyon, D., Pardanaud, L., Breant, C., Karkkainen, M.J., Alitalo, K., and Eichmann, A. (2002). Abnormal lymphatic vessel development in neuropilin 2 mutant mice. Development 129, 4797–4806.